Principles and Measuring Techniques of Turbulence Characteristics in Open-Channel Flows

GEOLOGICAL SURVEY PROFESSIONAL PAPER 802–A

Principles and Measuring Techniques of Turbulence Characteristics in Open-Channel Flows

By R. S. McQUIVEY

TURBULENCE IN WATER

GEOLOGICAL SURVEY PROFESSIONAL PAPER 802-A

UNITED STATES GOVERNMENT PRINTING OFFICE, WASHINGTON : 1973

UNITED STATES DEPARTMENT OF THE INTERIOR

ROGERS C. B. MORTON, *Secretary*

GEOLOGICAL SURVEY

V. E. McKelvey, *Director*

Library of Congress catalog-card No. 73-600207

For sale by the Superintendent of Documents, U.S. Government Printing Office
Washington, D.C. 20402 – Price $1.80 (paper cover)
Stock Number 2401-02405

CONTENTS

ILLUSTRATIONS

TABLE

SYMBOLS

Symbol	*Definition*	*Units*
a	Constant.	.....
A, A'	Constants in King's law.	.....
b	Constant.	.....
B, B'	Constants in King's law.	.....
B_e	Equivalent frequency band width.	sec^{-1}
c	Constant.	.....
C_p	Specific heat of the fluid at constant pressure.	Btu per lb °F
d	Characteristic dimension of the sensor.	ft
d'	Defined as $2B_eT$.	.....
D	Total depth of flow.	ft
e	Natural log base.	.....
e	Voltage fluctuation, defined as being equal to $\sqrt{\overline{e^2}}$.	volts
$\sqrt{\overline{e^2}}$	Root mean square of the voltage fluctuation.	volts
E	Instantaneous voltage output of the anemometer.	volts
$\overline{E}$	Mean voltage output of the anemometer.	volts
f	Frequency.	sec^{-1}
f_c	Cutoff frequency.	sec^{-1}
F	Body force.	lb
$F(f)$	Normalized energy-spectrum function of f.	sec
F_q	Digital normalized energy-spectrum function.	sec
g	Acceleration of gravity.	ft per sec per sec
G	Grashof number.	.....
h	Heat-transfer coefficient.	Btu per hr ft^2 °F
H	Thermal power (time rate of thermal heat) transferred between sensor and fluid.	Btu per hr
H_c	Convective heat transferred between sensor and fluid.	Btu per hr
H_j	Electrical (Joulean) heat produced in sensor.	Btu per hr
H_r	Radiant heat transferred between sensor and fluid.	Btu per hr

Symbol	Definition	Units
$\bar{i}$	Imaginary number, $\sqrt{-1}$.	.....
i, j, k	Indices in the x, y, and z directions, respectively.	.....
$\boldsymbol{i}, \boldsymbol{j}, \boldsymbol{k}$	Unit vectors in the x, y, and z directions, respectively.	.....
I	Electrical current.	amp
k	Thermal conductivity of the fluid.	Btu per hr ft °F
k_*	Wave-number vector.	ft^{-1}
K	Overheat ratio, defined as R_s/R_a.	.....
K_s	Height of roughness element.	ft
L	Eulerian length scale (macroscale of turbulence).	ft
L_L	Transverse Lagrangian scale.	ft
m	Index associated with digital autocorrelation function.	.....
M	Total number of lags in digital autocorrelation function.	.....
n	Exponent in King's law and index for digitized data.	.....
N	Total number of digitized data points.	.....
N	Nusselt number.	.....
o	Index associated with digital energy-spectrum functions.	.....
p	Pressure fluctuation at a point in the flow.	lb per ft^2
P	Instantaneous pressure at a point in the flow.	lb per ft^2
$\overline{P}$	Mean pressure at a point in the flow.	lb per ft^2
P	Prantl number.	.....
P_q, P_o, P_M	Digital energy-spectrum functions.	ft^2 per sec^2
q	Index associated with digital energy-spectrum functions.	.....
$Q(r)$	General correlation function of r.	ft^2 per sec^2
$\mathbf{Q}_{ij}(r)$	General correlation function of r (tensor).	ft^2 per sec^2
r	Distance between hot-film sensors at two points (x and $x+r$) in the flow.	ft
R	Hydraulic radius.	ft
R	Reynolds number.	.....
R_a	Electrical resistance of the sensor at fluid or environment temperature (cold).	ohms
R_s	Electrical resistance of the sensor at sensor temperature (hot).	ohms
R_m, R_o, R_M	Digital autocorrelation functions.	ft^2 per sec^2
$R(\tau)$	Eulerian time autocorrelation function of τ.	.....
$\mathbf{R}_{ij}$	Eulerian point correlation function of x (tensor).	.....
$\mathbf{R}_{ii}(r)$	Eulerian space correlation function of r (tensor).	.....
$\mathbf{R}_{ij}(r)$	Eulerian space correlation function of r (tensor).	.....
$\mathbf{R}_{ij}(r, \tau)$	Eulerian space-time correlation function of r and τ (tensor).	.....
$R_L(\tau)$	Lagrangian time correlation function of τ.	.....
$\mathbf{R}_{L_{ij}}(\tau)$	Lagrangian time correlation function of τ (tensor).	.....
s	Area of the sensor.	ft^2
S	Slope of the energy gradient.	ft per ft
S_x	Sensitivity term in the x direction.	volt sec per ft
S_y	Sensitivity term in the y direction.	volt sec per ft
t	Time.	sec
Δt	Sampling interval.	sec
T	Total sampling time, or length of record.	sec
T_a	Temperature of the fluid or environment.	°C
T_s	Temperature of the sensor.	°C
T_e	Eulerian integral time scale.	sec
T'	Eulerian integral space-time scale.	sec
T_L	Lagrangian integral time scale.	sec
u	Velocity fluctuation in the x direction, defined as being equal to $\sqrt{\overline{u^2}}$.	ft per sec
$\sqrt{\overline{u^2}}$	Root mean square of the velocity fluctuation in the x direction, defined as the longitudinal turbulence intensity.	ft per sec
U	Instantaneous velocity at a point in the x direction.	ft per sec
$\overline{U}$	Mean velocity at a point in the x direction.	ft per sec
U_{tot}	Total instantaneous velocity in the x direction at a point in the flow.	ft per sec
U_A	Average velocity of the entire flow field.	ft per sec
U_*	Shear velocity in the x direction, defined as $\sqrt{gRS}$.	ft per sec
$\overline{u^2}, \overline{uv}, \overline{uw}$ $\overline{vu}, \overline{v^2}, \overline{vw}$ $\overline{wu}, \overline{wv}, \overline{w^2}$	Turbulence shear stresses.	ft^2 per sec^2
v	Velocity fluctuation in the y direction, defined as being equal to $\sqrt{\overline{v^2}}$.	ft per sec
$\sqrt{\overline{v^2}}$	Root mean square of the velocity fluctuation in the y direction, defined as the vertical turbulence intensity.	ft per sec

Symbol	*Definition*	*Units*
V	Instantaneous velocity at a point in the y direction.	ft per sec
$\overline{V}$	Mean velocity at a point in the y direction.	ft per sec
V_{tot}	Total instantaneous velocity at a point in the flow.	ft per sec
w	Velocity fluctuation in the z direction, defined as being equal to $\sqrt{\overline{w^2}}$.	ft per sec
$\sqrt{\overline{w^2}}$	Root mean square of the velocity fluctuation in the z direction, defined as the lateral or transverse turbulence intensity.	ft per sec
W	Instantaneous velocity at a point in the z direction.	ft per sec
$\overline{W}$	Mean velocity at a point in the z direction.	ft per sec
$W(f)$	Energy-spectrum function of f.	ft^2 per sec^2
W_q, W_o, W_M	Digital energy-spectrum functions.	ft^2 per sec^2
x	Coordinate in the direction of flow (longitudinal).	ft
y	Coordinate perpendicular to the direction of flow and perpendicular to the bottom (vertical).	ft
z	Coordinate perpendicular to the direction of flow and parallel to the bottom (lateral or transverse).	ft
α	Angle the boundary makes with respect to the horizontal.	radians
α'	Constant.	.....
β	Coefficient of expansion of the fluid.	ohm^{-1}
β', β_*	Constants.	.....
γ	Specific weight of the fluid.	lb per ft^3
γ'	Constant.	.....
ϵ	Dissipation term.	lb per ft^2 sec
ϵ_*	Energy conversion factor.	.....
λ_x	Eulerian length scale (microscale of turbulence in the x direction).	ft
Λ_L	Lagrangian length scale.	ft
μ	Dynamic viscosity of the fluid.	lb-sec per ft^2
ν	Kinematic viscosity of the fluid.	ft^2 per sec
ξ	Angle of yaw in space between sensor and x axis, defined as the sum of ϕ and ψ.	radians
ρ	Density of the fluid.	lb-sec^2 per ft^4
τ	Increment of time, or delay time defined as $m\Delta t$.	sec
ϕ	Instantaneous angle of yaw in the xy plane.	radians
$\overline{\phi}$	Mean angle of yaw in the xy plane.	radians
ϕ'	Fluctuation in angle of yaw in the xy plane.	radians
$\Phi(k_*)$	Energy-spectrum function of k_*.	ft
$\Phi_{ij}(k_*)$	Energy-spectrum function of k_* (tensor).	ft
ψ	Angle of yaw in the xz plane.	radians
ω	Angular frequency.	sec^{-1}

PRINCIPLES AND MEASURING TECHNIQUES OF TURBULENCE CHARACTERISTICS IN OPEN-CHANNEL FLOWS

By R. S. McQuivey

ABSTRACT

Turbulence velocity fluctuations in open-channel shear flows cause or strongly influence a large number of fluid-mechanics phenomena of interest to engineers. Turbulence measurements in fluids have been made with varying degrees of success, but only recently have measurements of turbulence in water been made with any degree of reliability. This recent improvement is due to the development of hot-film anemometry, which has given the researcher a tool for studying the structure of turbulence in open-channel flows. The fine spatial resolution (due to the small size of the sensor) and the good frequency response of the hot-film anemometer system are unmatched by any other system now available for making turbulence measurements in open-channel flows.

This report describes the statistical turbulence characteristics that best define the structure of the flow field and the relation between the characteristics and the equations of motion and energy. A detailed description of instrumentation, sensor selection, and theory of operation is presented along with a discussion of calibration characteristics, heat-transfer relations, hot-film and hot-wire measurements, and possible sources of errors in turbulence measurements. The report explains in detail a procedure to circumvent contamination problems so that measurements can be made in natural rivers and streams; it also presents a mathematical and experimental justification for the procedure. Aspects of analog and digital data reduction are discussed along with some guidelines to insure meaningful measurement of turbulence characteristics.

INTRODUCTION

As a part of the research program of the Water Resources Division of the U.S. Geological Survey, several projects have been organized to study the mechanics of water and sediment movement in open-channel flow. Answers to problems of flow resistance, sediment transport, turbulent diffusion, dispersion, and related topics have been sought. Early attempts to find solutions to these problems only considered the mean-flow variables and the fluid properties. In mean-flow studies, as has been a common procedure in open-channel-flow studies, the turbulent motions have been intentionally ignored, and the fluid has been treated as a fictitious "laminar flow" with special fluid properties. However, many fluid-mechanics phenomena are entirely caused or strongly influenced by the turbulent velocity fluctuations and scales and, therefore, by the statistical characteristics which have been used to describe the turbulence structure. Therefore, an attempt should be made to statistically define the turbulence structure.

Several early attempts were made by various investigators to develop phenomenological theories of turbulence. These theories are essentially simplified models of turbulent mass and momentum transfer. They include certain supposedly universal constants determined on the basis of laboratory measurements of mean velocity and average boundary shear, and they involve endowing the fluid with a property called "eddy viscosity," or more generally, "eddy diffusion coefficient." If an attempt is made to account for behavior in terms of "eddy viscosity," the fluid appears to be very peculiar. It might be described as non-Newtonian because of the dependence of the viscosity on the rate of shear. "Eddy viscosity" varies from point to point in one part of the flow and remains practically constant in other parts, and the numerical value is often hundreds of times larger than that of ordinary viscosity and bears no definite relation to it. Even more unconventional is the fact that "eddy viscosity" increases with the size of the flow field as well as with overall velocity. A fluid flowing in a large stream, for example, behaves as though it had a larger viscosity than the same fluid flowing in a small stream. Also, at high flow rates the viscosity appears to be larger than at low flow rates.

Neither the experimental investigations of gross parameters in turbulent flows nor the phenomenological theories of turbulence provides sufficient insight into the real structure of turbulence, nor

do they lead to any understanding of the turbulence mechanism or to quantitative estimates of the turbulence characteristics. These practices and theories have been maximally utilized, and no additional understanding of the mechanics of flow can be obtained by employing them.

Reference must always be made back to the turbulence mechanism in order to ultimately understand the structure of the flow field and the relation between the turbulence characteristics and the many basic flow processes.

The mechanism of turbulent motion in open-channel flow is so complex that a general physical model on which to base an analysis has not been formulated; therefore, a statistical approach must be used to obtain some of the variables that are physically significant and convenient to measure experimentally. This report defines the statistical characteristics of turbulence as suggested by the equations of motion and energy.

The approach to the problem is to experimentally obtain as much information about the characteristics of turbulence in open-channel flows as possible, and then from the experimental results try to obtain a clear idea of the structure and motion of turbulence. This approach in delineating the kinematics of turbulent motion depends on becoming extremely familiar with the turbulence characteristics and their distributions in the various flow fields of interest.

From an energy standpoint, the production, growth, dissipation, and distribution of turbulence in the flow field are of fundamental importance to understanding fluid motion involving friction, drag, and diffusion and dispersion of heat, mass, and momentum. The statistical characteristics guide the experimenter as to what variables and parameters to measure.

Only recently has turbulence in water been measurable with any degree of reliability. The development of hot-film anemometry has given the experimenter a tool for studying the structure of turbulence in open-channel flow. Increased use of film sensors and constant-temperature compensating circuitry, supplemented by root-mean-square voltmeters, FM recording equipment, and digital computers, has made anemometry more practical. However, many experimenters are employing hot-film anemometry without understanding the limitations, the possible errors, and the details of data-reduction procedures.

This report discusses in detail several items relating to the use of hot-film anemometry: anemometers and hot-film sensors available and their selection, limitations, advantages, disadvantages, and possible frequency-response problems; useful readout and signal-conditioning equipment available; operational procedures; contamination, drift, and other operational problems associated with measurements in natural streams; types of measurements and possible sources of errors; mathematical analysis of the anemometer output for one- and two-sensor operation; heat-transfer relations, calibration characteristics, and advantages and disadvantages of linearization; and analog and digital data-reduction techniques. The information in this report provides guidelines that can assist researchers in organizing experiments and in making accurate, useful measurements.

TURBULENT FLUID MOTION

The mechanism of turbulent motion in open-channel flow is so complex that a general physical model on which to base an analysis has not been formulated. However, if the problem is approached using statistical mechanics, certain simplifying assumptions and concepts can be introduced that will allow a solution to be obtained for some of the variables that are convenient to measure experimentally and are of clear physical significance. The material discussed herein should thus be viewed as a reasonably rigorous mathematical presentation, with some simple and limited mechanistic ideas injected on the basis of experimental evidence. At present, the details of what is physically occurring in turbulent shear flows are simply not known, and a general model of turbulent motion cannot be expressed in complete mathematical terms at this point.

Flows which occur in open channels belong to a particular class known as shear flows. Shear flows are comprised of flow fields in which relative velocities have been induced by viscous and turbulent shear stresses rather than by pressure gradients. The flows are, therefore, rotational as opposed to potential. The discussion is restricted to shear flows because only in these flows can turbulent motions arise and sustain themselves.

When tangential stresses are applied to a fluid having internal friction, shearing motions are produced in line with the stresses and in conformity with the shape of the boundaries. In open-channel flow fields, various kinds of secondary motions can also be produced. Irregular secondary motions, called turbulence, are very important for mixing, diffusion, and dispersion in open-channel flows, but their direct cause is not obvious. The occurrence of turbulence does not

depend on the shape of the boundaries but, like all secondary flows, depends only on a generating mechanism which produces motions in directions other than that of the applied shear.

Turbulence in open-channel flows is convected downstream in the same manner as any other fluid property. The turbulence which is convected downstream is followed by other turbulence from upstream. A steady state is maintained if the turbulence leaving is as vigorous as that arriving.

Because turbulent motions require energy to produce the frictional stresses, a mechanism must exist by which turbulent motions capture kinetic energy from the mean flow. This energy is expressed by the production term in the energy equations, which consists of the turbulent shear stress times the local velocity gradient. In short, turbulence carries with it the mechanism for sustaining itself; the energy produced by turbulence is sufficient to balance the energy lost by diffusion, convection, and viscous damping, and thus a steady state is maintained at each point.

Even though the energizing of turbulence is expressible in terms of shear stresses, turbulent pressure gradients are required and must arise from interactions within the flow itself. These interactions can be imagined to take the form of collisions between fluid elements. The resulting motions can best be described as a superposition of eddies with various orientations. The eddies which make up the turbulence arise near the boundaries, where regions of high shear stress exist. As individual eddies move about, they combine with others or break down into smaller ones. The shearing action stretches the eddies with axes lying along directions in which the fluid is being strained and intensifies their vorticity. Some concentrated vortex motions can, therefore, be expected to exist in a very complex motion.

Various scales of motion occur in turbulent shear flows. The largest scale motion is the mean flow, whose dimensions are characterized by parameters such as flow depth and channel width. Next are the turbulent motions, whose superimposed eddies have various dimensions ranging from near that of the flow depth down to the so-called microscale. All turbulent motions are responsible for shearing stress in the presence of a mean shear, and, therefore, all extract energy from the mean flow to sustain themselves. However, the amount of energy extracted by the turbulent action decreases with decreasing scale, so most of the energy is generally thought to enter the turbulence by way of the larger eddies at or near the boundaries. Correspondingly, the amount of energy lost through the damping action of viscosity is assumed to be negligible in the mean flow and among the large eddies but to increase progressively with decreasing size until it finally becomes dominant among the smallest eddies.

If energy enters the turbulence more by way of the large eddies than by the small ones and leaves more by way of the small eddies than by the large ones, then energy must be transferred from the larger scale motions to the smaller ones. The succession of transfer is generally regarded as taking place from size to size down the scale, and the number of stages increases with Reynolds number.

Frictional effects, mean velocity distributions, rate of spreading, and other features of turbulent flow bear little resemblance to features of laminar flow. The differences can be attributed to a diffusiveness of turbulence that far exceeds molecular diffusion and has a more intimate connection with the mean flow. The mechanism of turbulent diffusion, however, is similar to that of molecular diffusion, wherein a molecule moves and collides with another and so, by a process of random walk, migrates farther and farther from some initial point. In turbulent diffusion, large eddies wander randomly in generally curved paths and so produce a cumulative increase in the distance from an initial point.

The degree of energy transfer or of mixing by turbulent motions so surpasses that by molecular motions that the latter has little effect other than to smooth out the local conditions of properties in their new neighborhood.

Turbulent shear flow in open channels viewed mathematically is such a complex problem that any approach to it must lean heavily on experiments. The first stage in delineating the kinematics of the turbulence mechanism is to define the turbulence characteristics in terms of statistical relations of measurable parameters.

SIMPLIFYING ASSUMPTIONS

If statistical relations are to be used to define the turbulence characteristics, certain assumptions must be made about turbulent flow. A complex turbulent motion can be simplified as a mean that is time invariant and an irregular fluctuation that is a function of time about the mean value. (Any regular fluctuation would not be considered as turbulent motion.) (See fig. 1.)

The instantaneous velocity of turbulent motion at a point is given by

$$V_{tot}=Ui+Vj+Wk,$$

where U, V, and W are velocity components and i, j, and k are unit vectors in the x, y, and z directions, respectively. The instantaneous velocity components can be represented by their mean values and superimposed fluctuations as

$$U=\overline{U}+u,\ V=\overline{V}+v,\ \text{and}\ W=\overline{W}+w,$$

where U, V, and W are the mean values (bar over symbols denotes mean, or average) and u, v, and w are the random fluctuations in the x, y, and z directions, respectively.

In general, an averaging procedure can be carried out only if certain conditions are satisfied. Consider the average value of velocity in the x direction at a point of the flow field with respect to time. The average value is then defined by

$$\overline{U}=\lim_{T\to\infty}\frac{1}{2T}\int_{-T}^{+T}U\,dt. \qquad (1)$$

The period of time during which measurements are taken, T, cannot be infinitely long; it must be a finite time interval. The interval must be large compared with the time scale of the turbulence. On the other hand, it must be small compared with the period of any slow variations in the field of flow that would not be regarded as belonging to the turbulence. Obtaining a suitable average in open-channel flow is seldom any problem.

Other assumptions, such as homogeneity and isotropy, can be made about turbulent flow. These simplifying assumptions make the rather complex problem amenable to theoretical analysis.

The term "homogeneous turbulence" means that the velocity fluctuations in the system are random and that the average turbulence characteristics are independent of position in the flow field—that is, invariant to translation of the axis of reference.

The characteristic features of channel flow are to some extent a result of homogeneity of the turbulent motion in the direction of mean flow. In channel flows the motion is statistically similar in planes parallel to the boundary, and this considerable degree of homogeneity permits productive theoretical treatment of the problem without much necessity for arbitrary assumptions.

The term "isotropic turbulence" refers to a homogeneous system in which the velocity fluctuations are not only random but also independent of the axis of reference—that is, invariant to axis rotation and reflection. To illustrate the difference between homogeneous and isotropic turbulence,

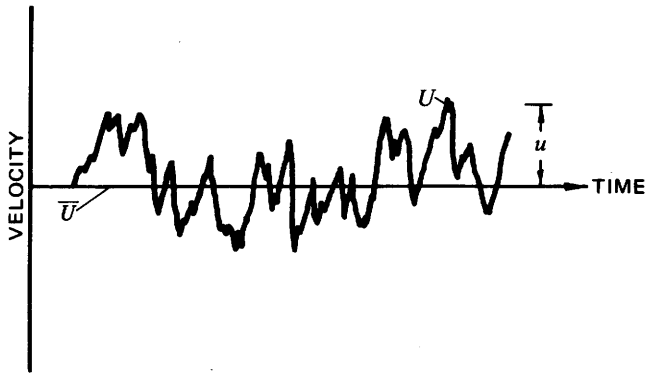

FIGURE 1.—Turbulent motion as a function of time. Only the component of motion in the x direction is shown. U, instantaneous velocity; $\overline{U}$, mean velocity; u, velocity fluctuation.

consider the root mean squares of the velocity fluctuations:

$$u=\sqrt{\overline{u^2}},\ v=\sqrt{\overline{v^2}},\ \text{and}\ w=\sqrt{\overline{w^2}},$$

where u, v, and w are used to simplify the notation in equations. (The root-mean-square notation is retained in this report to denote actual measurements.) In homogeneous turbulence, the root-mean-square values could all be different, as in open-channel flows, but each value must be constant over the entire turbulence field. In isotropic turbulence, the spherical symmetry requires that the fluctuations be independent of direction, or that the root-mean-square values all be equal, which is not true of open-channel flows. Isotropic flow has no cross velocity terms ($\overline{uv}$, $\overline{uw}$, $\overline{vu}$, $\overline{vw}$, $\overline{wu}$, $\overline{wv}$) because the random motion means that $\overline{uv}$, for example, would have just as many positive as negative values. Consequently, the average $\overline{uv}$ would be zero. Isotropic flow, therefore, has no shearing stresses and no gradients of mean velocity. Such a state of motion cannot exist in laboratory experiments or in nature.

Turbulent shear flows may be divided into flows that are nearly homogeneous in the direction of the flow and those that are not homogeneous in the direction of flow. Experiments have indicated that nearly homogeneous flows are restricted, as are steady and (or) uniform open-channel flows. Inhomogeneous shear flows are unrestricted, as are unsteady and (or) nonuniform open-channel flows.

STATISTICAL RELATIONS

INTENSITY OF TURBULENCE

One of the best visualizations of turbulence is obtained by measuring the velocity fluctuations at various points in the flow.

The intensity of turbulence is defined as the standard deviation, or root mean square, of the fluctuating velocity:

$$u=\sqrt{\overline{u^2}},\ v=\sqrt{\overline{v^2}},\ w=\sqrt{\overline{w^2}}.$$

The relative turbulence intensity is usually expressed as a ratio of the root mean square to the mean flow velocity, $\overline{U}$, or to the shear velocity, U_*. For example, relative turbulence intensity in the x direction is

$$\sqrt{\overline{u^2}}/\overline{U} \text{ or } \sqrt{\overline{u^2}}/U_*,$$

where $U_*=\sqrt{gRS}$, in which g is the gravitational acceleration, R is the hydraulic radius, and S is the slope of the energy gradient.

CORRELATION FUNCTIONS

Correlation functions often play a major role in making and analyzing primary experimental measurements. Taylor (1935) was the first to suggest that a statistical correlation can be applied to fluctuating-velocity terms in turbulence. He pointed out that no matter what the diameter of an eddy is, a high degree of correlation will exist between the velocities at two points in space if the separation between the points is small compared with the eddy diameter. Conversely, if the separation between the points is many times the eddy diameter, then little correlation can be expected. This concept is very important in considering the various scales of motion in turbulent flows and in examining the role of scale in open-channel flow processes.

Consider the velocity fluctuation at two points separated by a distance r. A correlation may exist between the velocities and can be defined as a function of r:

$$Q(r)=\overline{u(x)\ u(x+r)}. \tag{2}$$

The bar denotes an averaging of measurements taken for many points at one given time. Physically, taking so many measurements at one time is nearly impossible, so the fluctuations at two given points are measured at different times as the fluid moves past the measuring instruments. The basis of statistical turbulence characteristics is the assumption that statistical averages can be used to describe the system. Three components of u exist at x [$u(x)$, $v(x)$, $w(x)$], and three components of u exist at $x+r$ [$u(x+r)$, $v(x+r)$, $w(x+r)$]. One-to-one correlation yields nine possible combinations of components. $Q(r)$ will have nine terms and can be expressed as a second-order tensor in Cartesian coordinates:

$$\mathbf{Q}_{ij}(r)=\overline{u_i(x)\ u_j(x+r)}, \tag{3}$$

where i and j are indices, and each gives u three values. For example, $u_i(x)$ expands to: $u_1(x)=u(x)$; $u_2(x)=v(x)$; and $u_3(x)=w(x)$.

Correlation measurements in the Eulerian frame of reference system are the most convenient to obtain with present-day equipment. The Eulerian space correlation function for the velocity fluctuation in homogeneous flow is

$$\mathbf{R}_{ij}(r)=\frac{\overline{u_i(x)\ u_j(x+r)}}{\sqrt{\overline{u_i^2(x)}}\cdot\sqrt{\overline{u_j^2(x+r)}}}, \tag{4}$$

where u_i, for example, represents the three root-mean-square values of u, v, and w which can exist at two points, x and $x+r$. (See fig. 2.)

By the ergodic hypothesis, when the flow is statistically homogeneous in one or more directions, mean turbulence values along lines in these directions are identical with the time means.

Because the root-mean-square values are independent of separation, equation 4 becomes

$$\mathbf{R}_{ij}(r)=\frac{\overline{u_i(x)\ u_j(x+r)}}{\sqrt{\overline{u_i^2}}\cdot\sqrt{\overline{u_j^2}}}. \tag{5}$$

This measurement is difficult to make in the direction of the flow because of probe and sensor interference. For isotropic homogeneous turbulence, the root mean squares are all identical, and equation 5 becomes

$$\mathbf{R}_{ii}(r)=\frac{\overline{u_i(x)\ u_i(x+r)}}{\sqrt{\overline{u_i^2}}\cdot\sqrt{\overline{u_i^2}}}. \tag{6}$$

Using the covariance between velocity components at two separated points in the flow to describe a turbulent flow has become standard practice, although the covariance is recognized to be an essentially incomplete one and does not include time.

Because shear flows are not isotropic, the turbulent shear stresses are not zero, and a correlation exists between the various cross velocity terms when the separation distance, r, is zero or finite. For zero separation, equation 4 reduces to a Eulerian point correlation function, which is

$$\mathbf{R}_{ij}=\frac{\overline{u_i\ u_j}}{\sqrt{\overline{u_i^2}}\cdot\sqrt{\overline{u_j^2}}}. \tag{7}$$

Even though the function is still dependent on x,

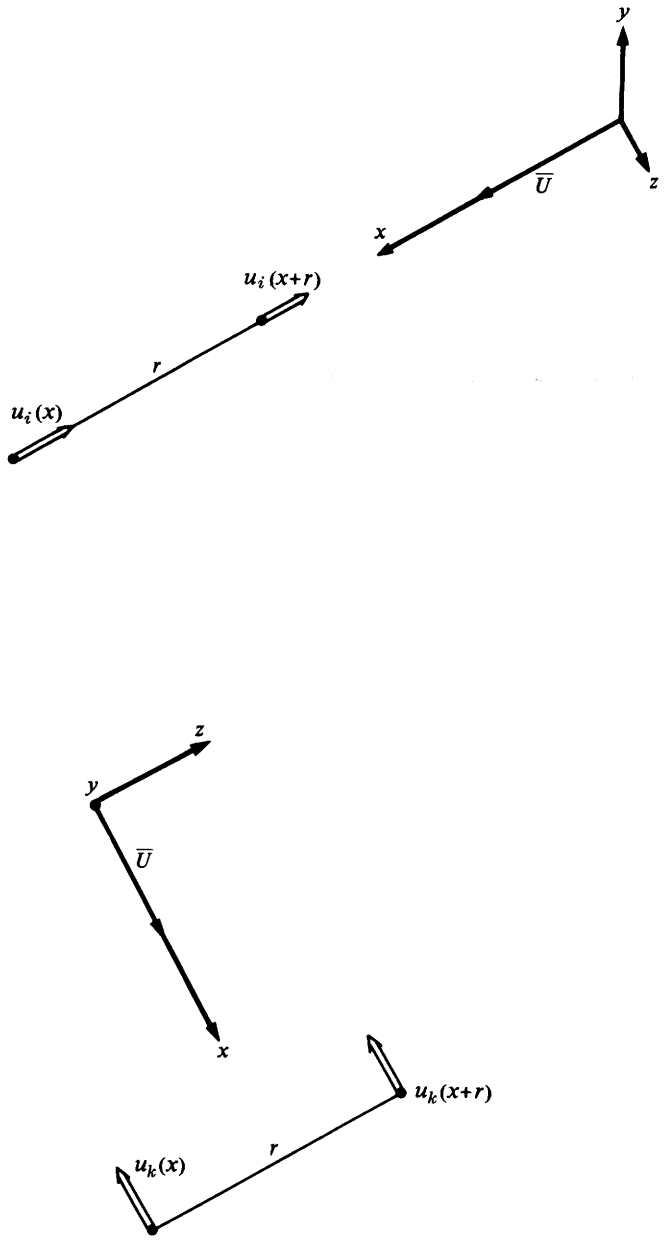

FIGURE 2.—Probe arrangement for double velocity correlations. Dots at the bases of the open arrows represent four probe locations—two for each pair of covarying velocities.

the x is usually dropped from the notation because all terms are understood to apply to a single point for a given computation of $\mathbf{R}_{ij}$. The value of $\mathbf{R}_{ij}$, however, will vary from point to point in the flow. This variation determines the Reynolds stresses, or turbulence shear stresses.

Measurements needed for the Eulerian space correlation are not always possible or convenient to make because of probe interference or limited equipment; however, by assuming that $x=\overline{U}t$ is applicable and by replacing the space coordinate, x, with an equivalent time coordinate, t, the Eulerian space correlation function can be equated with a Eulerian time correlation function (a process called autocorrelation) to give

$$R(\tau)=\frac{\overline{u_r(t)\ u_r(t+\tau)}}{\sqrt{\overline{u^2}}\cdot\sqrt{\overline{u^2}}}, \tag{8}$$

where τ is an increment of time. This correlation function can be obtained from the output signal of a single sensor and is much easier to obtain than the space correlation function. The time correlation part, the numerator, of equation 8 is an average of the velocities taken at two times for one point. Although the autocorrelation technique can be very convenient, it is limited to uniform flow, where $\sqrt{\overline{u^2}}$ is much less than $\overline{U}$, and thus may not be valid in certain shear flows. Hinze (1959, p. 40) further discussed this point.

Another informative correlation function is the Eulerian space-time correlation. This function correlates velocity fluctuations both with respect to separation distance, r, and with respect to time separation, τ. The result is a mixed Eulerian correlation function:

$$\mathbf{R}_{ij}(r,\tau)=\frac{\overline{u_i(x,t)\ u_j(x+r,\ t+\tau)}}{\sqrt{\overline{u_i^2(x,t)}}\cdot\sqrt{\overline{u_j^2(x+r,\ t+\tau)}}}. \tag{9}$$

By calculating this function for many values of r, the function can be mapped into an $r\tau$ plane, which may be more descriptive of the flow structure.

In the previous discussion, the Eulerian coordinate system has been utilized; in this system, the space correlation function, $\mathbf{R}_{ij}(r)$, correlates the velocity fluctuations at one time for two points, and the time correlation function, $R(\tau)$, correlates the velocity fluctuations at two times for one point. In turbulence diffusion and dispersion applications, the Lagrangian coordinate system is more convenient; in this system, the time correlation function, $\mathbf{R}_{L_{ij}}(\tau)$, correlates the velocity fluctuations of one fluid particle at two times and at two corresponding points along the particle path. Thus,

$$\mathbf{R}_{L_{ij}}(\tau)=\frac{\overline{u_i(t)\ u_j(t+\tau)}}{\sqrt{\overline{u_i^2(t)}}\cdot\sqrt{\overline{u_j^2(t+\tau)}}}. \tag{10}$$

Although this system of coordinates is often much easier to use, measurement of $\mathbf{R}_{L_{ij}}(\tau)$ is complicated. At best, $\mathbf{R}_{L_{ij}}(\tau)$ has only been estimated from turbulent diffusion measurements in turbulent shear flows and from measurements of decaying isotropic turbulence in the wake of a grid in a wind tunnel. In isotropic turbulence, the form becomes less complex:

$$R_L(\tau)=\frac{\overline{u(t)\,u(t+\tau)}}{\sqrt{\overline{u^2}}\cdot\sqrt{\overline{u^2}}}. \quad (11)$$

Note that $\sqrt{\overline{u^2}}$ in the Lagrangian system is the root mean square of the velocity fluctuations averaged for many fluid particles at different times and points along their respective paths and not averaged for many times at one point in space, as for the Eulerian system. The Eulerian and Lagrangian time correlations do not yield the same values; however, additional information may prove that they are related. The Eulerian system is used when measuring velocity by fixed probes, but the Lagrangian system is more convenient when measuring turbulent diffusion and dispersion, because these mixing processes are measured by the spread of contaminating particles to different points in the flow.

ENERGY-SPECTRUM FUNCTIONS

The energy spectrum provides information on how turbulent energy is distributed with respect to frequency or wave number. The concept of energy spectra is important in comparing and understanding turbulent shear flows, and yet little information and data are available for flow in open channels.

An analysis of energy spectra involves taking the Fourier transformation of the various correlations already considered. The Fourier transformation is simply the means by which the complex random wave form of the turbulent motion can be broken into a sum of sine waves of various amplitudes and frequencies. The sum of the sine waves must equal the original wave form. The transformed correlations form an energy spectrum, which is reported as a plot of the amplitudes of the various sine waves against the respective frequencies of the waves. The spectrum can provide insight into the distribution of the kinetic energy of turbulence for various frequencies of the velocity fluctuations.

Taylor (1938) considered only the one-dimensional spectrum. However, his theory indicates that the theory of Fourier transformation can be applied to a statistically steady field to derive the Fourier transform of the velocity-correlation tensor. Thus, using tensor notation, the three-dimensional spectrum is

$$\Phi_{ij}(\boldsymbol{k}_*)=\frac{1}{(2\pi)^3}\int_{-\infty}^{+\infty}\mathbf{Q}_{ij}(r)\,e^{-\bar{i}\boldsymbol{k}_*\cdot r}dr, \quad (12)$$

where $\bar{i}$ in the exponent is $\sqrt{-1}$ and $\boldsymbol{k}_*$ is the wave-number vector. The components of this vector are related to the frequency, f, by

$$k_{*_i}=2\pi f_i/\overline{U}_i. \quad (13)$$

The spectrum tensor is the transformation of the general correlation tensor from Eulerian space to wave-number space; this tensor describes how the energy, which is associated with each velocity component, is distributed over various wave numbers or frequencies. In essence, a Fourier analysis of the complex turbulence fluctuations gives a spectrum of the turbulence energy associated with a given wave number or frequency. In effect, a complex wave (in real space) has been broken down into a number of sine waves (in frequency space).

The reverse transformation, from the spectrum tensor to the general correlation tensor, gives:

$$\mathbf{Q}_{ij}(r)=\int_{-\infty}^{+\infty}\Phi_{ij}(\boldsymbol{k}_*)e^{\bar{i}\boldsymbol{k}_*\cdot r}d\boldsymbol{k}_*. \quad (14)$$

if $r=0$, then this reduces to

$$\mathbf{Q}_{ij}(0)=\int_{-\infty}^{+\infty}\Phi_{ij}(\boldsymbol{k}_*)\,d\boldsymbol{k}_*, \quad (15)$$

where $\mathbf{Q}_{ij}(0)$ is the general correlation tensor. The energy-spectrum tensor, $\Phi_{ij}(\boldsymbol{k}_*)$, shows the density of energy in wave-number space.

Owing to experimental convenience and certain limitations, measurements for the spectrum function have been limited to the one-dimensional spectrum function in the direction of the mean velocity, which is readily measured from the output signal of a single sensor. The one-dimensional energy spectrum, $\Phi(\boldsymbol{k}_*)$, of the root mean square of the velocity fluctuation in the x direction, $\sqrt{\overline{u^2}}$, as registered from a hot-film anemometer can be expressed by

$$\int_{-\infty}^{+\infty}\Phi(\boldsymbol{k}_*)d\boldsymbol{k}_*=\overline{u^2}. \quad (16)$$

In turbulent shear flows, the relation between the one-dimensional spectrum function, $\Phi(\boldsymbol{k}_*)$, and the three-dimensional spectrum function, $\Phi_{ij}(\boldsymbol{k}_*)$, is not known. However, the one-dimensional function is often assumed to be an integral effect of the three-dimensional function. In spite of experimental difficulties, the study of energy spectra has led to several interesting conclusions.

A normalized spectrum function, $F(f)$, is expressed in terms of frequency, f, by

$$\int_{-\infty}^{+\infty} F(f)df=1. \quad (17)$$

SCALES

The scales of turbulence are important in evaluating the structure of various shear flows. Furthermore, they play a major role in understanding and evaluating turbulence diffusion processes and the dissipation and diffusion of energy in open-channel flows.

The macroscale, which is sometimes considered the average size of the eddies, is descriptive of the large eddy structure and has several possible definitions depending upon the choice of the correlation function. First consider the Eulerian system of coordinates. A Eulerian length scale, sometimes called the macroscale of turbulence, can be defined as the area under the space correlation curve:

$$L=\int_0^{\infty} \mathbf{R}_{ij}(r)\, dr. \quad (18)$$

The Eulerian integral time scale of turbulence is defined as the area under the time correlation curve, which was derived by autocorrelation:

$$T_e=\int_0^{\infty} R(\tau)\, d\tau. \quad (19)$$

By applying Taylor's hypothesis (1935), a longitudinal Eulerian length scale can be obtained:

$$L=\overline{U}T_e. \quad (20)$$

This relation has meaning only as long as the flow remains steady. Another Eulerian time scale can be defined as the area under the space-time correlation curve:

$$T'=\int_0^{\infty} R(r,\tau)\, d\tau. \quad (21)$$

The microscale is used to describe the small eddy structure. A microscale relation for the x direction, λ_x, can be developed using the cosine transformation of the Eulerian autocorrelation function and is given by

$$\frac{1}{\lambda_x^2}=\frac{4\pi^2}{(\overline{U})^2}\int_0^{\infty} f^2 F(f)\, df. \quad (22)$$

This length scale gives a measure of the smallest eddies responsible for the dissipation of energy. The microscale relation can be developed using another statistical method. Assuming a normal and independent distribution of the velocity fluctuations, the microscale can be calculated from

$$\frac{1}{\lambda_x}=\frac{\pi}{\overline{U}}\times \text{Average number of zero crossings of } u \text{ per second.} \quad (23)$$

In the Lagrangian coordinate system the path of a particle is followed, and the correlation is given by equation 10. Several macroscales can be defined in the Lagrangian system. The Lagrangian integral time scale is the area under the time correlation curve:

$$T_L=\int_0^{\infty} \mathbf{R}_{Lij}(\tau)\, d\tau. \quad (24)$$

This scale is usually estimated from the results of turbulence diffusion experiments. Several other Lagrangian length scales can be defined; the transverse Lagrangian scale is defined as

$$L_L=\sqrt{\overline{v^2}}\, T_L. \quad (25)$$

The Lagrangian length scale is defined as

$$\Lambda_L=\overline{U}\, T_L. \quad (26)$$

EQUATIONS OF MOTION

Fluctuations which occur in turbulent flow necessitate added terms in the basic equations of laminar motion. If an exact representation of these fluctuations were known, a general solution could be obtained to account for turbulence. The additional terms were first investigated by Reynolds (1895). He assumed that the velocities in the laminar-flow equations could be replaced be the instantaneous velocities for turbulent motion and that the equations would still be completely valid. He combined the Navier-Stokes equations for laminar motion with the concept of an average velocity and a superimposed fluctuating component; he then averaged the resulting equation and used certain rules of approximation, which he formulated, to allow calculation of mean values. These rules are not rigorous, but they provide good approximations when the fluctuations are sufficiently numerous and are distributed at random.

Reynolds (1895) found, for incompressible flow, that the equation of continuity for turbulent flow was identical with that for laminar flow but that the instantaneous velocity at a point was now replaced by the average velocity at that point.

The two equations are

Laminar flow:

$$\frac{\partial U}{\partial x}+\frac{\partial V}{\partial y}+\frac{\partial W}{\partial z}=0 \text{ or } \frac{\partial U_i}{\partial x_i}=0 \text{ and}$$

Turbulent flow:

$$\frac{\partial \overline{U}}{\partial x}+\frac{\partial \overline{V}}{\partial y}+\frac{\partial \overline{W}}{\partial z}=0 \text{ or } \frac{\partial \overline{U}_i}{\partial x_i}=0. \quad (27)$$

The simplified equations on the right are in general Cartesian notation, in which the i is a repeated index and indicates summation of the three component values.

For the Navier-Stokes equations, Reynolds found that average properties again appeared in place of instantaneous properties and that a term associated with the fluctuations was added. The two equations in general Cartesian notation are

Navier-Stokes equation for laminar flow:

$$\rho\left(\frac{\partial \overline{U}_i}{\partial t}+\overline{U}_j\frac{\partial \overline{U}_i}{\partial x_j}\right)=-\frac{\partial \overline{P}}{\partial x_i}+\overline{F}_i+\mu\frac{\partial^2 \overline{U}_i}{\partial x_j \partial x_j} \text{ and} \quad (28)$$

Reynolds equation for turbulent flow:

$$\rho\left(\frac{\partial \overline{U}_i}{\partial t}+\overline{U}_j\frac{\partial \overline{U}_i}{\partial x_j}\right)=-\frac{\partial \overline{P}}{\partial x_i}+\overline{F}_i+\mu\frac{\partial^2 \overline{U}_i}{\partial x_j \partial x_j}-\frac{\partial \rho\overline{u_i u_j}}{\partial x_j}. \quad (29)$$

For a given i, the repeated index in any one term is j and indicates summation of the three component values. Each equation, because of the Cartesian notation, actually represents three equations. For example, the Reynolds equation of motion for the x direction is given by equation 29 when $i=1$:

$$\rho\left(\frac{\partial \overline{U}}{\partial t}+\overline{U}\frac{\partial \overline{U}}{\partial x}+\overline{V}\frac{\partial \overline{U}}{\partial y}+\overline{W}\frac{\partial \overline{U}}{\partial z}\right)=-\frac{\partial \overline{P}}{\partial x}+\mu\left(\frac{\partial^2 \overline{U}}{\partial x^2}+\frac{\partial^2 \overline{U}}{\partial y^2}+\frac{\partial^2 \overline{U}}{\partial z^2}\right)+\overline{F}_x-\left(\frac{\partial \rho\overline{u^2}}{\partial x}+\frac{\partial \rho\overline{uv}}{\partial y}+\frac{\partial \rho\overline{uw}}{\partial z}\right). \quad (30)$$

The additional term has nine components, three of which are shown in the x equation (eq 30). The terms given by $\rho\overline{u_i u_j}$ in equation 29 are called the Reynolds stresses, or turbulent stresses. The tensor in Cartesian coordinates is

$$\rho\begin{pmatrix}\overline{u^2} & \overline{uv} & \overline{uw}\\ \overline{vu} & \overline{v^2} & \overline{vw}\\ \overline{wu} & \overline{wv} & \overline{w^2}\end{pmatrix}. \quad (31)$$

The tensor is symmetrical, since $\overline{uv}=\overline{vu}$, $\overline{uw}=\overline{wu}$, and $\overline{vw}=\overline{wv}$. Thus, there are only six independent terms.

The Reynolds equations for incompressible turbulent motion cannot be solved, because there are ten unknowns and only four equations available—three motion equations and one continuity equation. The unknowns are the mean pressure, the three mean-velocity components, and the six Reynolds stresses.

Although obtaining complete solutions to any problem in open-channel flow from the Reynolds equations of motion appears prohibitively difficult, the equations do indicate which mean flow parameters and turbulence characteristics are convenient to measure and of reasonable physical significance.

The special case of fully developed turbulent open-channel flow, where the viscous and dynamic processes have reached a statistically stable state imposed by the rigid boundaries, leads to several simplifying conditions. Thus, for a two-dimensional flow having the appropriate boundary conditions, the Reynolds equations after one integration become

$$\left.\begin{aligned} &x \text{ direction:} && \gamma DS(1-y/D)=\mu\frac{d\overline{U}}{dy}-\rho\overline{uv},\\ &y \text{ direction:} && \overline{P}=(D-y)\gamma\cos\alpha-\rho\overline{v^2}, \text{ and}\\ &z \text{ direction:} && \rho\frac{\partial \overline{vw}}{\partial y}=0, \end{aligned}\right\} \quad (32)$$

where D is the depth of flow, S is the slope of the energy gradient, γ is the specific weight of the fluid, and α is the angle the boundary makes with respect to the horizontal. These equations are simpler but are still insufficient to give a general solution. However, the measured terms can now be compared with the balance of terms predicted by the Reynolds equations.

ENERGY EQUATION

The production, dissipation, and diffusion of turbulent energy are particularly important in understanding the mechanism of turbulent motion.

The Reynolds equation of motion can be converted to an expression for the kinetic energy of the velocity fluctuations. The equation of motion for each coordinate direction is multiplied by the velocity in that direction, and the velocity and pressure fluctuations are introduced as

$$U=\overline{U}+u \text{ and } P=\overline{P}+p.$$

The three component equations are then summed and averaged according to the Reynolds rules of averaging. Then the kinetic energy of the mean motion is subtracted. This procedure yields the following energy equation for homogeneous flow:

$$\underset{(1)}{\frac{1}{2}\frac{\partial\overline{u_i^2}}{\partial t}}+\underset{(2)}{\overline{u_iu_j}\frac{\partial\overline{U}_i}{\partial x_j}}+\underset{(3)}{\frac{\partial}{\partial x_j}\left[\overline{\left(\frac{P}{\rho}+\frac{u_i^2}{2}\right)u_j}\right]}+\underset{(4)}{\frac{\partial}{\partial x_j}\left(\overline{\frac{u_i^2}{2}}\,\overline{U}_j\right)}$$
$$\underset{(5)}{-\nu\frac{\partial^2}{\partial x_j\partial x_j}\overline{\frac{u_i^2}{2}}}\underset{(6)}{+\nu\overline{\left(\frac{\partial u_i}{\partial x_j}\right)^2}}=0, \quad (33)$$

where ν is the kinematic viscosity of the fluid. Each term in equation 33 represents a rate of change of turbulent energy per unit mass—specifically: (1) time rate of change of the turbulent kinetic energy, (2) production of turbulent kinetic energy by shearing stress (that is, energy transfer from the mean motion), (3) diffusion of energy by kinetic and pressure effects, (4) transfer of energy by convection, (5) the work done by viscous shear stresses in the turbulent motion, (6) dissipation of turbulent kinetic energy.

One of the main reasons for obtaining such an energy relation is that insufficient turbulence information is available from the time-average momentum equation (eq 29). Averages over periods of time eliminate a great deal of information concerning the contributions of turbulence to the characteristics of the flow field. To completely describe the turbulent flow field, not only the time averages of the turbulence quantities appearing in the momentum and energy equations need to be known, but also all higher order terms that might be obtained by taking higher moments of the momentum equation. At the present time, obtaining all these terms is neither practical nor, for that matter, possible; thus, experimental work has been directed mainly toward obtaining the relative magnitude of the quantities in the energy equation.

The energy equation for two-dimensional flow, considering relevant orders of magnitude, may be written as

$$\underset{(1)}{\rho\overline{uv}\frac{d\overline{U}}{dy}}=\underset{(2)}{\frac{d}{dy}\left[\overline{\rho v(u^2+v^2+w^2)+vp}\right]}+\underset{(3)}{\mu\overline{\left(\frac{\partial u_i}{\partial x_j}\frac{\partial u_i}{\partial x_j}\right)}}. \quad (34)$$

This equation expresses the fact that energy produced by the turbulent shear forces at a point in the flow field is partly diffused and partly dissipated. Although measurements are not sufficient to study the complete turbulence energy balance in an open channel, the production term can be measured, and the dissipation term can be estimated. Term 1 is the energy produced by the turbulence shearing stresses; it can be obtained directly from measurements of $\overline{uv}$ and from the mean-velocity profile. Term 2 is the energy diffused by the turbulence. Term 3 is the energy dissipated because of the breakdown of large eddies into small ones.

The dissipation and diffusion terms need to be expressed in easily measurable quantities. For isotropic turbulence, Taylor (1935) evaluated the dissipation term, abbreviated as ϵ, using the microscale of turbulence in the x direction, λ_x, and obtained

$$\epsilon=15\mu\frac{\overline{u^2}}{\lambda_x^2}. \quad (35)$$

When the distributions of the energy production and dissipation are known, the diffusion of energy can be estimated from equation 34. Note that because of the approximations involved in the calculations of dissipation, the conclusions derived are chiefly qualitative. In effect, the energy equation has not been completely defined by measurable quantities, but it has been used with some measured quantities to obtain a clearer understanding of turbulent shear flows.

INSTRUMENTATION

Hot-wire anemometry has been used for many years as a standard technique for turbulence measurements in air. Recently, the application of anemometry has expanded greatly owing to better equipment and to more interest in details of fluid flow in liquids, such as water. Until recently, however, serious difficulties attended any attempt to adapt the anemometer to use in water. Some of these difficulties, such as contamination of the sensor by dirt or deposits, occur also in air; whereas others, such as boiling and electrolysis, occur in liquids only.

Electrolysis is by far the main source of trouble, causing corrosion of the sensor, generation of gases, and instability in the electronic control circuitry. It can be avoided by using nonconducting liquids. However, this does not solve the basic problem, and much work has therefore been done to eliminate or reduce the effect of electrolysis in conducting liquids. The most successful effective method is to coat the sensing element to provide

electrical insulation between the electrical system and the liquid, but the coating must be very thin in order not to affect the frequency response. This method permits stable operation of the anemometer in conducting liquids, such as water; moreover, contamination of the sensing element by fluid-borne particles appears to be greatly reduced as a result of this measure. The anemometer thus gives reproducible results and can be used for quantitative measurements in open-channel flows.

Increased use of film sensors and compensating circuitry, supplemented by sensitive accessory equipment and digital computers, has made anemometry more practical. The fine spatial resolution (due to the small size of the sensor) and the good frequency response of the hot-film anemometer system are unmatched by any other system now available for making turbulence measurements in open-channel flows.

ELECTRONIC CIRCUITRY

A very important part of high-frequency anemometry is the electronic circuitry. It supplies a controlled amount of electrical current to heat the sensor and to provide frequency compensation for the sensor.

The anemometer circuit used for operating sensors in water should have the following characteristics for best all-around application to turbulence measurements in open-channel flows:

1. *Low noise level.*—Because the overheat ratio of the sensor (ratio of hot to cold resistance) is low (1.1) and the turbulence level of the water is often low (less than 10 percent), the lowest possible internal electronic noise level is desirable.
2. *Adequate frequence response.*—Direct current to 2 kHz (kilohertz) is sufficient for most measurements in water (10 kHz represents a reasonable upper limit in air). Adequate high-frequency response is obtainable with most anemometers. However, low-frequency response (0–2 hertz) can vary. The coating of the sensing element must be very thin in order not to affect the low-frequency response.
3. *Adequate temperature compensation.*—Provision should be made for taking temperature changes into account to get accurate results.
4. *High power output.*—Water has high heat-transfer characteristics, and enough power to operate the largest sensor at the highest anticipated velocity is needed.
5. *Minimal long-term drift.*—Because the overheat ratio is low, electronic drift in the electronic components shows up more in water than in air. This drift must be kept at an insignificant amount.

The two basic types of anemometer circuitry are used with hot-wire and hot-film sensors: constant current and constant temperature. Experimenters need to know and understand the advantages and disadvantages of the operating characteristics of both anemometer systems.

CONSTANT-CURRENT ANEMOMETER

The constant-current anemometer maintains the current of the sensor at an essentially constant level by using a large resistor in series with the sensor. The current is selected so that the sensor is operated at the desired temperature in the fluid. If the velocity of the fluid increases, the heat transfer from the sensor to the fluid increases, and the sensor will cool; this results in a decrease in sensor resistance. If a constant current is maintained in the sensor, the decrease in resistance will cause a decrease in voltage at the terminal between the sensor and the resistor. An amplifier is used to detect this change in voltage and to amplify the voltage to a useful signal level for recording or monitoring. If the velocity change takes place very rapidly, the response of the sensor will lag the actual change in velocity, owing to the thermal inertia of the sensor. To compensate for this lag, the amplifier is given a nonlinear characteristic with frequency. By carefully matching the frequency characteristics of the amplifier to those of the sensor, a flat frequency response is possible up to 100 kHz.

The major drawback of the constant-current system is that the temperature frequency response of the sensor depends not only on sensor characteristics but also on flow characteristics. The response depends on both the thermal capacity of the sensor and the heat-transfer coefficient between the sensor and its environment. Because the sensor response changes with changes in flow, the frequency compensation of the amplifier must be readjusted whenever the mean flow changes. This is not practical for fast changes. Therefore, the constant-current anemometer is most applicable where the fluctuations in velocity are small compared with the mean velocity.

CONSTANT-TEMPERATURE ANEMOMETER

The constant-temperature anemometer maintains the resistance, and thus the temperature, of the sensor at an essentially constant level by using a feedback loop (Thermo Systems Inc., 1968). As

the fluid velocity increases, the sensor will tend to cool, and its resistance will tend to decrease. This decrease in resistance, as measured by a Wheatstone bridge, will cause the voltage across the bridge to decrease, so the input to the amplifier will decrease. The phase of the amplifier is such that this decrease in voltage will cause an increase in the voltage output of the amplifier that will increase the current through the sensor and balance the bridge. If the amplifier has a sufficient gain, it will keep its inputs very close to the balanced conditions. Therefore, any change in the sensor resistance will be immediately corrected by an increase or decrease in the current through the sensor. By keeping the sensor temperature constant, this anemometer system overcomes the main disadvantage of the constant-current system.

The output of the constant-temperature system is the voltage output of the amplifier, which in turn is the voltage required to drive the necessary current through the sensor. Using the feedback control, the resistance in the bridge is constant, the voltage across the bridge is directly proportional to the current through the sensor, and the power is equal to the current squared times the resistance. Therefore, the square of the voltage measured across the bridge is directly proportional to the instantaneous heat transfer between the sensor and its environment. No matching of frequency characteristics for the amplifier and the sensor is required, because the feedback circuit makes the match automatically.

Present-day constant-temperature systems are comparable to the constant-current systems in both noise level and frequency response. However, the constant-temperature systems are superior in convenience of operation and in flexibility. Several other basic advantages of constant-temperature anemometry over constant-current anemometry include the following:

1. Constant-temperature systems are more compatible with hot-film sensors because the frequency response of hot-film sensors is so complex.
2. Operation of a sensor at constant temperature prevents sensor burnout when the velocity past the sensor suddenly decreases.
3. Constant-temperature operation is more practical for measurements in water where large changes in sensor temperature occur in response to velocity changes.
4. Constant-temperature systems can be temperature compensated.
5. Constant-temperature systems give a direct direct-current output. In a constant-current system, the measurement of mean voltage levels is typically made by manually balancing a built-in bridge, and the minimum frequency limit of the amplifier system generally is about 2 Hz (hertz).
6. Constant-temperature systems can measure large velocity fluctuations, whereas constant-current systems cannot under most circumstances.

For these reasons, constant-temperature systems have essentially replaced constant-current systems for use in making turbulence measurements.

When choosing among the various constant-temperature systems, the experimenter should compare three basic variables: high- and low-frequency response, background noise, and power output.

No basic problems are associated with the electronic circuitry of present-day constant-temperature anemometers. Rather, the primary problem is in selecting a hot-film sensor and in understanding its operation and limitations for specific fluid-mechanics measurements.

HOT-FILM SENSORS

The basic concept of hot-film sensors was introduced over ten years ago by Ling and Hubbard (1956), and this type of sensor has been replacing the hot-wire sensor for many applications in recent years.

The hot-film sensor is essentially a conducting metallic film on a ceramic substrate. (See figs. 3–6.) Plating, commonly gold, delineates the sensitive area and provides electrical leads to the circuitry through the probe, to which the sensor is attached. The metallic film in a typical hot-film sensor is less than 1 micron thick; therefore, the physical strength and the effective thermal conductivity of the sensor are determined almost entirely by the substrate material, which is commonly quartz. Most films are platinum, because platinum resists oxidation and thus has long-term stability.

Hot-film sensors for water are coated with quartz about 1 micron thick; for further protection, the tip of the probe, except for the film itself, is coated with a temperature- and corrosion-resistant varnish. This treatment ensures good insulation that is able to prevent electrolysis with little sacrifice to frequency response.

Four problems pertaining to the operation of hot-film anemometers in open-channel flows are directly related to the sensor and to the measure-

ment of the basic data: (1) drift caused by fluid-borne contaminants, (2) calibration for the voltage-velocity relation, (3) sensitivity to velocity fluctuations, and (4) noise caused by mechanical vibrations or introduced through ground loops.

Drift is a change of the output voltage of an anemometer when there has been no change in either the velocity, temperature, or properties of the fluid. Accumulation of dirt, scale, or lint—in fact, any organic or inorganic material—on the sensor surface will reduce the heat transfer to the water and cause a change in voltage. This one problem has discouraged many researchers from using hot-film anemometry. However, in open-channel flows, the problem is always present, and techniques must be developed to minimize it.

Noise caused by mechanical vibration is always a problem in taking measurements in open-channel flows. Caution should be taken to insure that mechanical vibrations are insignificant. Noise introduced through ground loops is always possible when additional signal-conditioning equipment is being used. Disconnecting the power-source ground for all the signal-conditioning equipment (but not the anemometer) permits the equipment to be connected to the anemometer-chassis ground through the cable shield, thereby reducing ground-loop noise.

Calibration for the voltage-velocity relation is essential for operating hot-film sensors in open-channel flows. In fact, when drift due to contamination is possible, a calibration at each point in the flow is advised. Contamination problems preclude the use of general heat-transfer relations and a one-time calibration procedure for reducing turbulence data.

Sensitivity of the hot-film sensor to changes in velocity is particularly problematic in obtaining meaningful turbulence measurements. Because the sensitivity is a derivative of the voltage-velocity calibration, the calibration at each point must be made much more precisely than if accuracy of only a few percent for velocities were needed. This is particularly true when the voltage-velocity calibration can change because of contaminant accumulation.

Many problems associated with operating hot-film sensors in water can be eliminated or reduced by understanding each sensor and by choosing the right sensor for a particular measurement in a particular environment.

SHAPES

The cylindrical hot-film sensor is shown in figure 3. It is well suited for detailed studies, particularly in water, if it is subject to velocities less than about 8 fps (feet per second) and if the fluid has been filtered of all fluid-borne contaminants. Where contaminants are present in the water, the cylindrical hot-film sensor is virtually impossible to operate with any degree of reliability; and at velocities greater than 8 fps, flow separation can occur. Cylindrical hot films generally require higher power output and give better sensitivity than solid sensors. Furthermore, they have better low-frequency response than sensors of other shapes. For two- and three-dimensional work, they are more convenient, and the output is easier to analyze because of good directional properties. These sensors can be mounted in single-, two (cross)-, or three-sensor probe arrangements.

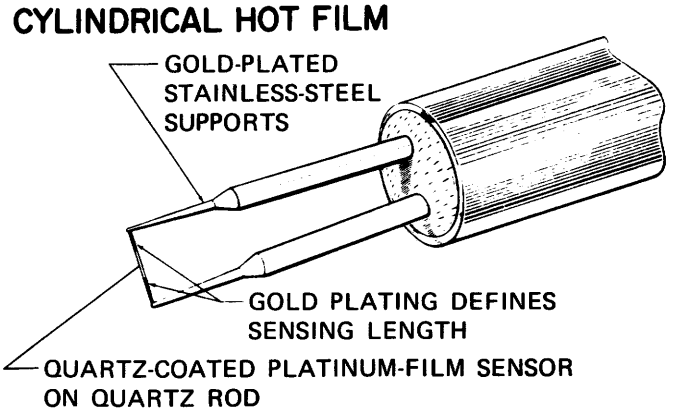

FIGURE 3.—Cylindrical hot-film sensor.

The wedge sensor is shown in figure 4. It is very strong, does not have flow-separation problems, and has good high-frequency response. Owing to high conduction losses, they are not recommended for turbulence measurements at low velocities (less than about 1 fps). The directional response of these probes is not well known and requires

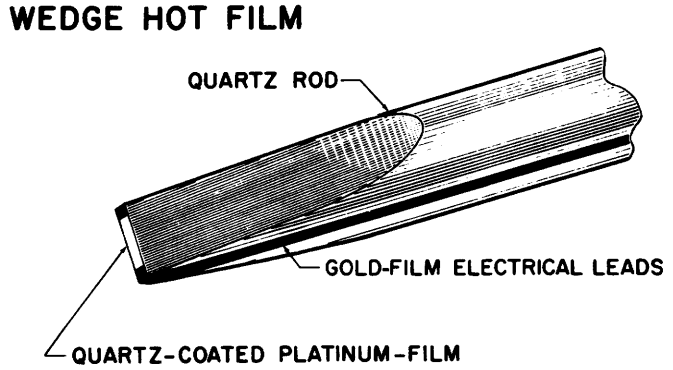

FIGURE 4.—Wedge hot-film sensor.

that the wedge be alined with the flow stream. Foreign matter can accumulate on the flat leading edge, but it does not accumulate as readily as on the cylinder.

The main advantage of the conical sensor, shown in figure 5, is the lack of surfaces on which to catch foreign matter. Also, this sensor is very insensitive to direction, owing to the cone angle and the sensor placement.

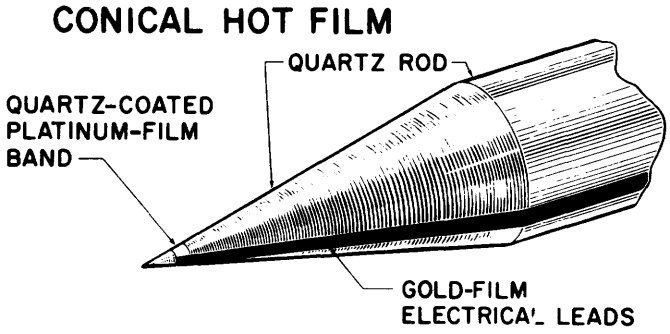

FIGURE 5.—Conical hot-film sensor.

The Parabolic sensor is shown in figure 6. It has the advantages of both cones and wedges. It has a rounded tip to minimize foreign-matter pickup, yet it has the sensor on the leading edge to give high-frequency response. The direction of flow should be within about a 10°-angle of the probe axis to avoid adverse directional response. Parabolic sensors are less vulnerable to breakage than other sensors because they have no sharp edges, points, or fragile structure. Adequate high-frequency response is obtainable during measurements in open-channel flows. However, an evaluation of the low-frequency response (less than 2 Hz) has never been carried out. These low frequencies are of particular interest in open-channel flows, and possible errors may be reported because of inadequate low-frequency response.

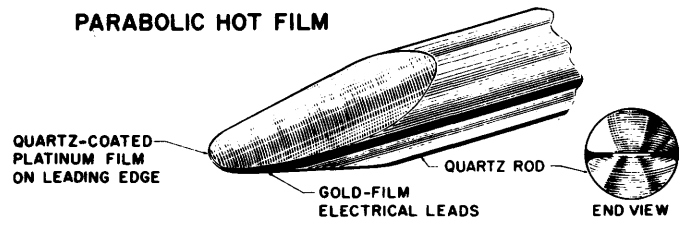

FIGURE 6.—Parabolic hot-film sensor.

SELECTION

Various factors must be considered when selecting a sensor: minimum and maximum flow velocity to be measured; strength of the sensor and rigidity of the sensor supporting structure; sensor shape, size, and temperature; fluid contamination of the sensor; and stability of the sensor calibration.

The minimum flow velocity measurable by a heated sensor depends on the free convection currents generated by the heat from the sensor. In water, free convection currents affect fluctuating-velocity measurements below a mean velocity of about 0.5 fps, because at these velocities, the free convection boundary layer has not had time to come into equilibrium with the flow. Solid sensors —such as cones, wedges, and parabolas—present a problem at low velocities because of the high heat conduction from the film into the substrate. At low frequencies this conduction causes both the film and the substrate, not just the film, to heat and cool, creating a calibration offset when compared with a steady flow calibration. This effect is most critical at low velocities (less than 1 fps). For this reason, cylindrical hot-film sensors are generally recommended for making turbulence measurements in low-velocity flows.

In high-velocity flows (over about 8 fps), extraneous turbulence can easily be generated by a vibrating probe, so a rigid sensor supporting structure is needed. High-velocity flow may also induce breakage of the sensor, so a strong sensor, such as the wedge or parabola, should be used.

In high-velocity flows, cylindrical sensing elements have two disadvantages due to flow separation on the downstream side. Eddies can be formed by this separation; they are picked up as fluctuating signals and can be confused with the turbulence. Cavities in the flow can also be created downstream from a cylindrical sensor; a combination of high sensor temperatures and high velocities tends to generate cavitation. Conical, wedge, and parabolic sensors circumvent both these difficulties.

At high velocities, collision of sediment particles with the sensor induces a high-frequency spike on the signal, as shown in figure 7. The experimenter should be aware of this possible alteration in the signal, but the additional energy due to the collisions is usually insignificant. Collision of sediment particles with the sensor also decreases its usable operation time. The abrasion removes the protective quartz coating and allows electrolysis to occur; once this happens a new sensor must be used. The approximate useful operation time of sensors in a sediment-laden stream is about 15 hours.

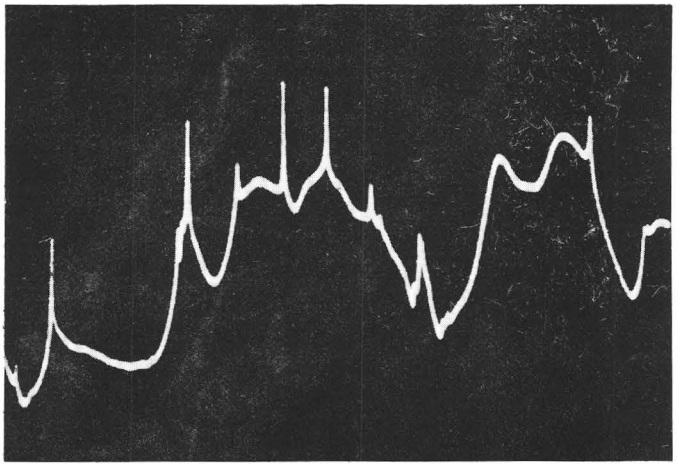

FIGURE 7.—Photograph of voltage trace from a hot-film sensor, showing spikes due to sediment particles colliding with the sensor.

Dirt and foreign particles within a flow field present the greatest difficulty to making stable and meaningful measurements. Natural open-channel flow is usually laden with particles, which tend to collect on the sensing element and affect the calibration. The tendency for a sensor to collect foreign matter is related to its shape and size. The cylindrical sensor is recommended over sensors of other shapes as long as the fluid can be filtered of all foreign matter. When the fluid cannot be filtered, then one of the solid sensors—notably, the parabolic sensor—is recommended.

Any hot-film sensor can and should be cleaned after each use with a small camel's-hair brush. This is a tedious procedure, but it helps prolong the life of the sensor. Strong solvents or chemicals should not be used to remove foreign matter. Repeated brushings during operation, when the sensor is still in water, are also suggested.

For a mean-flow measurement to be valid, the sensor must maintain its calibration over long time periods, which is possible only under ideal operating conditions. Compared with stability in air, stability in water can be a more difficult problem because of foreign contaminants, gas-bubble formation on the sensing element at low velocities, and electrical-conductivity problems. Gas-bubble formation and electrical-conductivity problems are usually characteristic of a thin quartz coating or a hot spot on the sensing element where no quartz coating is present. Major stability problems are usually detected by an increasing value of the cold resistance. When this is detected, the sensor should be replaced.

In summary, the parabolic sensor is the best sensor for general use in open-channel flows. Its geometry minimizes contaminant buildup, decreases the possibility of damage due to breakage, insures adequate frequency response in high-velocity flows, and circumvents cavitation and eddy formation. However, the cylindrical sensor is best for low-velocity flows where contaminants can be filtered out.

CALIBRATION CHARACTERISTICS

Typical voltage-velocity calibration curves for 0.002- and 0.006-inch-diameter cylindrical hot-film sensors and a 0.0002-inch-diameter hot-wire sensor in airflow are shown in figure 8 (Richardson and McQuivey, 1968). The calibration curves are nonlinear; sensitivity is a maximum at low velocities and decreases toward high velocities. The disadvantages of a nonlinear output in terms of convenient reading and recording are well known. A significant advantage of the nonlinear output is that measurements can be made over a wide range of flow velocities while maintaining a nearly constant percentage of reading accuracy. Measurements of velocities from a few feet per minute to supersonic can be made with no change in either the sensor or the scale reading.

The anemometer output signal is a voltage and is usually related to the flow velocity as follows:

$$\overline{E}^2 = A + B\,(\rho\overline{U})^n\,(T_s - T_a), \tag{36}$$

where

$\overline{E}$ = mean voltage,
A and B = constants depending on fluid properties,
ρ = fluid density,
$\overline{U}$ = mean flow velocity in the x direction,
n = an exponent that varies with velocity and with fluid and sensor properties,
T_s = sensor temperature (hot), and
T_a = fluid or environment temperature (cold).

This relation, known as King's law when $n=0.5$, illustrates the nonlinearity of the anemometer output. It also shows how voltage is related to density, velocity, and temperature. Although the basic variable is mass flow, $\rho\overline{U}$, velocity is indicated whenever density is constant. Hot-wire and hot-film sensors have been used to measure temperature, velocity, mass flow, thermal conductivity, basic heat transfer, and mass fractions because of the many variables that can be sensed. Because so many variables can be sensed, care must be

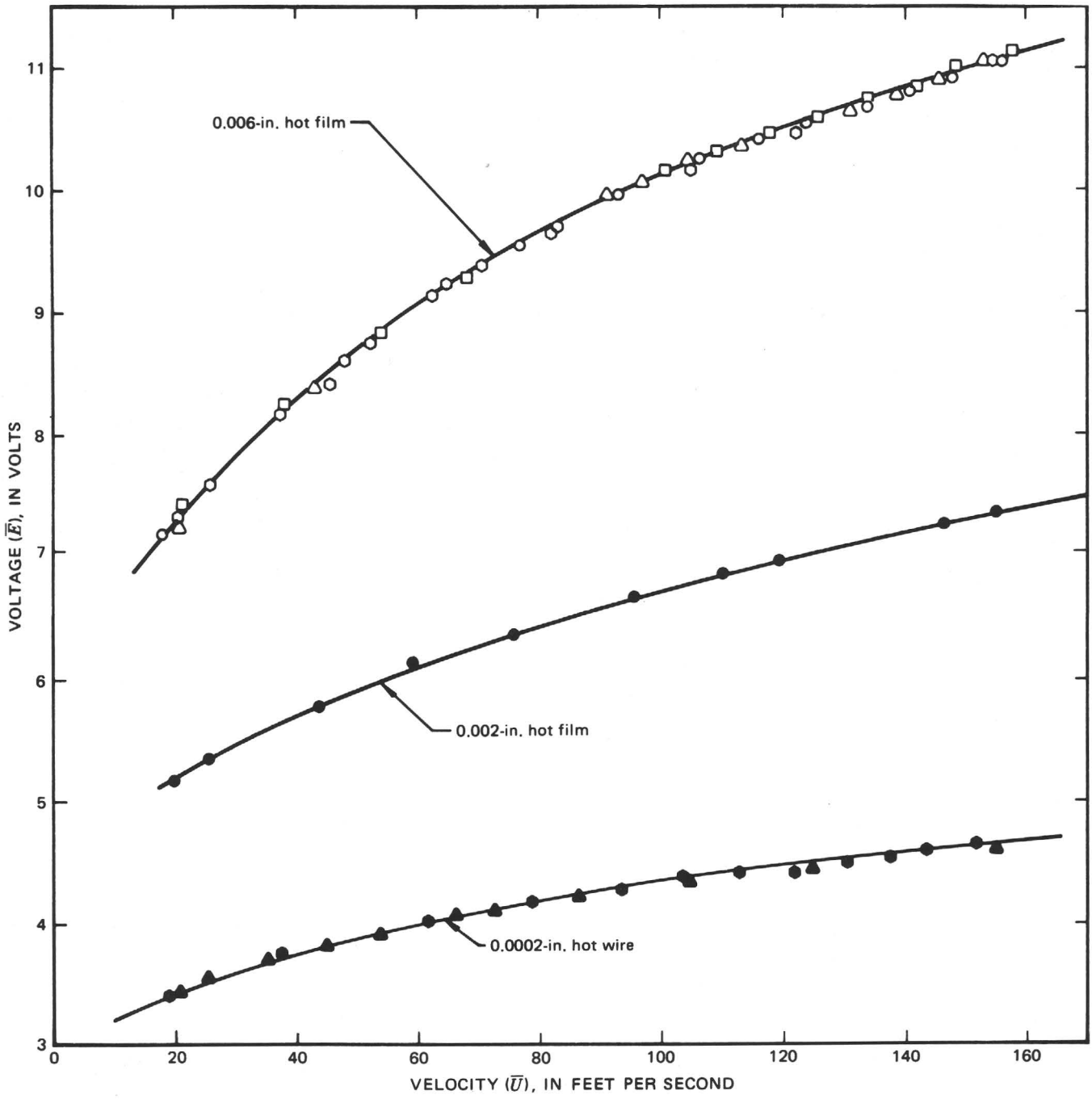

FIGURE 8.—Relation between mean voltage, $\overline{E}$, and mean velocity, $\overline{U}$, in airflow. (From Richardson and McQuivey, 1968.) Different symbols represent different sets of data for a given sensor. Curve represents average of the sets.

taken to isolate or control all the variables that are not pertinent when measuring a single variable. Temperature compensation is of particular importance when measuring velocity or mass flow.

King (1914) determined that $n=0.5$; this value gives the typical fourth-power relation between velocity and voltage, as shown in figure 9. In practice, anemometer sensors do not follow King's law precisely, but cylindrical sensors follow more closely than do sensors of finite length, such as the conical, wedge, and parabolic sensors.

Most hot-film anemometry data can be obtained using the basic nonlinear output, but linearizing circuits are becoming standard additions to an anemometry system. Making mean-flow measurements is more convenient when the voltage output

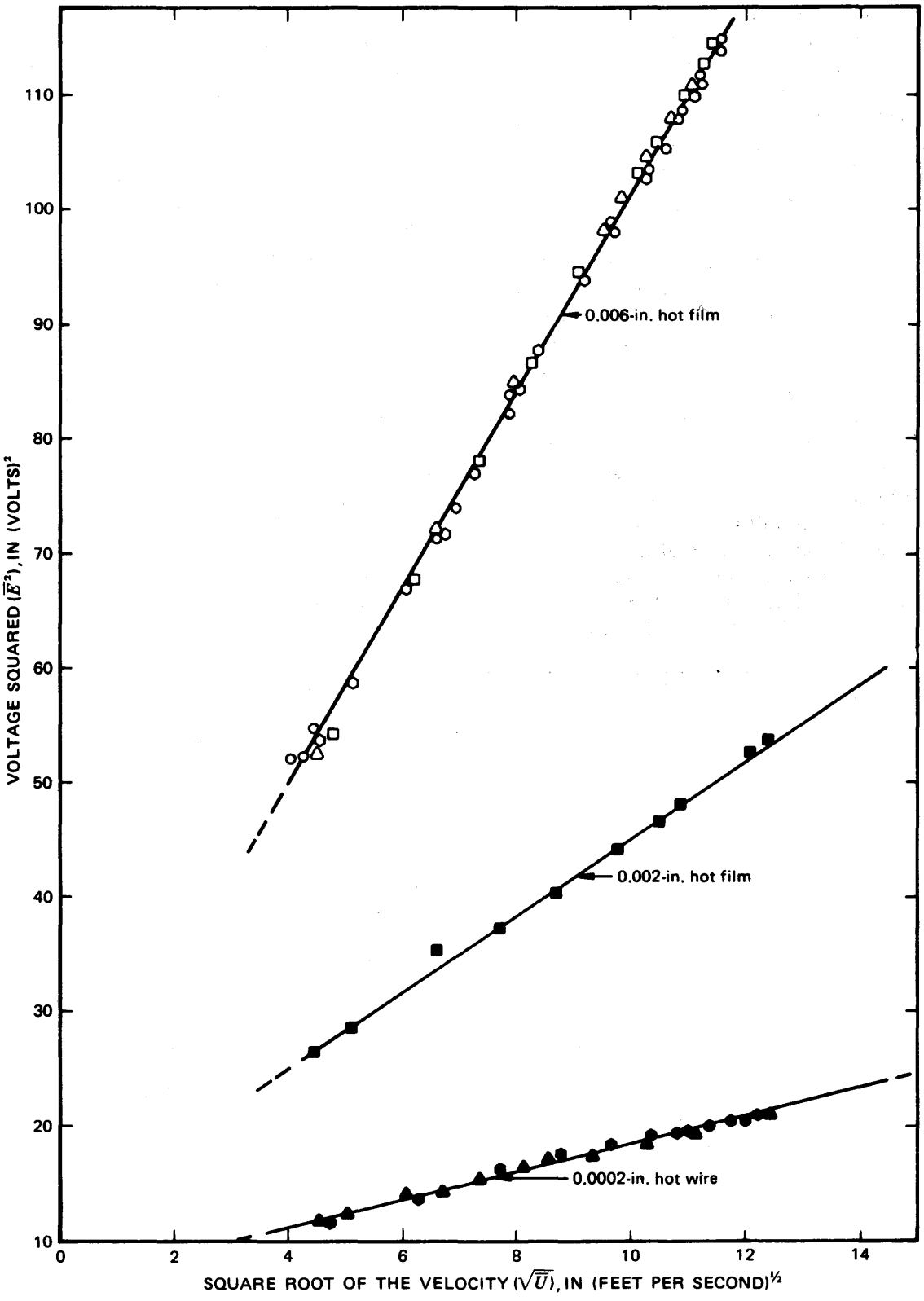

FIGURE 9.—Relation between the mean voltage squared, $\overline{E^2}$, and the square root of the mean velocity, $\sqrt{\overline{U}}$. Different symbols represent different sets of data for a given sensor. Curve represents average of the sets.

is linearly related to flow. However, some accuracy is lost when the output goes through any signal-conditioning circuit, so for highest accuracy, the nonlinear output is best. Where contamination is a problem and sensor calibration cannot be maintained, linearizing circuits cannot be used, and the nonlinear output must suffice.

COMPARISON WITH HOT-WIRE SENSORS

In order to evaluate the hot film as a transducer in turbulence investigation, Richardson, McQuivey, Sandborn, and Jog (1967) measured turbulence intensities in airflow at the centerline of a 5.75-inch-diameter pipe using 0.002- and 0.006-inch-diameter cylindrical hot films and 0.0002-inch-diameter hot wires. Hot wires were used as the standard with which to compare the hot films, because the response characteristics of hot wires have been extensively investigated and hot wires are standard transducers in wind-tunnel investigations. The results of the measurements showed that the 0.002-inch-diameter hot film indicated the same turbulence intensities as the 0.0002-inch-diameter hot wires, but the 0.006-inch-diameter hot film indicated smaller intensities, as shown in figure 10. The reason the 0.006-inch-diameter hot film indicated smaller intensities than the other sensors was attributed to end losses (heat loss by conduction through the sensor ends to the supports) and to a possible heat loss to the ceramic backing. Bellhouse and Schultz (1967) concluded that thermal feedback from the glass backing is important in air but not in water, so hot-film sensors are satisfactory transducers for turbulence investigations.

HEAT-TRANSFER RELATIONS

The heat transferred between the fluid and the sensor depends on the fluid velocity, the physical properties of the fluid, the dimensions and physical properties of the film or wire, and the difference in temperature between the film or wire and the fluid.

The convective heat transfer from a cylindrical sensor—either wire or film—has had extensive theoretical and experimental treatment. The theoretical study that is most extensively quoted was done by King (1914), who, for potential flow, derived an expression for the heat transfer from a cylinder. King's relation can be expressed as

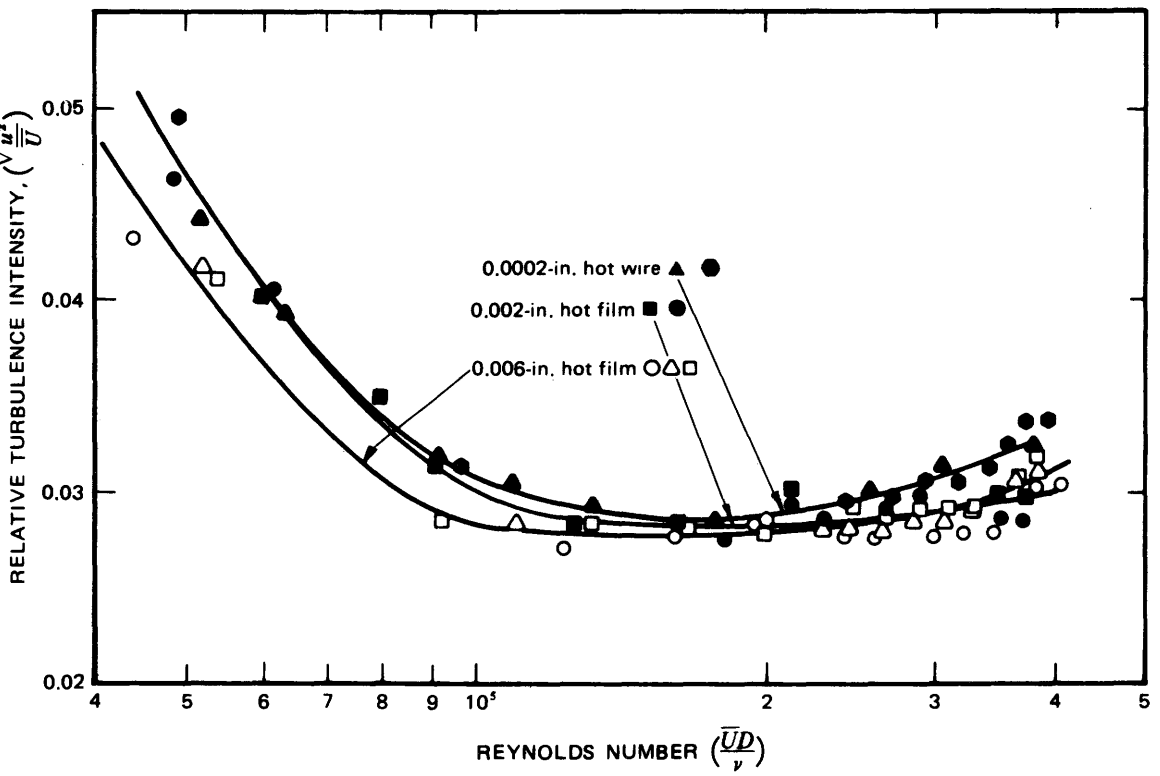

FIGURE 10.—Comparison of turbulence-intensity measurements made using hot-film and hot-wire sensors in airflow. (From Richardson and others, 1967.) Different symbols represent different sets of data for a given sensor. Curve represents average of the sets.

$$\frac{I^2R_s}{R_s-R_a}=A+B\sqrt{\overline{U}}, \tag{37}$$

where

I=electrical current,
R_s=electrical resistance of the sensor at sensor temperature (hot),
R_a=electrical resistance of the sensor at fluid temperature (cold),
A and B=constants depending on fluid properties, and
$\sqrt{\overline{U}}$=square root of the mean velocity of the flow in the x direction.

King's relation at best only holds for continuum flow at large Reynolds numbers. This is not surprising because the flow around a cylinder is very complex.

The heat-transfer relation has been expressed in nondimensional terms (Hinze, 1959):

$$\mathbf{N}=f(\mathbf{R}, \mathbf{P}, \mathbf{G}), \tag{38}$$

where

$\mathbf{N}=Hd/sk(T_s-T_a)$, the Nusselt number;
$\mathbf{R}=\overline{U}D/\nu$, the Reynolds number;
$\mathbf{P}=\mu C_p/\mathbf{R}$, the Prandtl number; and
$\mathbf{G}=g\rho^2d^3\beta(T_s-T_a)/\mu^2$, the Grashof number;

in which

H=thermal power transferred between the sensor and the fluid,
d=characteristic dimension of the sensor,
s=area of the sensor,
k=thermal conductivity of the fluid,
T_s=sensor temperature (hot),
T_a=fluid or environment temperature (cold),
$\overline{U}$=mean velocity of the flow in the x direction,
D=depth of flow,
ν=kinematic viscosity of the fluid,
μ=dynamic viscosity of the fluid,
C_p=specific heat of the fluid at constant pressure,
g=gravitational acceleration,
ρ=density of the fluid, and
β=coefficient of expansion of the fluid.

For a hot-wire sensor, which has a length much greater than its diameter, the heat-transfer relation can be expressed as (Hinze, 1959)

$$\mathbf{N}=0.42\mathbf{P}^{0.2}+0.57\mathbf{P}^{0.33}\mathbf{R}^{0.5}. \tag{39}$$

For solid hot-film sensors, specific heat-transfer relations have not been established, but the general heat-transfer relation can reasonably be expressed as

$$\mathbf{N}=a+b\mathbf{P}^{\alpha'}+c\mathbf{P}^{\beta'}\mathbf{R}^{\gamma'}, \tag{40}$$

where a, b, c, α', β', and γ' are constants that have different values according to the characteristics of the fluid and the sensor. The a represents heat transfer between film and probe or substrate, the b term represents conduction and free convection between film and fluid, and the c term represents forced convection between film and fluid.

For continuum incompressible flow, the best experimental relation between mean heat loss and mean velocity is

$$\frac{I^2R_s^2}{R_s(R_s-R_a)}=A+B\,\overline{U}^n. \tag{41}$$

This relation is similar to King's (eq 37). However, n is a function of the fluid medium, overheat ratio, sensor, and mean velocity. As will be shown later, changes in n greatly affect the conversion of voltage fluctuations, which result from fluctuating heat loss, to velocity fluctuations. The value of n for a 0.002-inch-diameter hot film in air is 0.30 for velocities of 20–60 fps and 0.41 for velocities of 60–150 fps. In water, the value of n for the same sensor is 0.31 for velocities of 0.2–0.6 fps, 0.35 for velocities of 0.6–1.5 fps, and 0.45 for velocities of 1.5–3.0 fps.

For a constant-temperature hot-film anemometer in a flow with constant fluid properties (temperature, density, and viscosity), equation 41 can be written as

$$\overline{E}^2=A'+B'\,\overline{U}^n, \tag{42}$$

where A' and B' are constants depending on fluid properties.

Deviations in the above-discussed equations, properly applied, are often less than other errors due to less-than-ideal experimental conditions. End losses and nonuniformities in sensor surface temperature can cause errors in specific situations. However, for measurements in open-channel flows, general heat-transfer relations are not sufficient for the reduction of data. Calibration is recommended whenever accuracy is required and when noncylindrical sensors are used. In fact, a continuous calibration is suggested for all operations in open-channel flows.

VOLTAGE-VELOCITY RELATIONS

Hot-film sensors can become heated above ambient temperature by the electric current in the anemometer system. However, by using a constant-temperature hot-film anemometer, the electrical resistance and, therefore, temperature of the film can be kept constant. A slight variation in velocity will result in a variation in heat loss from the hot film, which in turn produces an imbalance in the Wheatstone bridge. Any imbalance in the bridge is compensated for by means of an electronic feedback system, which senses the imbalance in the bridge and alters the current to the bridge to rebalance it. Such a feedback system operates almost instantaneously and is effective for frequencies up to several kilohertz.

Because fluctuating-velocity measurements are desired rather than mean-velocity measurements, the fluctuations in heat transfer from the hot film must be considered. The velocity fluctuations can be approximated by assuming that the film responds as a first-order system; the fluctuations can then be evaluated from a calibration of the relation between the film heat loss and the fluctuating velocity. The film heat loss must be known very accurately so that the first derivative of heat loss with respect to velocity fluctuation can be obtained.

Operation of the hot film in the electronic circuit is assumed to be ideal, so problems of frequency response do not need to be considered. The problem is now to find a technique to obtain the turbulence velocity components from the hot-film voltage output and the calibration curve (fig. 8).

At least four assumptions are made in converting the voltage fluctuations sensed by the hot-film anemometer to velocity fluctuations:

1. The total instantaneous-velocity vector, U_{tot}, can be expressed by a mean value, $\overline{U}$, in the x direction and by fluctuation components—u, v, and w—in the x, y, and z directions, respectively.
2. A hot-film sensor held perpendicular to the flow is sensitive only to the mean and fluctuating component of the velocity in the direction of flow, the x direction. In other words, the hot film is sensitive to the first order of $\overline{U}$ and u but is sensitive to only the second order of v and w; the second-order terms are negligible and can be considered to be zero where the fluctuations are much less than the mean.
3. The relation between mean voltage, $\overline{E}$, and mean velocity, $\overline{U}$, can be used to convert voltage fluctuations to velocity fluctuations.
4. The change in the slope, $d\overline{E}/d\overline{U}$ (the sensitivity), of the voltage-velocity calibration curve is small in relation to the velocity fluctuations normally measured; thus, the tangent of the curve at the mean velocity can be used to convert voltage fluctuations to velocity fluctuations.

These assumptions imply that the fluid properties, overheat ratio, film diameter (characteristic), film length, angle of attack, and heat transfer from the hot film to the fluid are constant. That is, the heat transfer is a function of only the velocity of the flow.

The first assumption is the usual one made in fluid mechanics along with the Reynolds method of averaging to derive the Navier-Stokes equation for turbulent flow.

The second assumption is justified on an order-of-magnitude basis; it applies for low turbulence intensities (less than 15 percent). The total instantaneous-velocity vector for a hot-film sensor placed perpendicular to the mean flow is illustrated in figure 11.

The total instantaneous velocity is expressed as

$$U_{tot}=\sqrt{(\overline{U}+u)^2+v^2+w^2} \tag{43a}$$

or

$$U_{tot}=\overline{U}\sqrt{1+\frac{2u}{\overline{U}}+\left(\frac{u}{\overline{U}}\right)^2+\left(\frac{v}{\overline{U}}\right)^2+\left(\frac{w}{\overline{U}}\right)^2}. \tag{43b}$$

By expanding the square-root part by a binomial series expansion,

$$U_{tot}=\overline{U}\left[1+\frac{1}{2}\left(\frac{2u}{\overline{U}}+\left(\frac{u}{\overline{U}}\right)^2+\left(\frac{v}{\overline{U}}\right)^2+\left(\frac{w}{\overline{U}}\right)^2\right)+(\text{higher order terms})\right]. \tag{44}$$

Therefore, considering only first-order terms,

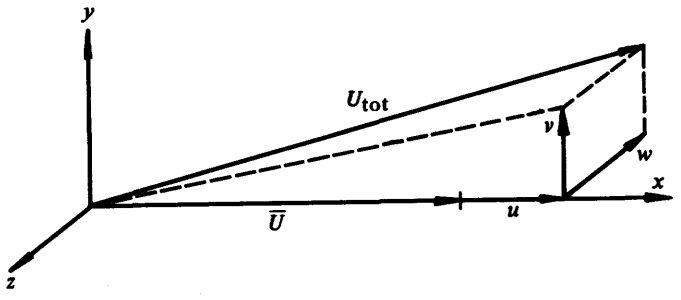

FIGURE 11.—Diagram defining the total instantaneous-velocity vector.

equation 44 reduces to

$$U_{tot} \approx \overline{U} + u. \tag{45}$$

For small fluctuations, where $\overline{U}$ is much greater than $|u|$, $|v|$, or $|w|$, a sensor normal to the flow would be sensitive only to the mean velocity and its fluctuation in the x direction. Note that equation 45 is true regardless of whether v and w are parallel or perpendicular to the hot film.

The third assumption says that the same heat-transfer relation exists for both the mean and the fluctuating quantities of voltage and velocity. According to Sandborn (1966), turbulence does not affect the heat-transfer characteristics of the hot film; turbulence effects on heat transfer are negligible for most anemometry work.

The fourth assumption, that the change in slope of the calibration curve is small in relation to the velocity fluctuations, is necessary to convert the measured voltage fluctuations to the velocity fluctuations. Sandborn (1966) investigated the effect of assuming that the voltage-velocity curve is linear over the range of measured root-mean-square voltage fluctuations. He found that for a 0.0002-inch-diameter tungsten wire, only 1-percent error in the turbulence intensity was introduced by the actual nonlinearity of the calibration curve for intensities up to 40 percent.

The equation for converting voltage fluctuations to velocity fluctuations for a hot film perpendicular to the flow is obtained as follows. The derivative of the instantaneous voltage output from the anemometer is

$$dE = \frac{\partial \overline{E}}{\partial \overline{U}} dU_{tot}. \tag{46}$$

From equation 43a

$$dU_{tot} = \frac{1}{\sqrt{(\overline{U}+u)^2+v^2+w^2}} [(\overline{U}+u)du + vdv + wdw]. \tag{47}$$

Where $\overline{U}$ is much greater than $|u|$, $|v|$, or $|w|$, equation 47 reduces to

$$dU_{tot} = du. \tag{48}$$

So

$$dE = \frac{d\overline{E}}{d\overline{U}} du. \tag{49}$$

The general assumption is that $dE=e$ and $du=u$ (that is, the derivatives are equal to the fluctuations). With this assumption, equation 49 becomes

$$e = \frac{d\overline{E}}{d\overline{U}} u. \tag{50}$$

The root mean square of the voltage fluctuation is normally the measured output of the hot-film anemometer; therefore, by assuming $e=\sqrt{e^2}$ and $u=\sqrt{u^2}$,

$$\sqrt{e^2} = \frac{d\overline{E}}{d\overline{U}} \sqrt{u^2}, \tag{51}$$

where $\sqrt{e^2}$ is the root mean square of the voltage fluctuation and $\sqrt{u^2}$ is the root mean square of the velocity fluctuation. The physical meaning of equation 51 and the assumptions leading up to it are illustrated in figure 12 for two overheat ratios.

To determine the sensitivity, $d\overline{E}/d\overline{U}$, equation 42 may be differentiated, giving

$$\frac{d\overline{E}}{d\overline{U}} = \frac{nB'\overline{U}^{n-1}}{2\overline{E}}. \tag{52}$$

If King's law is assumed to hold, n is 0.5, and equation 52 reduces to

$$\frac{d\overline{E}}{d\overline{U}} = \frac{B'}{4\overline{E}\sqrt{\overline{U}}}. \tag{53}$$

However, for most hot-film sensors the heat loss does not follow King's law; therefore, either $d\overline{E}/d\overline{U}$ must be determined empirically by plotting $\overline{E}^2$ against $\sqrt{\overline{U}}$ to obtain values of n and B' for equation 52, or $d\overline{E}/d\overline{U}$ must be determined graphically. Determining $d\overline{E}/d\overline{U}$ graphically is simpler. $\overline{E}$ is plotted against $\overline{U}$ for a given overheat ratio and fluid temperature (fig. 13). The tangent of this curve is $d\overline{E}/d\overline{U}$; it can be determined graphically and then plotted as a function of $\overline{U}$ (fig. 14).

The difference between $d\overline{E}/d\overline{U}$ determined graphically and $d\overline{E}/d\overline{U}$ determined by assuming that King's law holds and that equation 53 can be used is shown in figure 14. The graphical procedure has the advantage of accounting for variations in n, but it has the disadvantage of being more tedious and subject to human judgment in determining the tangent to the curve. Another advantage of the graphical procedure is in reducing data where drift due to contamination buildup on the sensor is a problem and where the voltage changes for a given velocity. The graphical procedure can be used to account for drift problems, as indicated in figure 12.

The method of determining the longitudinal turbulence intensity, u, for a single sensor has just been described. To determine the other com-

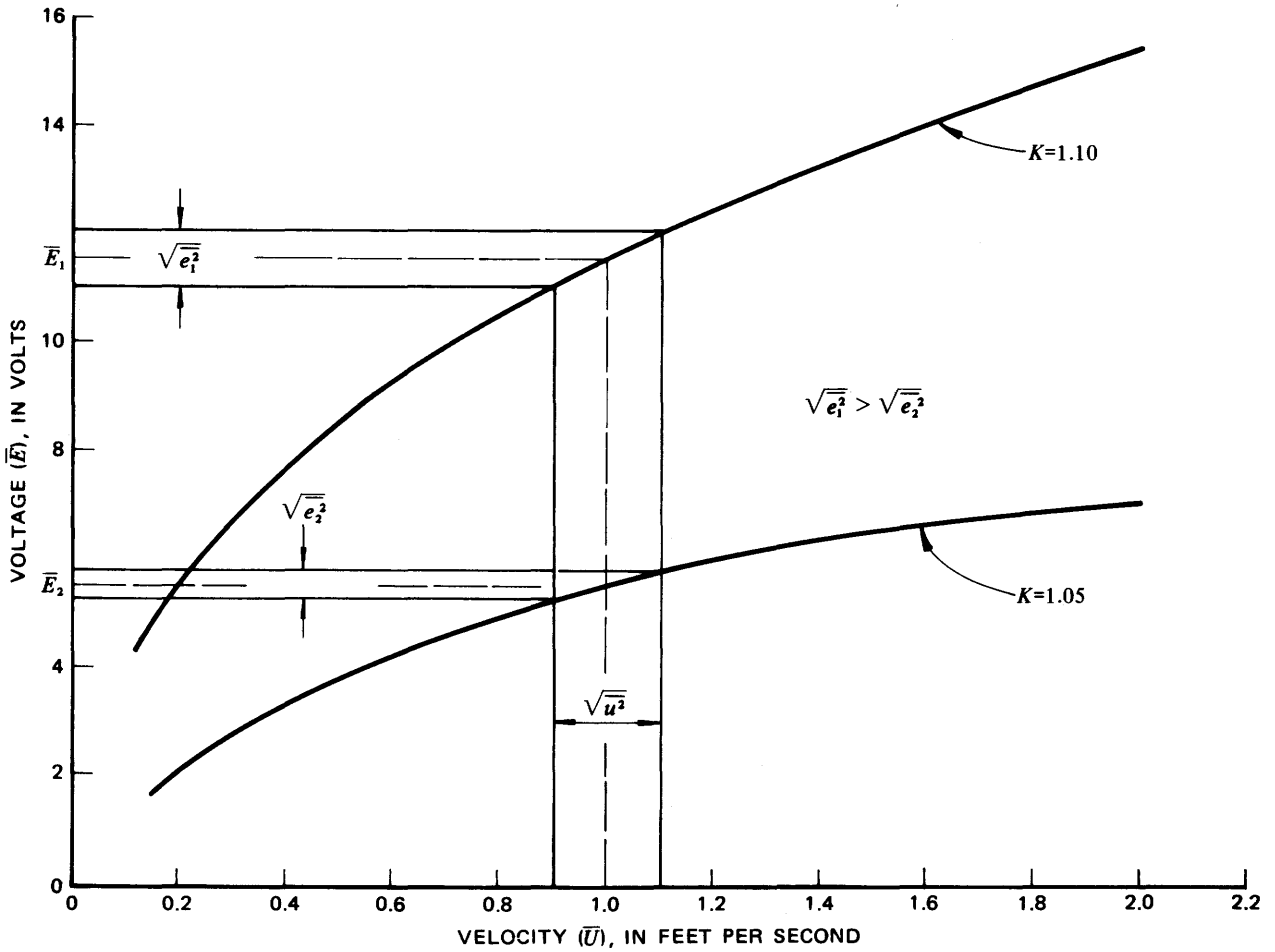

FIGURE 12.—Linearization schematic of the voltage-velocity relation. K, overheat ratio.

ponents of the velocity fluctuation, v and w, and the cross-velocity correlations—$\overline{uv}$, $\overline{vw}$, and $\overline{uw}$—a single sensor is held at two different angles to the mean flow, or two sensors are set in a cross arrangement.

The output, E, of the constant-temperature hot-film anemometer, which is indicative of the hot-film heat loss, can now be assumed to be a function of the total velocity, U_{tot}, and the angle of yaw, ξ, if the geometry and physical properties of the film remain constant:

$$E=f(U_{tot}, \xi). \tag{54}$$

The total velocity sensed by the hot film at any moment is given by equation 43. The rectangular coordinate system is placed so that the mean velocity, $\bar{U}$, is alined in the x direction (fig. 15). For very small u, v, and w in relation to $\bar{U}$, U_{tot} can be assumed to be essentially alined in the x direction. The angle ξ is the angle between the position of the hot film and the direction of the total velocity, the x direction. It is called the angle of yaw or the angle of attack, the angle between the sensor and a flow particle "attacking" the sensor. The angle ξ can be thought of as being made up of two angles, ϕ and ψ. Angle ϕ is the angle the hot film makes with the x axis when the film is rotated in the xy plane (fig. 15*A*), and angle ψ is the angle the hot film makes with the x axis when the film is rotated in the xz plane (fig. 15*B*). Any combination of ϕ and ψ coincides with one value for angle ξ. When the hot film is perfectly alined within the xy plane, then ψ is zero, and $\partial\bar{E}/\partial\psi$ is zero. The heat loss is quite sensitive to ψ for small deviations from perfect alinement. Therefore, a hot film placed in the xy plane must be alined exactly in this plane. Considering now a hot film so alined, the output of the constant-temperature hot-film anemometer can be assumed to be a function of the total velocity vector, U_{tot}, and the angle of yaw in the xy plane, ϕ:

$$E=f(U_{tot}, \phi). \tag{55}$$

In terms of differentials,

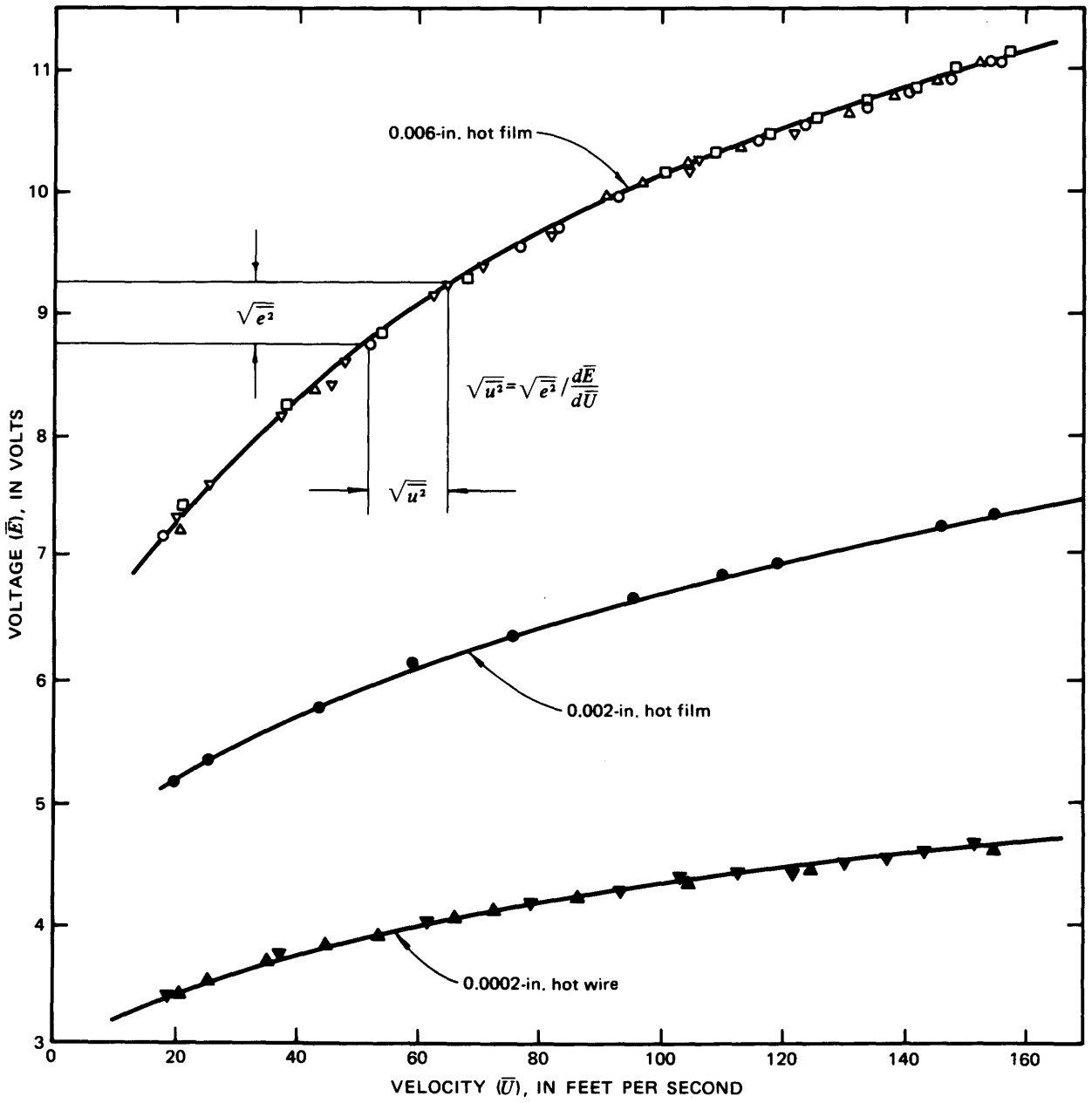

FIGURE 13.—Voltage-velocity relations for hot-film and hot-wire sensors.

$$dE=\frac{\partial \overline{E}}{\partial \overline{U}}dU_{\text{tot}}+\frac{\partial \overline{E}}{\partial \phi}d\phi. \tag{56}$$

The differential of the total velocity is the same as equation 47; again assuming $\overline{U}$ much greater than $|u|$, $|v|$, or $|w|$, the final results are the same as equation 48. Using figure 15, the instantaneous angle of attack in the xy plane, ϕ, can be written in terms of the angle fluctuation, ϕ', as

$$\phi'=\phi+\tan^{-1}\left(\frac{v}{\overline{U}+u}\right). \tag{57}$$

Its differential may be expressed as

$$d\phi=\frac{(\overline{U}+u)dv-vdu}{(\overline{U}+u)^2+v^2}. \tag{58}$$

By substitution in equation 56, one obtains

$$dE=\frac{\partial \overline{E}}{\partial \overline{U}}\frac{1}{\sqrt{(\overline{U}+u)^2+v^2+w^2}}[(\overline{U}+u)du+vdv+wdw]$$

$$+\frac{\partial \overline{E}}{\partial \phi}\left[\frac{(\overline{U}+u)dv-vdu}{(\overline{U}+u)^2+v^2}\right]. \tag{59}$$

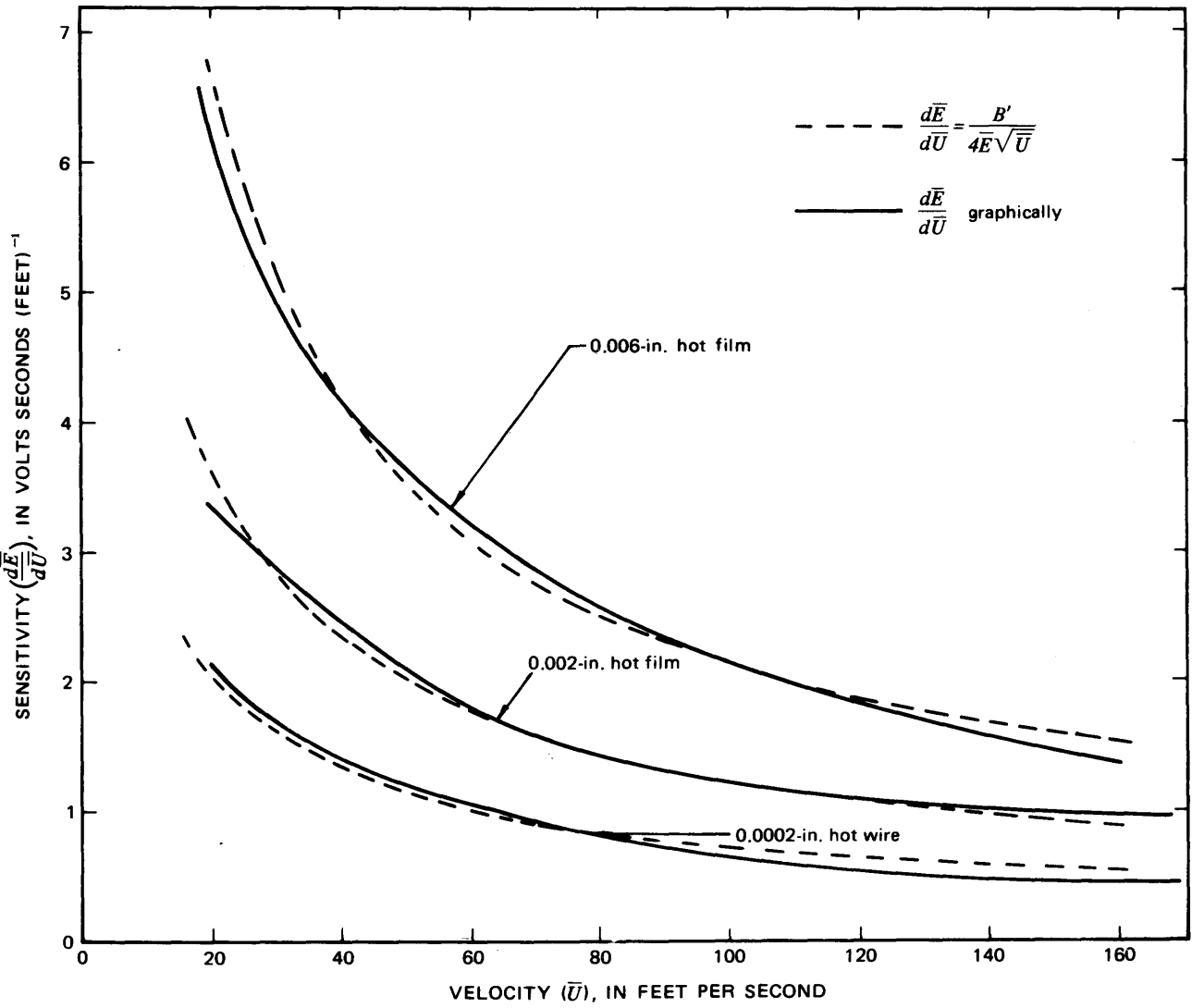

FIGURE 14.—Comparison of sensitivity-velocity relations for hot-film and hot-wire sensors as obtained graphically and from King's law.

This equation is still very complex, and additional assumptions are necessary to obtain a less complex expression in which the terms can be evaluated.

Once again the mean velocity, $\overline{U}$, is assumed to be much greater than the turbulence fluctuations (that is, $\overline{U} \gg |u|$, $|v|$, or $|w|$). With this assumption, equation 59 reduces to

$$dE=\frac{\partial \overline{E}}{\partial \overline{U}}du+\frac{\partial \overline{E}}{\partial \phi}d\phi. \tag{60}$$

Consequently,

$$E=f(U,\phi). \tag{61}$$

Assuming now that $f(U,\phi)$ is analytic everywhere in the flow field, the function can be expanded in a Taylor series about some convenient point of operation. The deviations of the velocity and the angle from their mean values are assumed to be small and will be denoted by $u=U-\overline{U}$ and $\phi'=\phi-\overline{\phi}$, respectively. Expanding the output of the hot film about $\overline{U}$ and $\overline{\phi}$, the following equation is obtained:

$$f(U,\phi)=f(\overline{U},\overline{\phi})+\left(\frac{\partial \overline{E}}{\partial \overline{U}}\right)u+\left(\frac{\partial \overline{E}}{\partial \overline{\phi}}\right)\phi'$$
$$+\frac{1}{2!}\left(\frac{\partial^2 \overline{E}}{\partial \overline{U}^2}\right)u^2+\left(\frac{\partial^2 \overline{E}}{\partial \overline{U}\partial \overline{\phi}}\right)u\phi'$$
$$+\frac{1}{2!}\left(\frac{\partial^2 \overline{E}}{\partial \overline{\phi}^2}\right)\phi'^2+\cdots. \tag{62}$$

The deviation of the hot-film voltage from its mean is denoted by e, where

$$e=f(U,\phi)-f(\overline{U},\overline{\phi}).$$

Neglecting higher order terms, the expansion can be written as

$$e=\left(\frac{\partial\overline{E}}{\partial\overline{U}}\right)u+\left(\frac{\partial\overline{E}}{\partial\overline{\phi}}\right)\phi', \tag{63}$$

where $(\partial\overline{E}/\partial\overline{U})$ is the sensitivity of the hot-film voltage to a deviation in velocity from the mean velocity, and $(\partial\overline{E}/\partial\overline{\phi})$ is the sensitivity of the hot-film voltage to a deviation in angle from the mean angle.

Using figure 15, the sine of ϕ' can be written as

$$\sin\phi'=\frac{v}{\sqrt{(\overline{U}+u)^2+v^2}}. \tag{64}$$

After expansion

$$\phi'=\frac{v}{\sqrt{(\overline{U}+u)^2+v^2}}+\frac{1}{6}\left(\frac{v}{\sqrt{(\overline{U}+u)^2+v^2}}\right)^3+\cdots. \tag{65}$$

As before, the mean velocity, $\overline{U}$, is assumed to be much larger than the turbulence fluctuations; consequently, $\phi'\approx v/\overline{U}$ and

$$e=\frac{\partial\overline{E}}{\partial\overline{U}}u+\frac{1}{\overline{U}}\frac{\partial\overline{E}}{\partial\overline{\phi}}v. \tag{66}$$

To employ this expression, it must be written in terms of quantities which can be measured, such as root mean squares or mean squares of fluctuating quantities. Therefore, equation 66 is squared and averaged to give

$$\overline{e^2}=\left(\frac{\partial\overline{E}}{\partial\overline{U}}\right)^2\overline{u^2}+2\frac{\partial\overline{E}}{\partial\overline{U}}\frac{1}{\overline{U}}\frac{\partial\overline{E}}{\partial\overline{\phi}}\overline{uv}+\left(\frac{1}{\overline{U}}\frac{\partial\overline{E}}{\partial\overline{\phi}}\right)^2\overline{v^2}. \tag{67}$$

Letting $\partial\overline{E}/\partial\overline{U}=S_x$ and $(1/\overline{U})(\partial\overline{E}/\partial\overline{\phi})=S_y$, one obtains

$$\overline{e^2}=S_x^2\,\overline{u^2}+2S_xS_y\overline{uv}+S_y^2\,\overline{v^2}, \tag{68}$$

where S_x is the sensitivity to velocity fluctuations in the x direction and S_y is the sensitivity to velocity fluctuations in the y direction (sensitivity to fluctuations from mean angle between sensor and x axis in xy plane).

Equation 68 requires that the hot film be calibrated with respect to angle and velocity in order to obtain a value for $\overline{uv}$, from which the turbulent shear stress in the x direction can be obtained. The sensitivities vary with angle and velocity; however, the two sensitivity terms, S_x and S_y, are

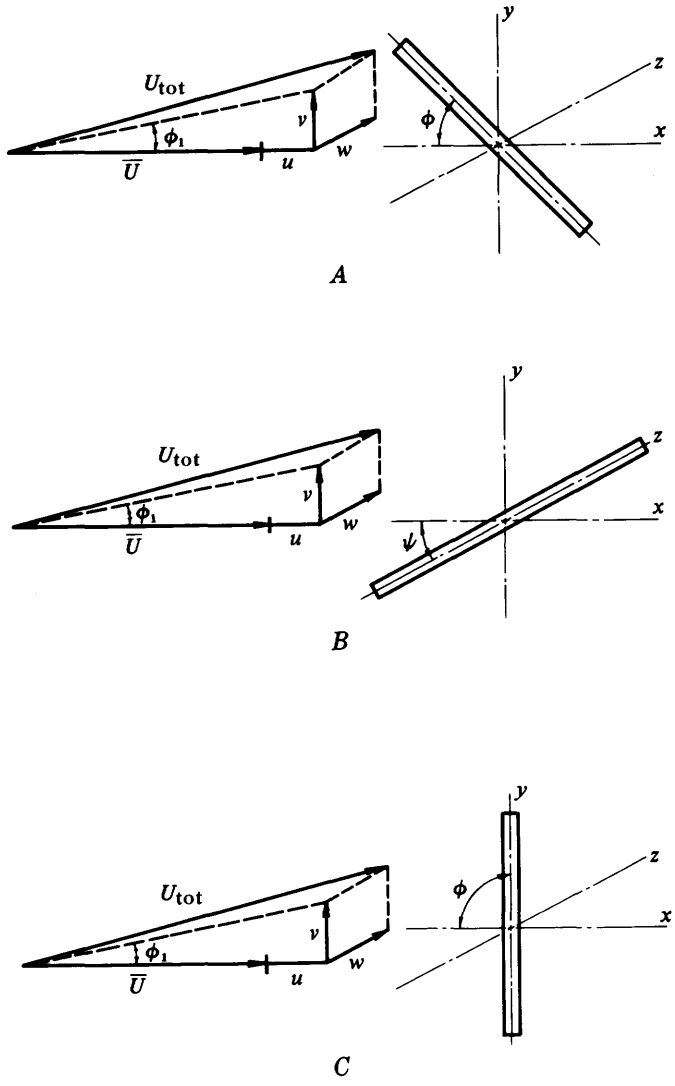

FIGURE 15.—Hot-film orientation with respect to the total velocity vector, U_{tot}. Position of hot film, which is a linear object, is represented by oblong rectangle in coordinate systems shown on right-hand side of figure. For very small u, v, and w in relation to $\overline{U}$, U_{tot} can be assumed to be essentially alined in the x direction. A shows angle ϕ, the angle the film makes with the x axis when the film is rotated in the xy plane. B shows angle ψ, the angle the film makes with the x axis when the film is rotated in the xz plane (ψ=90°). C shows a commonly used sensor position, where ψ=0 and ϕ=90°.

of equal magnitude at an angle of approximately $\overline{\phi}$=40°. On the basis of this information and previous experiments, I suggest that the hot film be operated at angles of plus and minus 40° from the x axis in the xy plane. First, however, measurements should be taken at ϕ=90°, when the film is perpendicular to the mean flow; then, the angle sensitivity is zero (fig. 15C), and equation 68 becomes

$$\overline{e^2}=S_x^2\,\overline{u^2}. \quad (69)$$

From this expression, the magnitude of $\overline{u^2}$ can be obtained when the film is properly calibrated for velocity and when the mean velocity at the point of measurement is known.

Knowing the magnitude of $\overline{u^2}$, the values of $\overline{v^2}$ and $\overline{uv}$ can now be obtained by using the measurements of $\overline{e^2}$ at the hot-film positions of plus and minus 40°. A plot (fig. 16) of hot-film voltage output versus angle of attack indicates that for positive quantity and for negative angles of attack S_y is a negative quantity. Therefore, two equations can now be written; one for the positive angle of attack

$$(\overline{e^2})_{+40}=(S_x^2)_{+40}\overline{u^2}+2(S_x)_{+40}(S_y)_{+40}\overline{uv}+(S_y^2)_{+40}\overline{v^2} \quad (70)$$

and one for the negative angle of attack

$$(\overline{e^2})_{-40}=(S_x^2)_{-40}\overline{u^2}+2(S_x)_{-40}(S_y)_{-40}\overline{uv}+(S_y^2)_{-40}\overline{v^2}. \quad (71)$$

Two sensors can be used to obtain certain turbulence characteristics. The most common use is for obtaining space and space-time correlations, which were discussed earlier in this report. This application is straightforward, and each sensor output is treated as a single sensor. The data analysis is also the same.

Hot films can be placed in a cross configuration. This configuration is useful in obtaining two components of the velocity fluctuation at once. The analysis of the system output is almost identical to that just discussed. This arrangement has some disadvantages. The configuration must be used under ideal conditions where no contaminant is present. For turbulence measurements in most open-channel flows, the cross configuration has little chance of being operated satisfactorily.

SOURCES OF ERRORS IN MEASUREMENTS

The preceding discussions might indicate that turbulence velocity components would be easy to

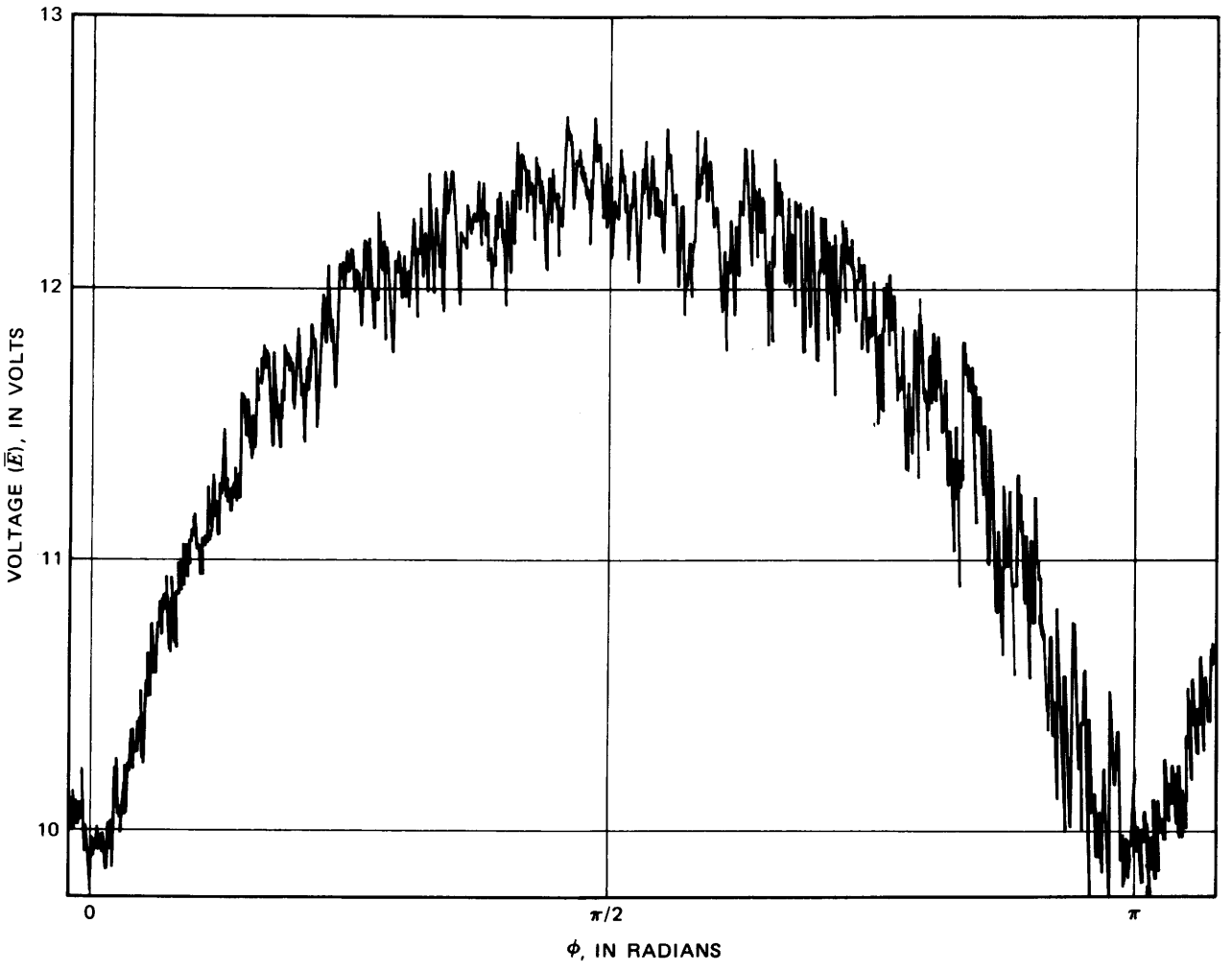

FIGURE 16.—Variation of voltage, $\bar{E}$, with angle of yaw in the xy plane, ϕ.

measure. However, these measurements are subject to a great deal of uncertainty.

The two major sources of error in hot-film anemometry are (1) an inaccurate heat-transfer relation due to heat-transfer effects other than convection and to an incorrect convective heat-transfer relation, and (2) a frequency response insufficient to give a true representation of the instantaneous heat transfer between the sensor and its environment. Heat transfer is normally considered as a combination of conduction, convection, and radiation. Equations such as equation 37 represent convection only. For hot-film sensors, heat conduction takes place primarily between the sensor and its supports, and radiation heat exchange can take place between the sensor and the external solid surfaces.

SOLID BOUNDARY

When a hot film is used close to a solid boundary, errors are introduced owing to the effect of the boundary on the rate of heat loss from the film (radiation). When a platinum film is used at an overheat ratio of $R_s/R_a=1.10$, the film temperature is approximately 180°F. Consequently, when this hot film is used near a solid boundary, the film can be 110°F hotter than the surface. Besides losing heat to the water, because of forced convection, the hot film may loose heat to the solid surface, because of radiation.

VELOCITY GRADIENTS AND TURBULENCE-INTENSITY GRADIENTS

When a hot film is operated in a flow with a velocity gradient, the heat transfer along the hot film is nonuniform. This results in a shift of the effective center of the sensor toward that part of the sensor with the higher heat transfer. If the film also experiences a turbulence-intensity gradient in the direction of the film orientation, a mathematical solution for the temperature distribution is almost impossible to obtain. For measurements of the longitudinal turbulence intensity (intensity in the x direction), the sensor can be placed so that these large gradients are not present along the hot film; however, for measurements of the turbulence shear stress, the hot film must be yawed so that it is partly projected in the y direction. The discrepancy in results from the horizontal and vertical hot films is about 2 to 3 percent when measurements are taken close to the boundary, where both gradients are greatest and the relative turbulence intensity is 20 percent (McQuivey, 1967).

LINEARIZATION OF THE VOLTAGE-VELOCITY RELATION

The sensitivity of the hot-film anemometer to velocity fluctuations was discussed in a previous section. The expression for the differential of the hot-film output was too complex, and additional assumptions had to be made. The usual assumption made was that the magnitude of the mean flow was much larger than the magnitude of the fluctuations.

In using the expression for the differential of the hot-film output, the calibration curve of the hot film is assumed to be linear around the point of operation. This assumption is valid for small turbulence intensities at high mean velocities; however, it must be questioned for intensities over the range required by $dE=\sqrt{\overline{e^2}}$. The possible error due to nonlinear averaging of the hot-film output was checked graphically from a calibration curve. For a relative turbulence intensity of $\sqrt{\overline{u^2}}/\overline{U}=0.30$, an error of 3 percent was found when $\overline{U}=1.0$ fps. At lower mean velocities and at the same turbulence intensities (a higher relative turbulence intensity), the error was slightly greater (McQuivey, 1967).

LARGE-SCALE TURBULENCE

Large-scale turbulence is common in open-channel flows. The common method of reducing turbulence data assumes flow fluctuations superimposed on a steady mean flow. During analysis, higher order terms are neglected which are significant when turbulence levels are high (above 15 to 20 percent).

Schraud and Kline (1965) have attempted to estimate the errors due to large turbulence fluctuations. The results show that errors of the order of 5 percent are possible for relative turbulence intensities of approximately 35 percent.

CONDUCTION LOSSES TO SENSOR SUPPORTS

Loss of heat through the sensor ends to the supports has been discussed in the literature, but the emphasis has been on making a heat balance on the sensor. The effects of end losses on frequency response seems to be less well known. However, Bellhouse and Schultz (1967), for wedge-shaped thin-film sensors, pointed out the strong influence on low-frequency response of what could be called end losses or side losses.

Figure 17 shows the effect of end losses on low-frequency response. Relative turbulence intensities obtained using a wedge sensor are compared with those obtained using a 0.002-inch-diameter cylindrical sensor in an 8-inch-wide flume. Heat

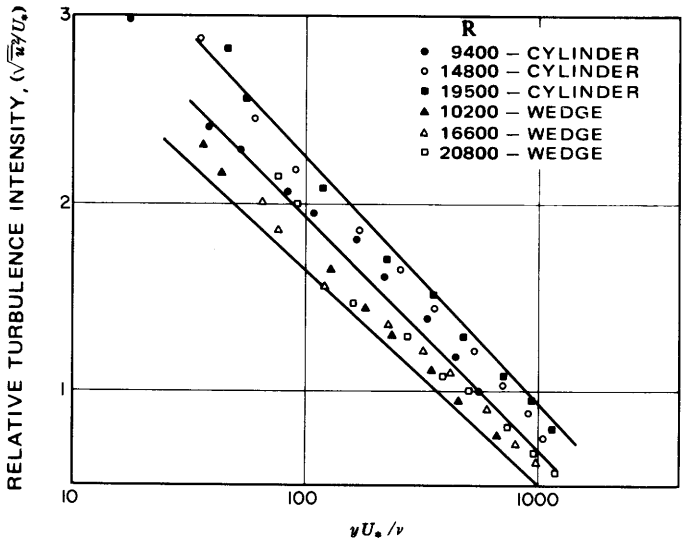

FIGURE 17.—Comparison of relative turbulence intensities obtained using a wedge sensor and those obtained using a 0.002-inch-diameter cylindrical sensor in an 8-inch-wide flume. The lines delineate the fields represented by the cylinder and the wedge.

transfer is better for the cylinder, and the heat loss from the wedge sensor is greater than the loss from the cylinder. The loss is due supposedly to a conduction loss (McQuivey, 1967). The mean velocity was fairly low and may have been approaching the limits of the wedge sensor's detection capabilities.

Figure 18 also shows the effect of end losses on low-frequency response. Relative turbulence intensities obtained using a parabolic sensor are compared with those obtained using a 0.002-inch-diameter cylindrical sensor in an 8-foot-wide flume. The results are similar, indicating that the two sensors were recording the same voltage output.

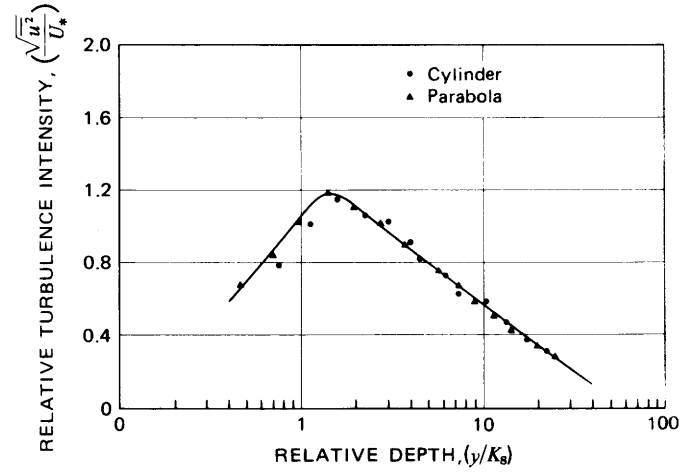

FIGURE 18.—Comparison of relative turbulence intensities obtained using a parabolic sensor and those obtained using a 0.002-inch-diameter cylindrical sensor in an 8-foot-wide flume.

These comparisons point out the need to investigate further the problems of errors in hot-film anemometry due to the influence of end losses on the low-frequency response.

READOUT AND SIGNAL-CONDITIONING EQUIPMENT

An anemometer system can be furnished with adequate readout equipment to make itself sufficient for mean-flow and turbulence measurements. A discussion of the output equipment that is used for various studies is helpful.

Several types of signal-handling equipment are used with anemometers for data analysis. The paragraphs below describe characteristics in the typical equipment used.

DIRECT-CURRENT MEASUREMENTS

Voltmeters. A basic d-c (direct-current) voltmeter is furnished with the anemometer for measurements of mean quantities. An accurate zero suppression circuit increases reading accuracy by subtracting a precise d-c voltage, allowing a very sensitive meter scale to measure the remainder. Accuracies of 0.1 percent are then possible. A digital voltmeter should be employed for highest accuracy. To improve on the accuracy of the d-c meter a 0.01 percent electronic digital voltmeter should be used. The servodriven digital voltmeters sometimes offered as anemometer accessories are usually not this accurate.

Sum-and-difference circuits. For a probe with two sensors in a cross arrangement, the instantaneous velocity components are proportional to the sum and difference of the signals from the two linearized anemometers. This is useful for directional work, but the sum-and-difference circuits must be capable of handling d-c signals as well as a-c (alternating-current) signals.

Recorders. Almost any strip-chart oscillographic or tape recorder can be used on the output of the anemometer. Since the anemometer is capable of high-speed measurements, a high-response recorder is often recommended.

Analog and digital computers. For computing vectors, angles, some correlations, phase shift, and so on, an external analog device (in addition to a sum-and-difference circuit) is sometimes utilized. Digitizing the anemometer output and analyzing data in a digital computer are also becoming popular.

ALTERNATING-CURRENT MEASUREMENTS

Root-mean-square voltmeters. The most common addition to any anemometer system is a true root-mean-square voltmeter to measure the root-mean-square average of flow fluctuations to get turbulence measurements. Recently, Thermo Systems Inc. introduced a root-mean-square meter optimally designed for mechanical-type measurements.

Output filters. For signals with a very wide frequency bandwidth, output filters can be used to eliminate signals not in the frequency range of interest. Also, some spectrum analysis can be done by bandpassing over the range of frequencies encountered.

Output amplifiers. When recorders do not have adequate sensitivity and (or) when very low level fluctuations are present, a calibrated low-noise amplifier can be very useful.

Correlators. Fluctuating signals are commonly correlated with one another with respect to location, direction, time, and so forth. A sum-and-difference correlator feeding its output into a true root-mean-square voltmeter can measure the cross-correlation functions for any two random signals. For autocorrelation measurements, a time-delay system must be incorporated. This can be a two-tape-head magnetic-tape system.

Spectral analyzers. For spectral analysis of turbulence, this type of instrument is a common addition. Spectral densities and probability densities can be obtained by variable bandpass filters, by a good commercial spectrum analyzer, or by autocorrelation.

Recorders. For high-frequency signals, an FM tape recorder is the best known method of recording. This allows for later analysis in a digital computer or other data-handling equipment. High-speed oscillographs are also common, but these are limited to frequencies on the order of 5–10 kHz.

OPERATION PROCEDURES

The researcher seeks to define turbulence characteristics in natural rivers and streams, where conditions are less than desirable for hot-film anemometry operations. Making turbulence measurements in water that is not filtered of all contaminants presents a constant problem. This section of the report explains in detail a procedure to circumvent contamination problems so that turbulence measurements can be made in natural rivers and streams. Mathematical and experimental justifications for using the procedure are presented.

MINIMIZING CONTAMINATION OF THE SENSOR

For turbulence measurements in water containing fluid-borne contaminants, the geometry of the parabolic sensor is much less conducive to contamination buildup than other sensor shapes. However, contamination is still a problem even with parabolic sensors.

Figure 19 illustrates four typical contamination problems that cause drift in the anemometer output signal. In figure 19*A*, the contamination was building up on the sensor slowly, causing a gradual decrease in the voltage. In figure 19*B*, the sensor was brushed at the beginning of the signal trace, and after a period of time the voltage drifted to a point where it remained fairly constant. This behavior is typical. After the sensor had been operating in a contaminated flow field for a short period, the contamination buildup seemed to reach a maximum, and the voltage then remained fairly constant. These voltage measurements are acceptable and can be interpreted with fairly good accuracy. They are about the best that can be expected in natural rivers and streams. In figure 19*C*, the sensor was hit by some foreign matter that remained attached to the sensor, reducing the heat transfer considerably and causing a sudden drop in the output voltage. In figure 19*D*, the sensor was being operated in a natural channel during spring runoff; the river was carrying about 6,000 milligrams per liter of suspended sediment as well as a great deal of foreign matter. The sudden voltage drops were caused by foreign matter becoming attached to the sensor. The voltage returned to its initial value after the foreign matter was swept off the sensor by the mean flow. These four conditions are common and must be remembered when such signals are used to obtain turbulence characteristics. To insure that the data are usable after the sensor becomes contaminated as illustrated in figures 19*A*, *C*, and *D*, measurements should be repeated until the voltage output trace is like those in figure 20, where no trends or discontinuities are present. A signal free of voltage drift will insure meaningful determination of turbulence characteristics. Where contamination problems are severe, obtaining a drift-free signal is time consuming but is worth the effort.

Figure 21 illustrates what happens to the output signal when sediment particles with a median diameter of about 0.2 millimeter collide with the hot-film sensor. In figure 21*A*, the sensor was not in a sediment-laden part of the flow; therefore, the output signal shows no pertubations other

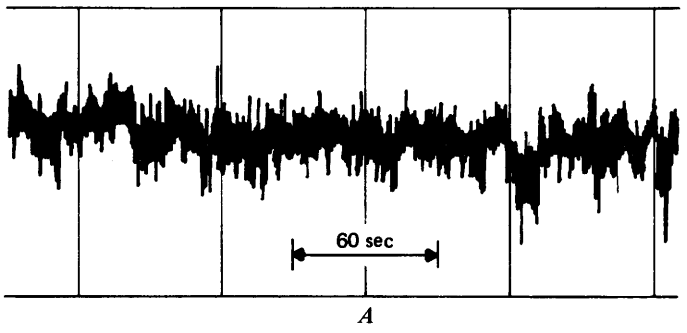

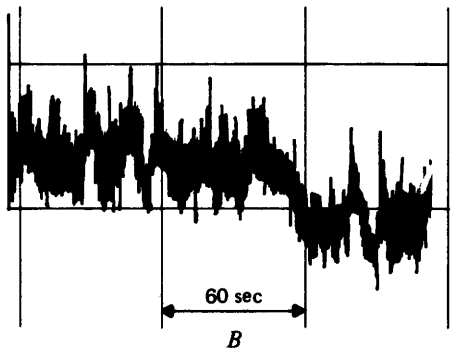

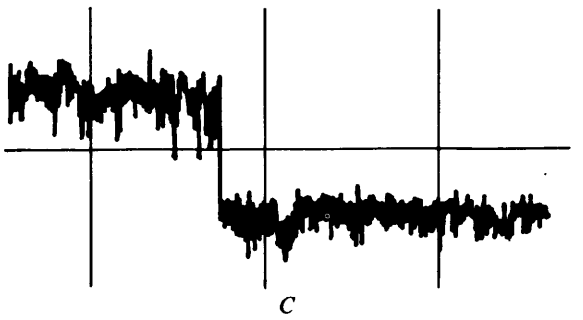

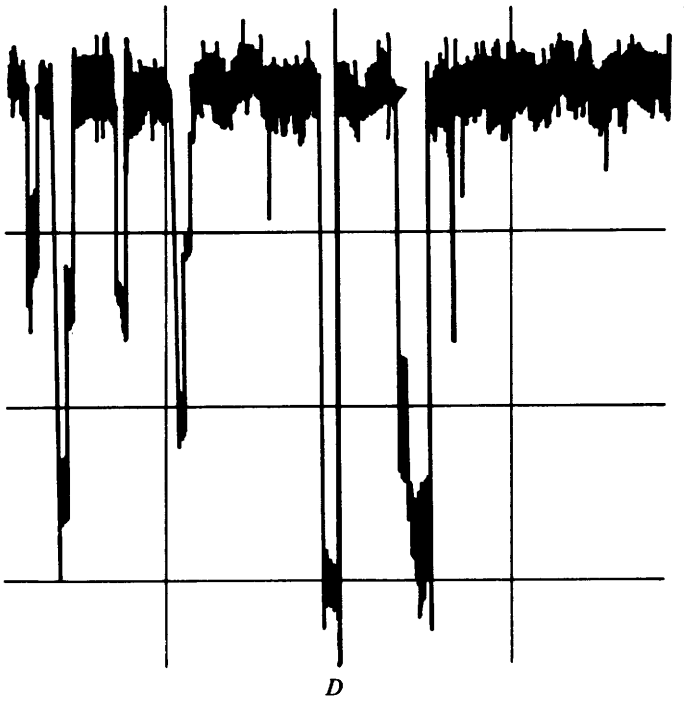

FIGURE 19.—Voltage traces of anemometer output with respect to time, showing drift due to contamination of the hot-film sensor. *A*, Contaminants build up gradually; *B*, contamination reaches a maximum and remains constant; *C*, a contaminant strikes the sensor and remains attached; *D*, contaminants become attached to the sensor but are soon swept away.

than those due to the flow field. In figure 21*B* and *C*, spikes are superimposed on the output signal as a result of sediment particles colliding with the sensor. The spikes are always in an increasing voltage direction. Their presence can complicate the data reduction.

Abrasion due to sediment particles hitting the sensor at the flow velocity wears the quartz coating off the sensor and thus exposes the platinum film. At an overheat ratio of 1.10, air bubbles are produced at the point of exposure; they affect the output voltage as illustrated in figure 22. The voltage rises gradually as an air bubble is formed and then falls sharply as the bubble is released owing to the convection of the flow. Bubbles can also form on a new sensor if the manufacturer has not completely covered the platinum film with quartz. Such sensors must be replaced, and the measurements must be repeated using a sensor that is completely covered with quartz.

CONVERTING VOLTAGE FLUCTUATIONS TO VELOCITY FLUCTUATIONS UNDER NATURAL FLOW CONDITIONS

The main problem in the use of hot-film anemometers is the conversion of measured voltage fluctuations to meaningful velocity fluctuations. When the actual voltage-velocity relation does not change with time, the conversion is accomplished by assuming that the mean values hold; thus, the relation can be linearized around the mean values, at which the tangent is assumed equal to the derivative, $d\overline{E}/d\overline{U}$, for the complete excursion of the fluctuations (fig. 12). When the water is contaminated, the conversion problem is further complicated by the fact that the voltage-velocity relation changes with time. Also, in natural rivers and streams the water temperature may change

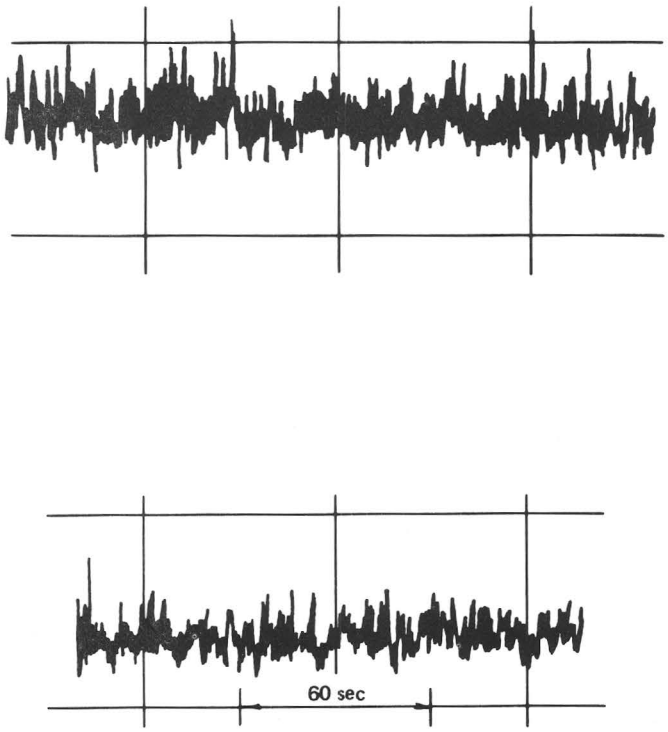

FIGURE 20.—Voltage traces of anemometer output with respect to time, showing no drift.

considerably during the measurement period, and this changes the voltage-velocity relation. In this section, a hypothesis and a procedure, along with mathematical and experimental justification, are outlined for converting voltage fluctuations to velocity fluctuations when the temperature of the flow field varies and (or) when the sensor is being contaminated by foreign matter in the flow.

HYPOTHESIS

The conversion of voltage fluctuations to velocity fluctuations when the actual mean voltage-velocity relation is changing because of probe contamination or fluid-temperature change is accomplished by assuming that at any point in time there is a new voltage-velocity relation for the contaminated probe. The change in the relation must remain constant during the measurement of the voltage fluctuation. The problem is to define the voltage-velocity relation at the time the voltage fluctuations are measured. The change in the voltage-velocity relation due to a contaminant buildup or fluid-temperature change can be assumed the same as the change which occurs for an uncontaminated sensor when the overheat ratio is decreased. The hypothesis (McQuivey, 1967) is that an accumulation of foreign matter on the sensor or an increase in the fluid temperature decreases the mean voltage for a given velocity but has only a minor effect on the frequency response of the sensor to velocity fluctuations.

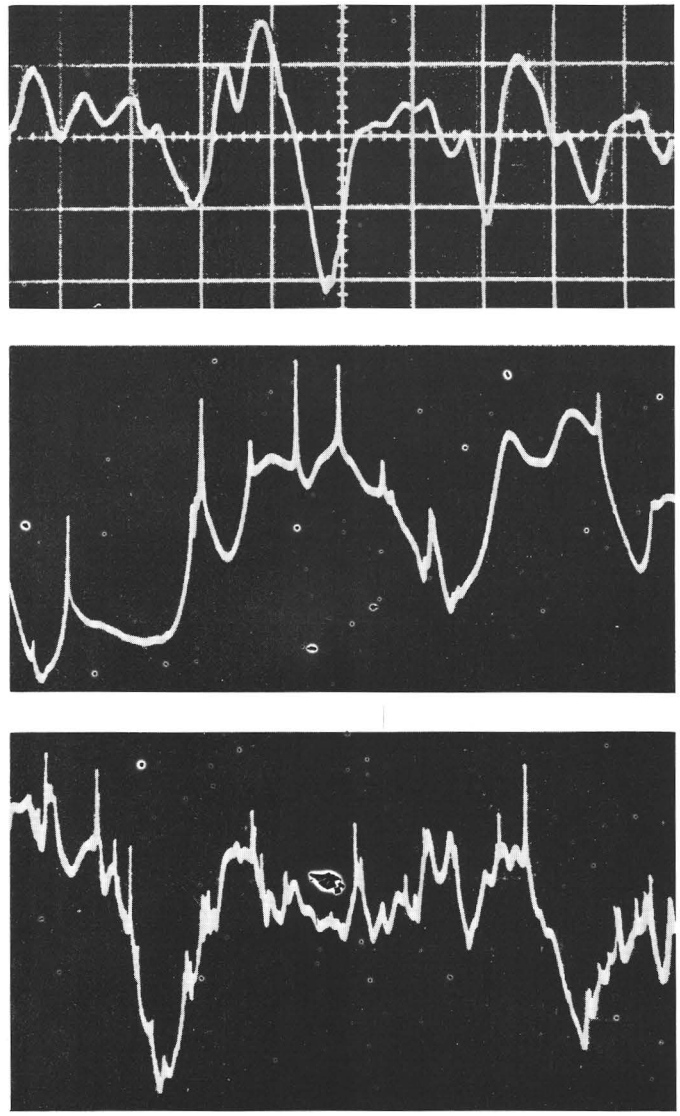

FIGURE 21.—Photographs of voltage traces of anemometer output with respect to time, showing superimposed spikes due to sediment particles colliding with the hot-film sensor. *A*, Normal trace; *B* and *C*, traces with spikes.

Each sensor has a unique family of voltage-velocity relations which can be defined by calibration with different overheat ratios.

To illustrate the hypothesis, consider figure 23. In a given flow field with constant $\overline{U}$ and $\sqrt{\overline{u^2}}$, $\overline{E}$ and $\sqrt{\overline{e^2}}$ will be equal to $\overline{E}_1$ and $\sqrt{\overline{e_1^2}}$ when the over-

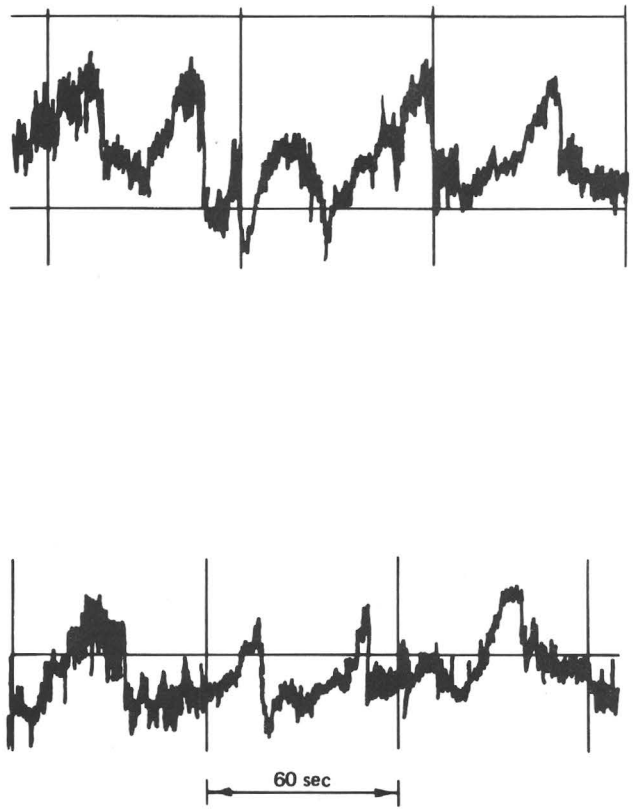

FIGURE 22.—Voltage traces of anemometer output with respect to time, showing the effect of air bubbles that form on the sensor.

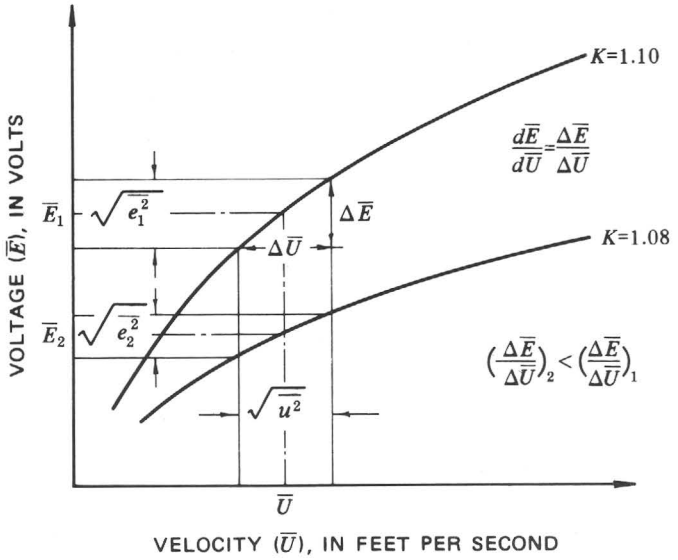

FIGURE 23.—Conversion of voltage fluctuations to velocity fluctuations in contaminated water.

heat ratio, K, is 1.10 and to $\overline{E}_2$ and $\sqrt{\overline{e_2^2}}$ when K is 1.08. The decrease of $\overline{E}$ from $\overline{E}_1$ to $\overline{E}_2$ and of $\sqrt{\overline{e^2}}$ from $\sqrt{\overline{e_1^2}}$ to $\sqrt{\overline{e_2^2}}$ is the direct result of the change in the voltage-velocity relation; if the correct relation is used to convert $\sqrt{\overline{e^2}}$ to $\sqrt{\overline{u^2}}$, the calculated $\sqrt{\overline{u^2}}$ will not change. If a sensor is operated at a constant K=1.10 but contamination buildup causes the voltage-velocity relation to change to that for K=1.08, then use of the calibration curve for K=1.08 to convert $\sqrt{\overline{e^2}}$ to $\sqrt{\overline{u^2}}$ will yield a more correct $\sqrt{\overline{u^2}}$.

MATHEMATICAL CONSIDERATIONS

The hypothesis implies that the voltage output from a sensor having a layer of contaminants (gaseous or solid) is the same as the output from a sensor having no layer of contaminants and being used at a reduced value of overheat ratio. This reduced value can be referred to as an apparent overheat ratio.

At equilibrium heat-transfer conditions, the heat produced in the film is equal to that which is radiated away plus that which is convected away by the flow. That is,

$$H_j=H_c+H_r, \tag{72}$$

where H_j is the electrical (Joulean) heat produced per unit length, H_c is the convective heat transferred per unit length, and H_r is the radiant heat transferred per unit length. Experimental work has shown that the radiant heat transfer is very small compared with the convective heat transfer and may be neglected. Thus,

$$H_j \approx H_c.$$

The major heat-transfer relation applied in hot-film and hot-wire anemometry is

$$H=sh\,(T_s-T_a), \tag{73}$$

where

H=thermal power (time rate of thermal heat) transferred from the sensor to the fluid,
s=area of the sensor,
T_s=sensor temperature (hot),
T_a=fluid or environment temperature (cold), and
h=heat-transfer coefficient.

The condition of thermal equilibrium requires that the rate of heat generated electrically in the sensor equal the heat passed to the fluid, so

$$H=\frac{\overline{E}^2}{R_s\epsilon_*}, \tag{74}$$

where $\overline{E}$ is the mean voltage across the sensor, R_s is the operating resistance of the sensor, and ϵ_* is the energy conversion factor. Thus, the energy balance becomes

$$\frac{\overline{E}^2}{R_s\epsilon_*}=sh\,(T_s-T_a). \tag{75}$$

To convert this to an expression involving the desired variables, the change in resistance of the sensing material due to a change in temperature is

$$R_s=R_a[1+\beta_*(T_s-T_a)], \tag{76}$$

where R_a is the resistance of the sensor at fluid temperature, T_a, and β_* is an experimentally determined constant. Equation 76 can be rearranged as

$$T_s-T_a=\frac{R_s-R_a}{R_a\beta_*}. \tag{77}$$

Substituting equation 77 into equation 75,

$$\frac{\overline{E}^2}{R_s\epsilon_*}=sh\left(\frac{R_s-R_a}{R_a\beta_*}\right), \tag{78}$$

which is solved for $\overline{E}^2$ as

$$\overline{E}^2=sh\,\frac{R_s\epsilon_*}{\beta_*}\left(\frac{R_s-R_a}{R_a}\right). \tag{79}$$

Defining R_s/R_a as the overheat ratio, K, equation 79 becomes

$$\overline{E}^2=sh\,\frac{\epsilon_*}{\beta_*}KR_a\,(K-1). \tag{80}$$

Or

$$\overline{E}=\left[sh\,\frac{\epsilon_*}{\beta_*}KR_a\,(K-1)\right]^{\frac{1}{2}}. \tag{81}$$

The assumption made is that the voltage output from a sensor having on it a layer of contaminants, which cause a reduction in the heat-transfer coefficient, is the same as the output from an uncontaminated sensor at a reduced value of the overheat ratio. Mathematically, this is equivalent to saying that at a given velocity the derivative of the output voltage with respect to the overheat ratio is a constant multiple of the derivative of the output voltage with respect to the heat-transfer coefficient.

The derivative of the output voltage, $\overline{E}$, with respect to the heat-transfer coefficient, h, is

$$\frac{\partial\overline{E}}{\partial h}=\frac{1}{2h^{\frac{1}{2}}}\left[s\,\frac{\epsilon_*}{\beta_*}KR_a\,(K-1)\right]^{\frac{1}{2}}. \tag{82}$$

Equation 81 can be rearranged as

$$\overline{E}=\left(sh\,\frac{\epsilon_*}{\beta_*}R_a\right)^{\frac{1}{2}}(K^2-K)^{\frac{1}{2}},$$

so the derivative of $\overline{E}$ with respect to the overheat ratio, K, can be expressed as

$$\frac{\partial\overline{E}}{\partial K}=\frac{1}{2}\left(sh\,\frac{\epsilon_*}{\beta_*}R_a\right)^{\frac{1}{2}}\left(\frac{2K-1}{(K^2-K)^{\frac{1}{2}}}\right).$$

This can be rearranged as

$$\frac{\partial\overline{E}}{\partial K}=\frac{1}{2K^{\frac{1}{2}}}\left(\frac{2K-1}{(K-1)^{\frac{1}{2}}}\right)\left(sh\,\frac{\epsilon_*}{\beta_*}R_a\right)^{\frac{1}{2}}. \tag{83}$$

Note from equations 82 and 83 that the change in $\overline{E}$ due to an incremental change in K is *not* directly proportional to the incremental change in h. Only if the expression

$$\frac{2K-1}{K-1} \tag{84}$$

behaves nearly as a constant over the range of change in K will this technique be valid. The most direct method of evaluating expression 84 is to substitute in typical values of K, as shown below:

K	$\frac{2K-1}{K-1}$
1.11	11.09
1.10	12.00
1.09	13.11
1.08	14.50

The deviation of the value of expression 84 from its value at $K=1.10$ is about 10 percent for a 1 percent change in K.

On the basis of these mathematical considerations, the hypothesis cannot be justified. However, such a mathematical exercise of a less-than-ideal and complicated heat-transfer process can only be, at best, a rough estimate. Experimental justification of the hypothesis is the only way to verify its applicability.

Experimental verification of the hypothesis is shown in figure 24 and Table 1 (Richardson and McQuivey, 1968). In this experiment, a 0.002-inch-diameter cylinder was used, and the water was contaminated by adding clay and fibers. The

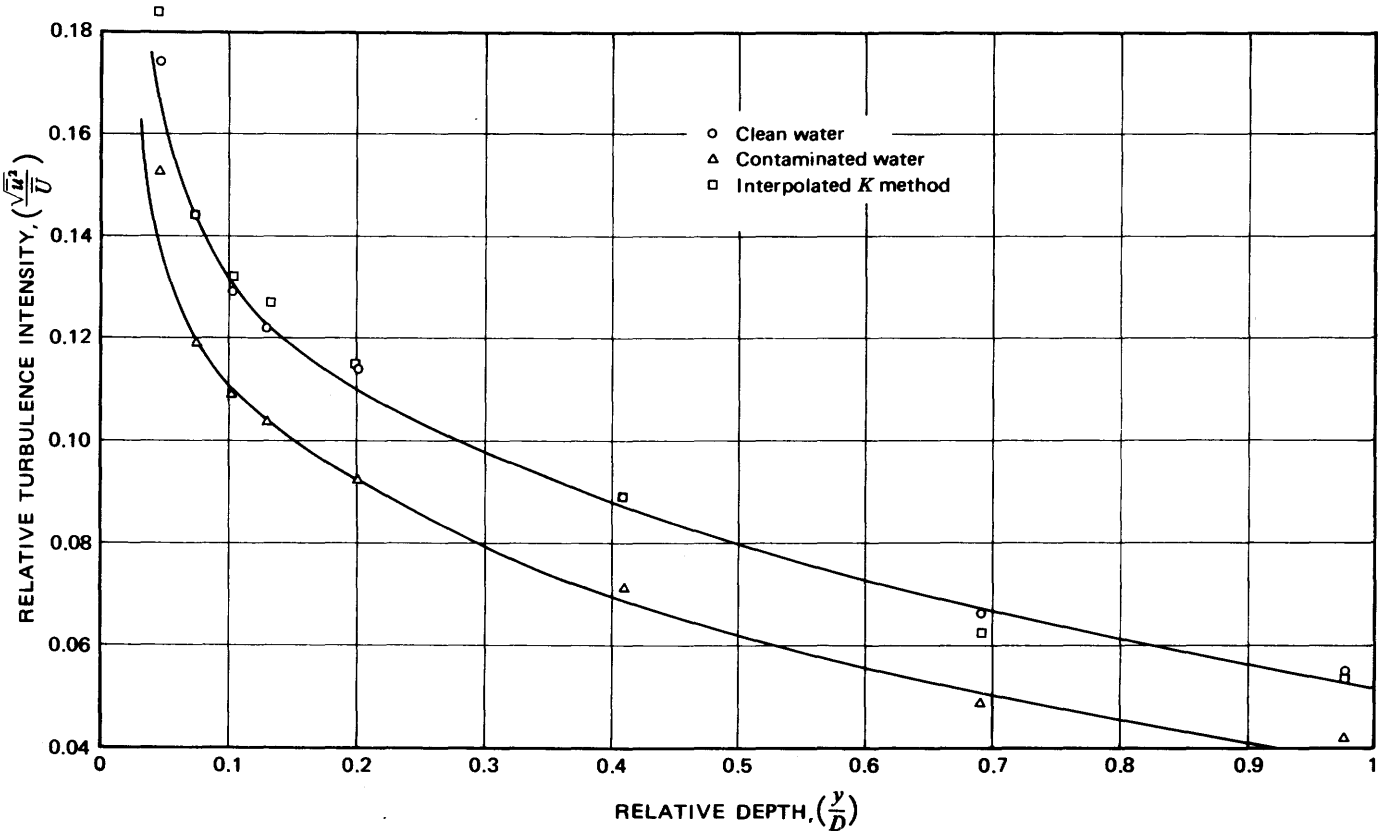

FIGURE 24.—Comparison of relative turbulence intensities measured in clean water, those measured in contaminated water, and those corrected (using interpolated K values) for measurements made in contaminated water.

change in mean voltage for a given velocity ranged from 15 to 20 percent.

The velocity ranged from about 1 to 3 fps and averaged 2.26 fps. Uncorrected values for turbulence intensity measured in contaminated water were about 12–25 percent below intensity values measured in clean, well-filtered water. The corrected values were within about 3 percent of the values measured in clean water.

Resch (1970) claimed to have verified the hypothesis in tests using a wedge hot-film sensor in flow velocities of 1–3 meters per second. Resch compared mean velocity values measured prior to contamination with corrected values of measurements made in contaminated water.

Experimental results seem to verify the hypothesis, which allows turbulence measurements to be made in flows where contamination is a constant problem. The correction technique yields turbulence intensities within about 3 percent of measurements made in well-filtered water where contamination is not a problem and where velocities are greater than 1 fps.

TABLE 1.—*Comparison of relative turbulence intensities,* $\sqrt{\overline{u^2}}/U_A$, *in percent, measured in clean and contaminated water*

Relative depth (percent)	Clean water (measured $\sqrt{\overline{u^2}}/U_A$)	Contaminated water			
		Uncorrected sensitivity		Corrected sensitivity	
		Measured $\sqrt{\overline{u^2}}/U_A$	Deviation from clean water (percent)	Measured $\sqrt{\overline{u^2}}/U_A$	Deviation from clean water (percent)
0.048	0.174	0.153	−12.05	0.186	6.90
.076	.143	.119	−16.78	.143	0
.103	.129	.109	−15.45	.132	2.32
.131	.122	.104	−14.75	.127	4.10
.201	.114	.092	−19.30	.115	.88
.410	.087	.072	−17.24	.089	2.30
.692	.066	.049	−25.80	.062	−6.07
.970	.055	.042	−23.65	.054	−1.82

CORRECTION PROCEDURE

The correction procedure as applied to measurements of turbulence intensity in contaminated water is as follows:

1. Define the voltage-velocity relation for an uncontaminated probe for different overheat ratios (fig. 25). This calibration can be done in nearly clean water if the probe is carefully brushed before each measurement. For the curves illustrated, the mean velocity was measured using a pitot tube, and the mean voltage was the output from a 0.002-inch-diameter cylindrical hot-film anemometer.

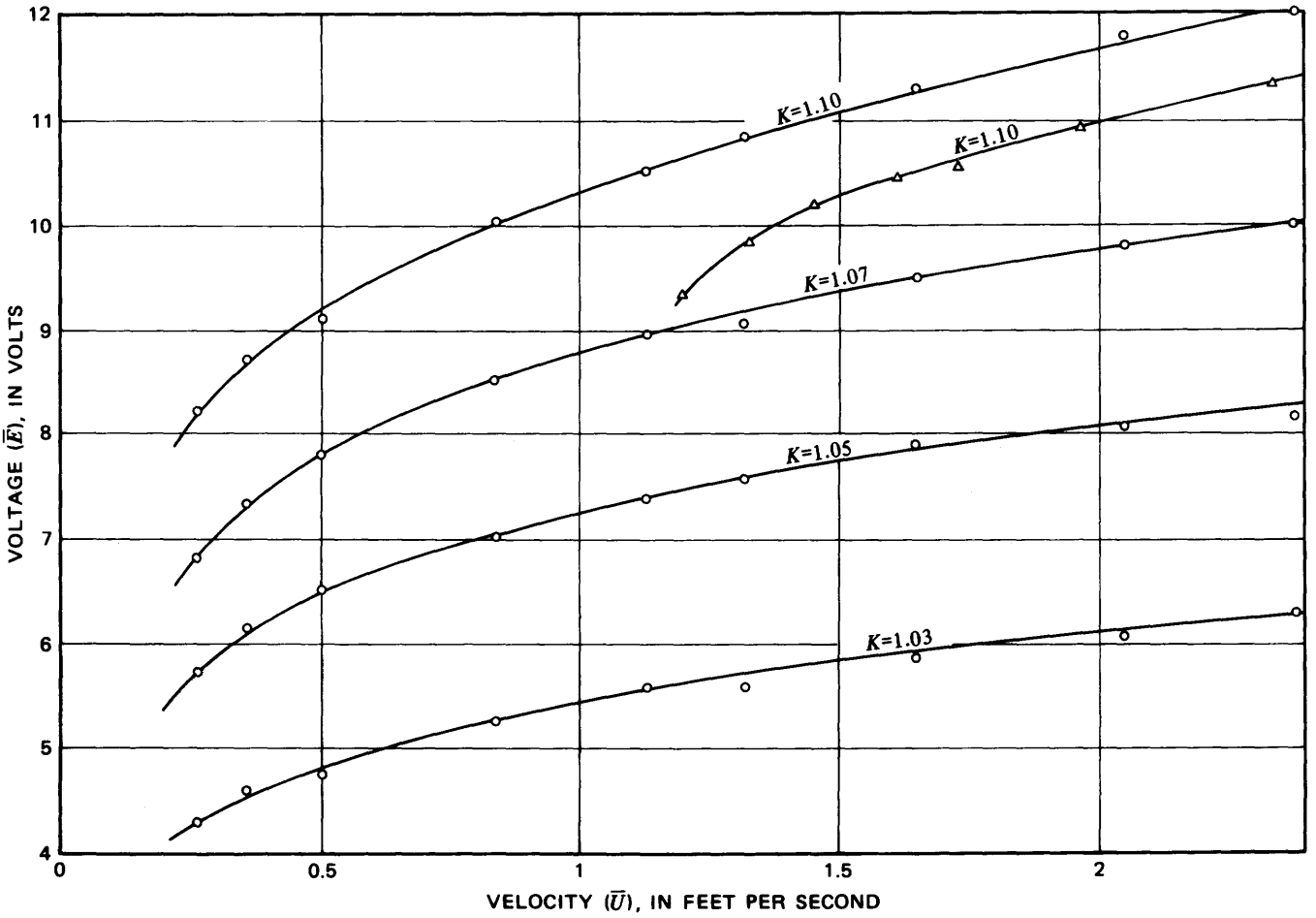

FIGURE 25.—Voltage-velocity relation for various overheat ratios in uncontaminated water. Triangles denote measurements in contaminated water.

2. Measure graphically the sensitivity, $d\bar{E}/d\bar{U}$, of the voltage-velocity relation, and plot it as a function of the mean velocity for various overheat ratios (fig. 26).
3. Now, in contaminated water, measure the mean voltage and the root mean square of the fluctuations at a point by using the hot-film anemometer, and measure the mean velocity at the point by using a pitot tube or some other suitable velocity transducer. The velocity measurements can be made either before, after, or simultaneously with the voltage measurements.
4. Plot the mean velocity and the mean voltage for the point in the flow on the voltage-velocity graph for uncontaminated water (note the triangles in fig. 25); the correct overheat ratio for the contaminated water can then be chosen. Use the mean velocity and the overheat ratio to determine the sensitivity of the voltage-velocity relation from figure 26. Of course, the voltage-velocity relation for the exact overheat ratio for every point in the voltage-velocity space cannot be determined, so the sensitivity is interpolated from the nearest overheat-ratio curve.
5. Calculate $\sqrt{\overline{u^2}}$ by using equation 51 or 69 and by substituting in the measured $\sqrt{\overline{e^2}}$ and the sensitivity as determined from the interpolated overheat ratio on the sensitivity-velocity graph. The turbulence intensity is then $\sqrt{\overline{u^2}}/\bar{U}$.

ANALYSIS OF DATA

ANALOG DATA REDUCTION

Because the data are initially in analog form, they can be analyzed by employing analog equipment. The analog output should be monitored continually to determine whether the measurements should be retaken.

The most common addition to any anemometer system is a root-mean-square voltmeter. This

analog instrument gives the root-mean-square value of the voltage fluctuation, a value sometimes referred to as the variance. Caution should be taken, however, in using this value as the true variance, because these voltmeters are not accurate at low frequencies (down to d-c level). Most presently available commercial root-mean-square voltmeters will underregister the power by 10–20 percent because of the low-frequency cutoff.

Correlations and power spectra can be obtained using analog instrumentation. If the experiment involves a great deal of data reduction, analog equipment may be cheaper to use than digital computer equipment. However, most available analog correlators and spectrum analyzers are not designed to analyze low-frequency input data, which are characteristic of open-channel turbulent shear flows.

For these reasons, the analog output signal is usually recorded on an FM magnetic-tape recorder and analyzed digitally. However, in order to obtain the turbulence intensities in natural channels, where contamination is a problem, the use of both analog and digital techniques is advisable.

DIGITAL DATA REDUCTION

A digital computing system and accessory equipment can be used in the data reduction. A schematic diagram of the system is shown in figure 27. The output voltage from the hot-film anemometer is recorded on FM magnetic tape. Although magnetic-tape recorders are useful for storing information, they introduce errors into the mea-

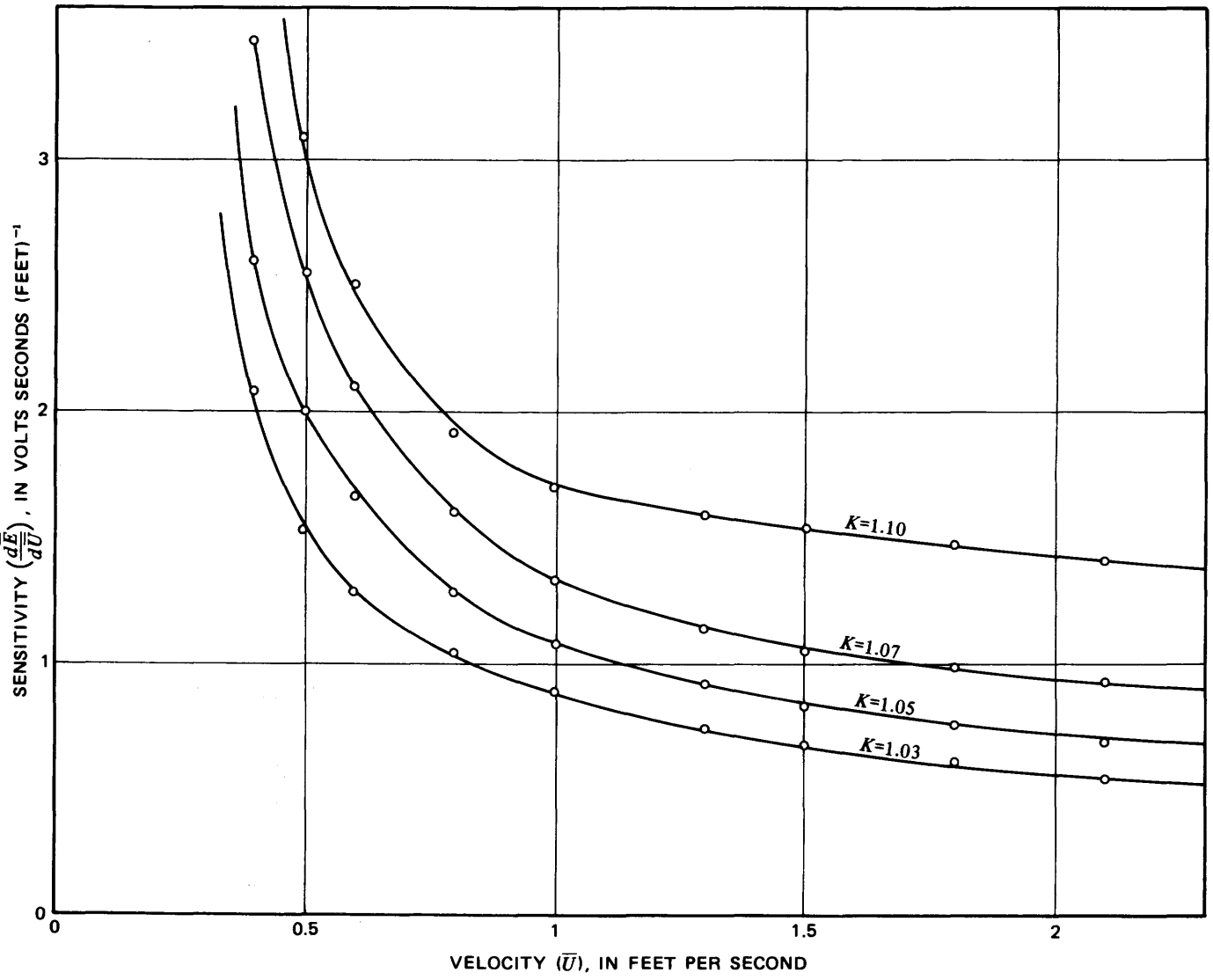

FIGURE 26.—Sensitivity-velocity relation for various overheat ratios in uncontaminated water.

surement process. Extraneous signals due to imperfect mechanical translations of the tape in both record and playback mode are possible. For these reasons, reference signals of known frequencies and root-mean-square levels are recorded along with the anemometer output. These reference signals are used in the digital data reduction to insure accuracy and to recover the original data which may have been subsequently changed in magnitude or frequency, owing to signal conditioning.

The data on the FM tapes are fed into a multiplexer and then into an analog-to-digital converter. The digital voltage outputs are stored on digital magnetic tape in a format compatible with the digital computing system. These data are then run through a computer program to obtain the mean voltage, $\overline{E}$; the root mean square of the voltage fluctuation, $\sqrt{\overline{e^2}}$; the variation of the autocorrelation function with time, $R(\tau)$; the energy-spectrum function, $F(f)$; and other desired statistical characteristics. A complete software documentation is given in the appendix. This program can be used to calculate the mean, the standard deviation, the skewness factor, and the flatness factor, and it can eliminate any trends; it can also be used to calculate and plot the number of crossings, the probability density and empirical density, the autocorrelation, the cross correlation, the power spectral density, the cross spectral density, the phase angle for one or two time series, the Hurst Range, and a self similarity analysis. The following paragraphs discuss the derivation of the major statistical characteristics.

The hot-film sensor must first be calibrated for the velocity range to be measured and for several overheat ratios. The calibration is not incorporated in the computer analysis because of possible voltage drift due to contaminant buildup; this drift can best be taken into account by the procedure already outlined. However, the digital value of the output variance, $\sqrt{\overline{e^2}}$, is used to calculate the intensity of turbulence.

The mean voltage and the root mean square of the voltage fluctuation are evaluated directly in the usual manner if all trends in mean voltage are removed; so

$$\overline{E}=\frac{1}{N}\sum_{n=1}^{N} E_n \tag{85}$$

and

$$\sqrt{\overline{e^2}}=\left[\frac{1}{N}\sum_{n=1}^{N}(E_n-\overline{E})^2\right]^{\frac{1}{2}},$$

where N is the total number of digitized data points and n is an index associated with the digitized data.

Digital analysis eliminates the problem associated with the low-frequency distortion caused by analog equipment, if the sample is taken for a sufficiently long period of time.

The accuracy of the root-mean-square value, the energy-spectrum function, the autocorrelation function, and other statistical computations depends largely on the digitized sampling interval, Δt, and the length of record, T. These two factors demand a compromise between economy and accuracy. This can be understood by considering the equations used in developing the computer program.

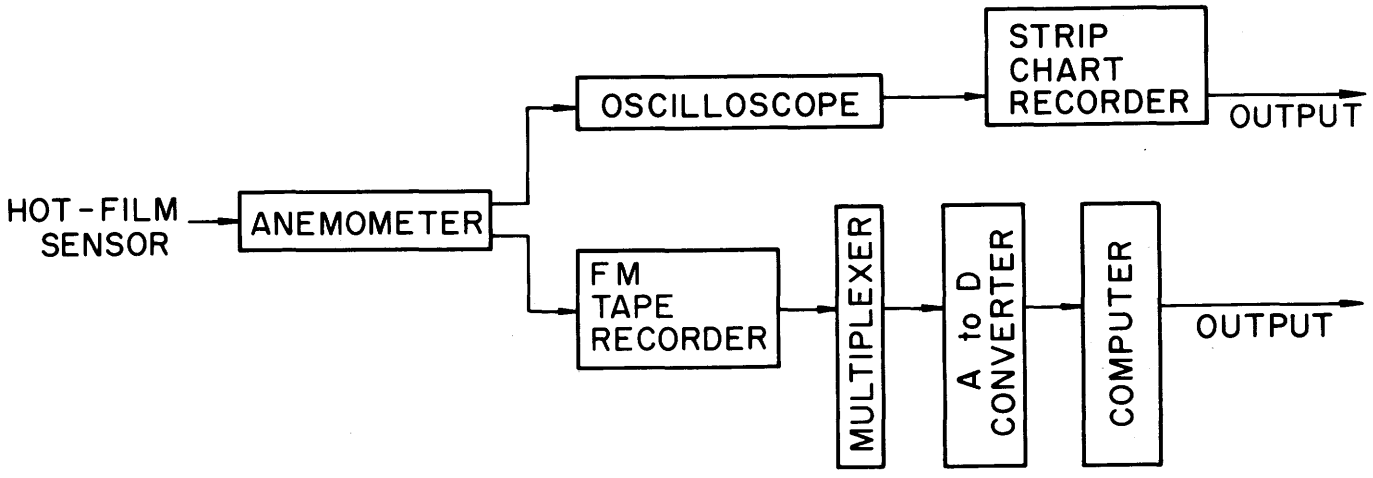

FIGURE 27.—Schematic diagram of the equipment system used in digital data reduction. A to D, analog to digital.

The autocorrelation function, $R(\tau)$, is defined in a continuous sense as

$$R(\tau)=\lim_{T\to\infty}\int_0^T \overline{u(t)\,u(t+\tau)}\,dt. \tag{86}$$

In the discrete form, equation 86 is

$$\left.\begin{aligned} R_m&=\frac{1}{N-m}\sum_{n=1}^{N-m}\overline{u_n\,u_{n+m}}\\ n&=1,\,2,\,3\ldots.N\\ m&=0,\,2,\,3\ldots.M\end{aligned}\right\} \tag{87}$$

where R_m is a digital autocorrelation function, m is an index associated with the function, and M is the total number of lags in the function. The autocorrelation lag is $\tau=m\Delta t$ for a data sampling interval, Δt. The distribution of the autocorrelation function with delay time τ provides an estimate of the eddy size associated with the turbulent flow.

The energy-spectrum function, $W(f)$, is defined as the cosine transformation of the autocorrelation function:

$$W(f)=4\int_0^\infty R(\tau)\cos\omega\,\tau d\tau, \tag{88}$$

where $f=\omega/2\pi$, in which f is the frequency, in hertz, and ω is the angular frequency, in radians per second.

The fraction of the turbulent energy associated with a frequency band, df, is then $W(f)df$; hence, the area under the energy-spectrum curve is equal to the root mean square of the turbulence fluctuation, $\sqrt{\overline{u^2}}$. Equation 88 can be rewritten, following the procedure of Blackman abd Tukey (1958), as

$$\left.\begin{aligned} P_q&=2\Delta t\,R_o+2\sum_{m=1}^{M-1}R_m\cos\frac{mq\pi}{M}+R_M\cos q\pi\\ q&=0,\,1,\,2\ldots M\\ m&=1,\,2,\,3\ldots M\end{aligned}\right\} \tag{89}$$

where R_o, R_m, and R_M are digital autocorrelation functions and P_q is a digital estimate of the energy-spectrum function associated with the discrete correlation function defined by equation 87 rather than the continuous function defined by equation 86. Because P_q is a discrete cosine transformation, the spectral estimates at any frequency are affected by the energy in neighboring frequencies (Bendat and Piersol, 1966). To obtain a better spectral estimate than that of equation 89, a simple smoothing operation can be performed. The Hanning procedure was used, and the final spectral estimates are given as

$$\left.\begin{aligned} W_o&=0.5\,P_o+0.5\,P_1\\ W_q&=0.25\,P_{q-1}+0.5\,P_q+0.25\,P_{q+1}\\ W_M&=0.5\,P_{M-1}+0.5\,P_M\end{aligned}\right\} \tag{90}$$

Equations 88, 89, and 90 form the basis for the numerical evaluation of the energy-spectrum function. A more detailed evaluation of these procedures is available in Blackman and Tukey (1958), Bendat and Piersol (1966), and in the appendix at the end of this report.

A normalized energy-spectrum function, $F(f)$, has already been defined (eq 17), where, in a continuous sense,

$$\int_0^\infty F(f)\,df=1.$$

Therefore, the digital counterpart of $F(f)$ is F_q, defined as $F_q=W_q/\sqrt{\overline{u^2}}$.

The values selected for the parameters N, M, and Δt in the equations above determine the amount of compromise between frequency resolution and length of record. Limits are largely dictated by f_c, the highest frequency component present. This requires prior knowledge of the spectral distribution or trial and error.

Once f_c has been selected, the time interval between samples, Δt, is governed by the requirement that two samples be measured per cycle of the highest frequency present; that is,

$$\Delta t=\frac{1}{2f_c}. \tag{91}$$

The resolution of the estimates is determined by the equivalent band width, B_e, of the digital filter, and

$$B_e=\frac{1}{T}=\frac{1}{M\Delta t}, \tag{92}$$

where T is the length of record.

The accuracy of the estimates is determined by the degrees of freedom of the chi square of the energy spectral density at a chosen confidence level. This is approximately twice the number of data points divided by the number of autocorrelation lags. In the interval $\Delta f=B_e$, the energy spectrum is customarily assumed to be the same as that for a band width limited to white noise. In this case,

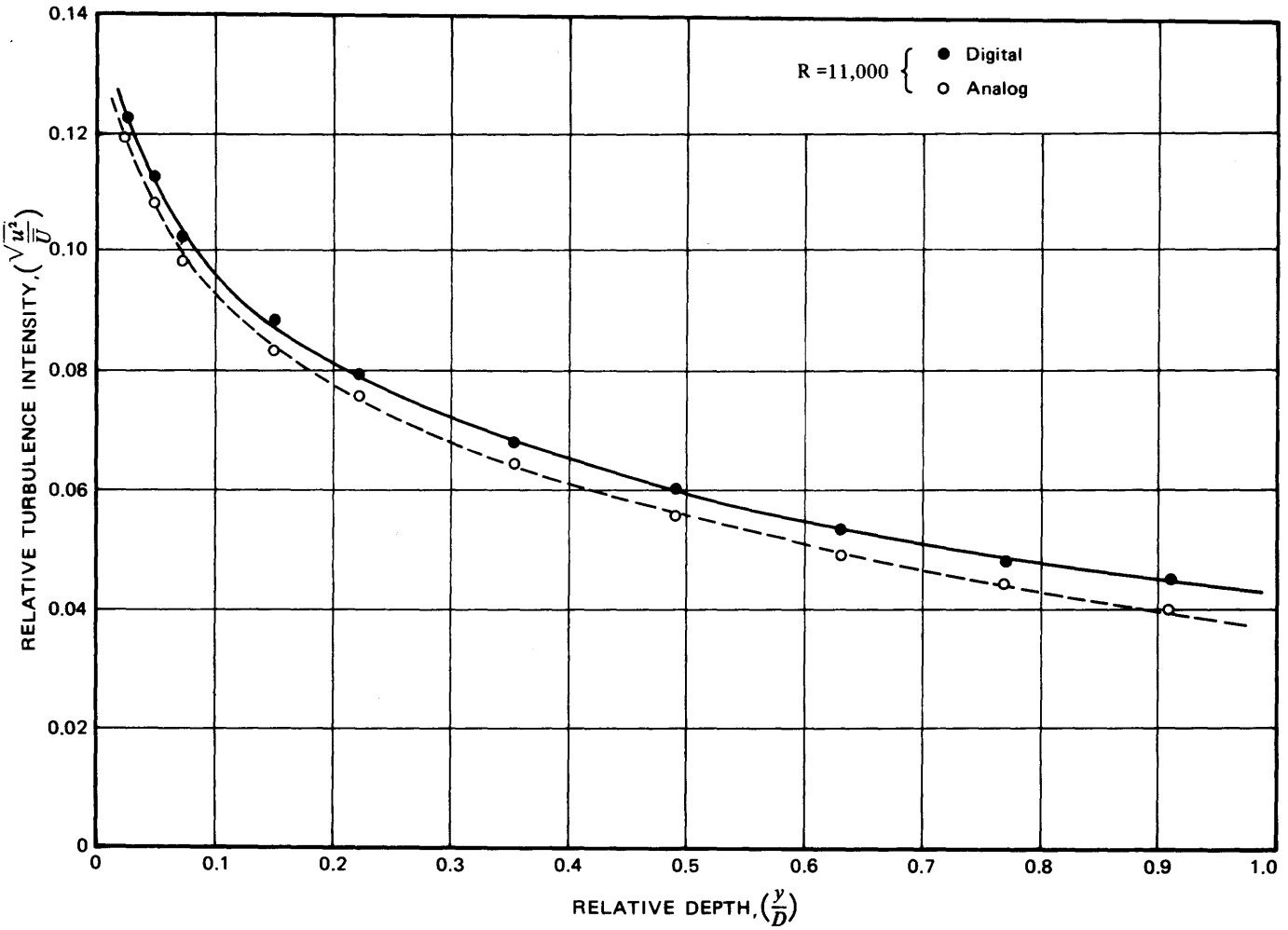

FIGURE 28.—Comparison of relative turbulence intensities obtained by analog and digital data-reduction techniques.

$$d' = 2B_e T \tag{93}$$

and

$$T = N\Delta t. \tag{94}$$

Therefore, d' controls the accuracy of the estimate, B_e controls the resolution, and T is governed by economic factors or computer storage limitations. Since the three are intimately related, a compromise is necessary in their selection.

ANALOG VERSUS DIGITAL ANALYSIS

Relative turbulence intensities obtained using the digital techniques are about 8–12 percent larger than those obtained using the analog techniques (fig. 28). The difference is due to the low-frequency cut off (0.5 Hz) of the analog root-mean-square voltmeter. In a large river system the difference was found to be as much as 25 percent because most of the energy was below 2 Hz. The digital system has the distinct advantage of having better resolution in the low-frequency range.

Figure 29 shows a typical energy spectrum computed by both analog and digital methods. The two methods are in good agreement. However, the analog curve was extrapolated for the frequencies less than 0.5 Hz.

In addition to having more accurate resolution at the low frequencies, the digital technique of data reduction has the advantage that the autocorrelation function, energy-spectrum function, and scales of turbulence can all be obtained using only one program. Analog data reduction employs a different piece of electronic equipment to obtain each of these turbulence characteristics. The disadvantages of digital data reduction are the problems of digitizing the data, the time lag between experiment and analysis, aliasing errors, filtering, and a bias of spectral estimates. Analog data reduction enables the results to be obtained

during the experiment or almost immediately thereafter. The time lag in digital data reduction depends on the particular institution and computer facilities. Nevertheless, analog data reduction is usually faster than digital.

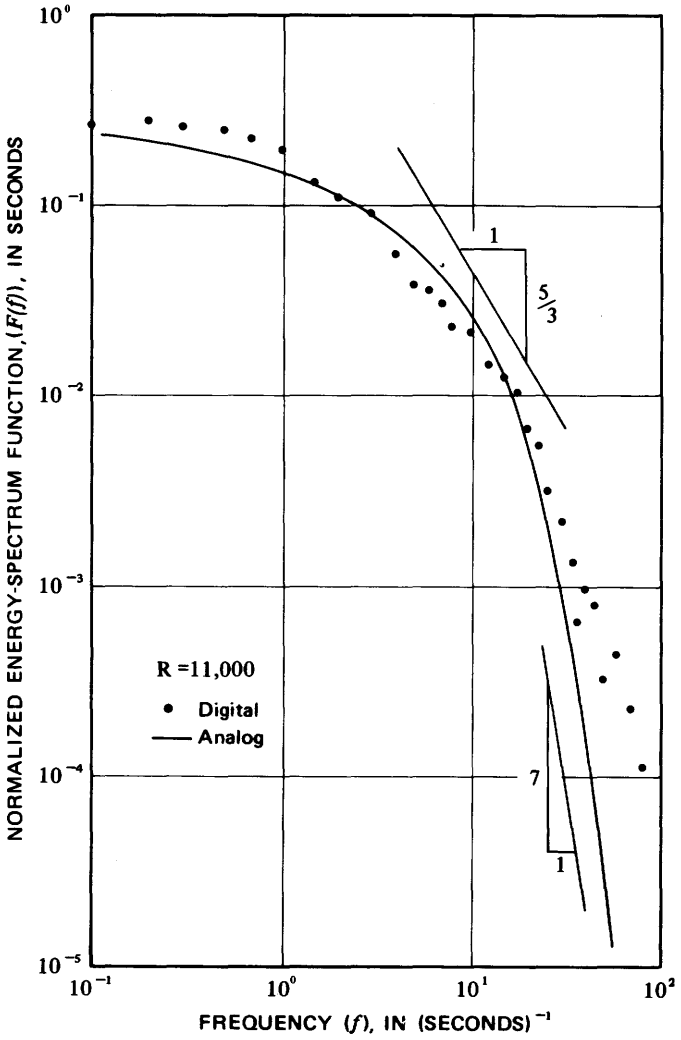

FIGURE 29.—Comparison of energy spectra obtained by analog and digital data-reduction techniques.

DETERMINATION OF PARAMETERS FOR DATA REDUCTION

The following questions must be answered before the energy spectra can be analyzed: (1) What length of record, T, shall be obtained? (2) How small shall the data sampling interval, Δt, be? (3) How many lags, M, shall be computed in the autocorrelation function?

Any investigation of the turbulence characteristics of a fluid flow, whether by analog or digital means, requires a minimum length of record. Figure 30 presents two examples of how sampling time affects measurements of the mean velocity and the root mean square of the velocity fluctuation.

In Figure 30*A*, 100 seconds of record, digitized at 0.01-second intervals, was obtained for an 8-inch-wide flume. Note that the mean velocity obtained after 1 second differs by less than 2 percent from the value obtained after 100 seconds. The root mean square of the velocity fluctuation shows a difference of about 20 percent for the same sampling interval. However, the difference in root-mean-square value at about 50 seconds compared with the value at 100 seconds is less than 2 percent. Therefore, a sampling time of greater than 50 seconds is needed to obtain a reasonable root-mean-square value.

In Figure 30*B*, 350 seconds of record, digitized at 0.01-second intervals, was obtained for the Mississippi River. Note that the mean velocity obtained after 1 second differs by about 10 percent from the value obtained after 250 seconds. The root mean square of the velocity fluctuation shows a difference of about 35 percent for the same sampling interval. However, the difference in root-mean-square value at 200 seconds compared with the value at 350 is less than 5 percent. Therefore, a sampling time of greater than 200 seconds is needed to obtain a reasonable root-mean-square value.

The first question can be answered on the basis of the results shown in figure 30. Because the area under the energy-spectrum curve is directly proportional to the root mean square of the velocity fluctuation, the length of record used for analyzing spectral content should be at least equivalent to that used for the root-mean-square determination.

The data sampling interval should be one-half the period of the highest frequency component observable in the record (Bendat and Piersol, 1966). An oscilloscope display of the hot-film output showed that the highest frequency component observable in the signal was 50 Hz for the Mississippi River and 100 Hz for the 8-inch-wide flume. Therefore, the highest frequency that can be detected in the spectrum is f_c, where $f_c=1/(2\Delta t)$. This frequency is usually referred to as the folding frequency or the cutoff frequency; the spectrum is "folded" about that point, and the energy at frequencies greater than f_c is transposed into the energy at frequencies less than f_c (Bendat and Piersol, 1966).

The third question, regarding the number of lags, is answered on the basis of the reliability of

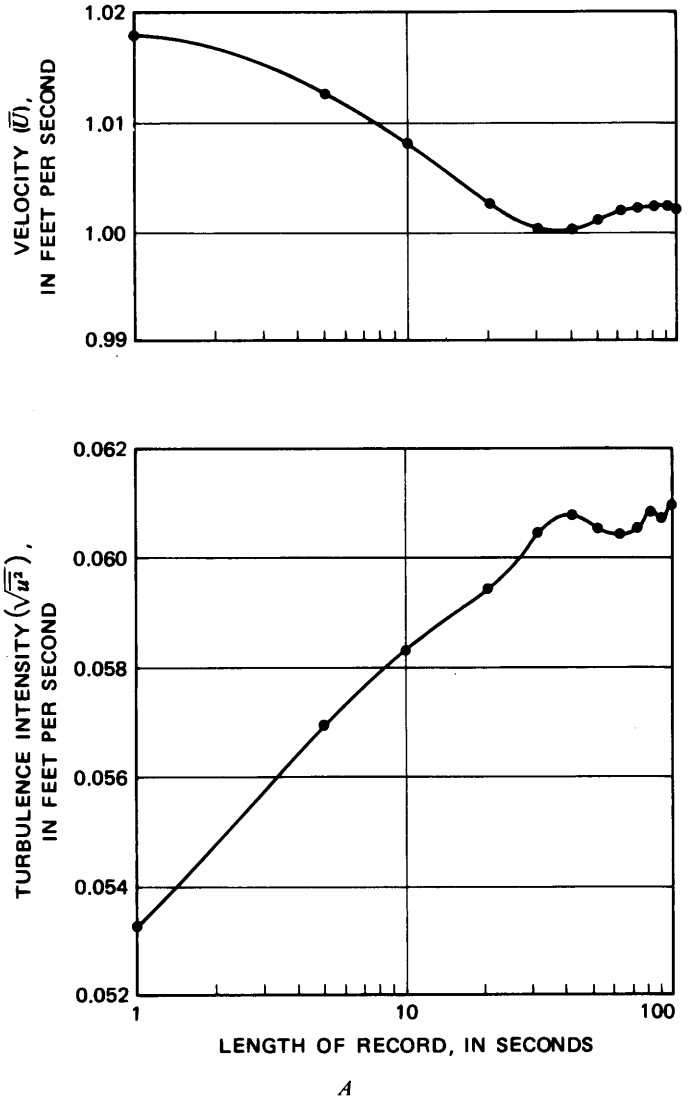

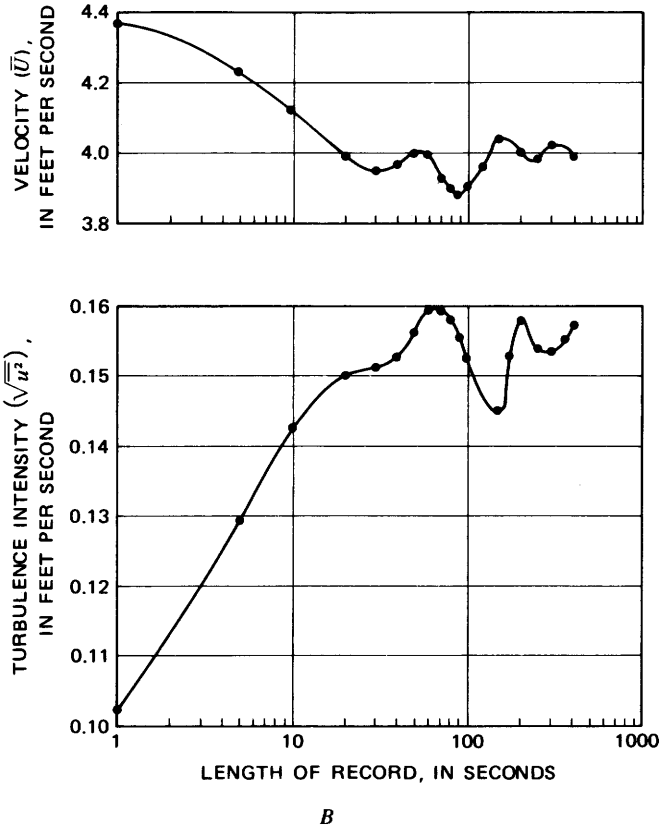

FIGURE 30.—Variation in the mean velocity and the root mean square of the velocity fluctuation with respect to time. *A*, 8-inch-wide flume; *B*, Mississippi River.

the spectral estimates and the frequency definition desired in the spectrum. The reliability is based on the degrees of freedom of the data, which is approximately twice the number of data points divided by the number of autocorrelation lags. The degrees of freedom defines the possible error in the computed spectrum; that is, it defines the 95- and 5-percent confidence limits of the spectrum (Raichlen, 1967). For the 8-inch-wide flume, f_c=100 Hz, Δt=0.005 second, and T=100 seconds, so there were 20,000 data points; the number of lags was 200, so there was 200 degrees of freedom. Two hundred degrees of freedom results in possible errors in the spectral estimates of 0.79 and 1.29 times the computed estimates for the 95- and 5-percent confidence limits, respectively. For the Mississippi River, f_c=50 Hz, Δt=0.01 second, and T=250 seconds, so there were 25,000 data points; the number of lags was 1,000, so there was 50 degrees of freedom. Fifty degrees of freedom results in possible errors in the spectral estimates of 0.75 and 1.45 times the computed estimates for the 95- and 5-percent confidence limits, respectively. Therefore, the number of lags should be chosen so that degrees of freedom and errors in the spectral estimates are low.

Once the three questions have been answered and measurements have been taken, the results should be scanned for possible problems that were not detected while collecting the data. Figures 31 and 32 illustrate a mechanical vibration problem of the probe holder and sensor that was not detected while collecting the data.

CONCLUSIONS

A large number of fluid mechanics phenomena are either entirely caused or strongly influenced by the turbulence structure of the flow. Therefore, an understanding of the mechanism of turbulent motion is essential to understanding these phenomena.

Because a general physical model on which to base an analysis has not been formulated, a statistical approach is used to obtain the variables

in the basic equations of motion and in the energy equation.

The approach to the problem is to experimentally obtain as much information about the characteristics of turbulence in open-channel flows as possible, and then from the experimental results try to obtain a clear idea of the structure and the kinematics of the turbulent motion.

Recent development of hot-film anemometry has enabled the researcher to study the structure of turbulent shear flows in water by providing a tool for obtaining the turbulence characteristics as defined from the statistical approach. Better accessory equipment and digital computers have also made anemometry more practical by providing more accurate measurements of turbulence characteristics.

Obtaining reproducible and meaningful turbulence measurements depends upon the following considerations:

1. Understanding the type of control circuitry being employed. Constant-temperature anemometry is best for measurements in open-channel flows.
2. Selecting the proper hot-film sensor to make the desired measurements under the experimental flow conditions. The parabolic sensor is the best all-around sensor for most open-channel flows. However, the cylindrical sensor is recommended for low-velocity flow and where contaminants are minimal.
3. Obtaining meaningful calibration curves with as much accuracy as possible.
4. Understanding the limitations of the instrument and the hot-film sensors, and recognizing possible problems due to drift, sensitivity, calibration, and noise.
5. Understanding the data-reduction procedures under ideal situations, where sensor contamination is not a problem.
6. Recognizing the possible sources of errors in the data reduction.

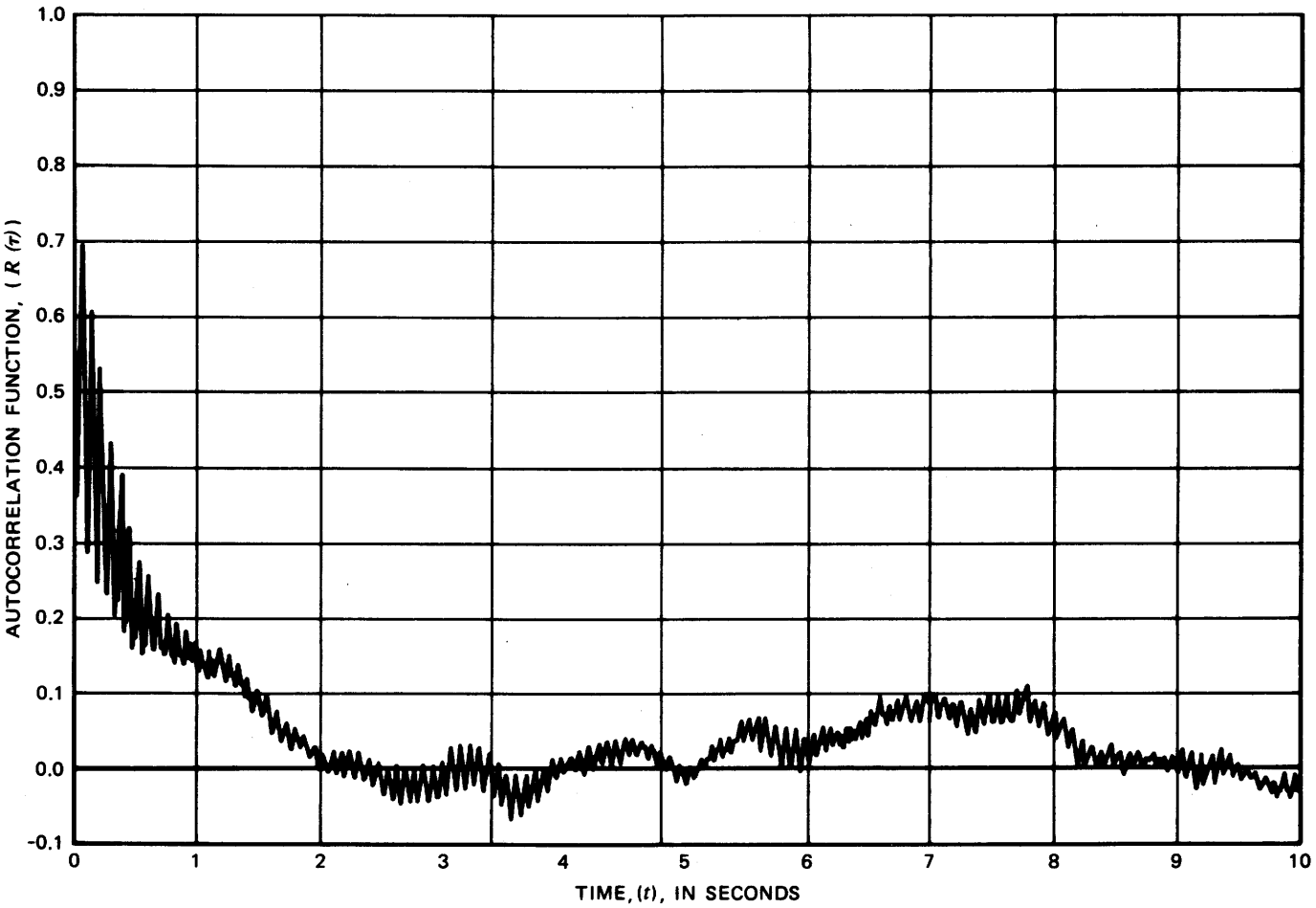

FIGURE 31.—Autocorrelation function, showing mechanical vibration superimposed on the turbulence signal.

7. Recognizing the possible problems of operating in a flow containing fluid-borne contaminants, and adjusting the data-collection procedures accordingly.
8. Making certain that the data collected at a point in the flow contain no trends or discontinuities.
9. Making certain that the period of record analyzed is of sufficient length.
10. Making sure that the low frequencies are accounted for if analog equipment is used in the data reduction.
11. Making sure, if digital equipment is used in the data reduction, that the sampling interval is small enough to account for all desired frequencies and that a sufficient number of lags is used to obtain the autocorrelation function. Digital data reduction has good low-frequency resolution and can be applied conveniently to obtain diverse turbulence characteristics.
12. Being flexible enough in the data collection procedures to adjust to the equipment and sensor capabilities and the data reduction techniques.

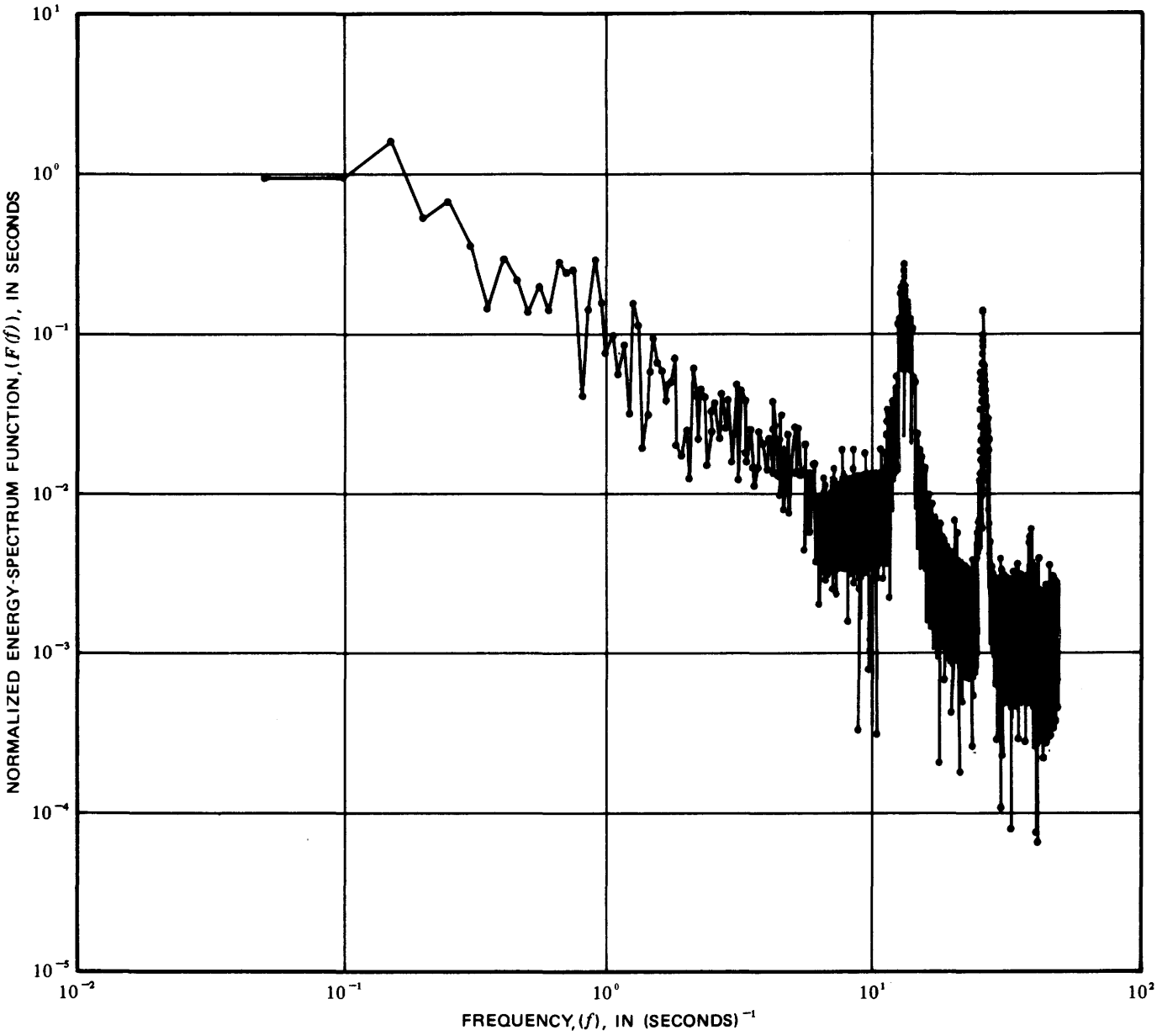

FIGURE 32.—Energy-spectrum function, showing mechanical vibration superimposed on the turbulence signal.

REFERENCES

Batchelor, G. K., 1953, The theory of homogeneous turbulence: London and New York, Cambridge University Press, 197 p.

Bellhouse, B. J., and Schultz, D. L., 1967, The determination of fluctuating velocity in air with heated thin film gauges: Jour. Fluid Mechanics, v. 29, pt. 2, p. 289–295.

Bendat, J. S., and Piersol, A. G., 1966, Measurement and analysis of random data: New York, John Wiley and Sons, 390 p.

Blackman, R. B., and Tukey, J. W., 1958, The measurement of power spectra: New York, Dover Publications, 190 p.

Hinze, J. O., 1959, Turbulence: New York, McGraw-Hill, 586 p.

King, L. V., 1914, On the convection of heat from small cylinders in a stream of fluid—Determination of the convection constants of small platinum wires with applications to hot-wire anemometry: Royal Soc. London Philos. Trans., v. 214, ser. A, p. 373–432.

Ling, S. C., and Hubbard, P. G., 1956, The hot-film anemometer—a new device for fluid mechanics research: Jour. Aeronautical Science, v. 23, p. 890–891.

McQuivey, R. S., 1967, Turbulence in a hydrodynamically rough and smooth open-channel flow: Ph. D. dissertation, Colorado State Univ., Fort Collins, Colo., 105 p.

McQuivey, R. S., and Richardson, E. V., 1969, Some turbulence measurements in open-channel flow: Am. Soc. Civil Engineers Proc., Jour. Hydraulics Div., v. 95, no. HY1, p. 209–223.

Raichlen, Fredric, 1967, Some turbulence measurements in water: Am. Soc. Civil Engineers Proc., Jour. Engineering Mechanics Div., v. 93, no. EM2, p. 73–97.

Resch, F. J., 1970, Hot-film turbulence measurements in water flow: Am. Soc. Civil Engineers Proc., Jour. Hydraulics Div., v. 96, no. HY3, p. 787–800.

Reynolds, Osborn, 1895, On the dynamical theory of incompressible viscous fluids and the determination of the criterion: Royal Soc. London Philos. Trans., v. 186, ser. A, p. 123–164.

Richardson, E. V., and McQuivey, R. S., 1968, Measurement of turbulence in water: Am. Soc. Civil Engineers Proc., Jour. Hydraulics Div., v. 94, no. HY2, p. 411–430.

Richardson, E. V., McQuivey, R. S., Sandborn, V. A., and Jog, P. M., 1967, Comparison between hot-film and hot-wire measurements of turbulence: 10th Midwestern Mechanics Conf., Colorado State Univ., Fort Collins, Colo., 1967, Proc., p. 1213–1223.

Sandborn, V. A., 1966, Meteorology of fluid mechanics: Colorado State Univ., Dept. Civil Engineering, Fort Collins, Colo., rept. CER66VAS32, 326 p.

Schraub, F. A., and Kline, S. J., 1965, A study of the structure of the turbulent boundary layer with and without longitudinal pressure gradients: Stanford Univ., rept. MD-12, 128 p.

Taylor, G. I., 1935, Distribution of dissipation of energy in a pipe over its cross-section: Royal Soc. [London] Proc., v. 151, ser. A, no. 874, p. 455–464.

_____1938, The spectrum of turbulence: Royal Soc. [London] Proc., v. 164, ser. A, no. 15, p. 476–490.

Thermo Systems Inc., 1968, Constant temperature anemometer: Instruction Manual, St. Paul, Minn., 53 p.

APPENDIX

```
C   EXECUTIVE ROUTINE
C   MAIN SEGMENT OF SYSTEM
C        DIGITAL ANALYSIS OF TURBULENCE DATA SYSTEM
C
C
      DIMENSION SPACE(3115)
      DIMENSION NTITLE(4),NOPTS(4),TITL(40)
      DIMENSION XARAY(10000,2),SIGMA(2),XMEAN(2)
      DIMENSION IARRAY(300),IDATA(600),MEAS(2),XMEAS(2,2),
     1 YMEAS(15,2),TITLE(75)
      DIMENSION ARAYX(20000)
      EQUIVALENCE (XARAY(1,1),ARAYX(1))
      REAL M3,M4
      COMMON /ARAY/XARAY,SIGMA,XMEAN
      COMMON /STORG/SPACE
      DIMENSION RMS(2),M3(2),M4(2)
      DATA NTITLE/6HNCROSS,6HAUTCOR,6HPOWDEN,6HNORMLD/
      EQUIVALENCE (TITLE(1),SPACE(2))
      EQUIVALENCE(SPACE(101),IARRAY(1)),(SPACE(501),IDATA(1))
      EQUIVALENCE (SPACE(3076),TITL(1))
C
C   READ GENERAL PARAMETERS
C
C
C  READ CODE CARD
C
1000  READ(5,8) ICODE
    8 FORMAT(A6)
      IF(ICODE.EQ.6H999999 ) GO TO 37
      IF(ICODE.EQ.6H******) GO TO 900
    1 FORMAT(24A6)
C
C  READ HEADER RECORDS FROM TAPE
C
      REWIND 11
      CALL IO(3,TITLE,20,1,2,IERR)
      IF(IERR.EQ.1) GO TO 900
      DO 104 I=1,20
  104 CALL HI2HU(TITLE(I))
      CALL IO(3,IARRAY,8,1,2,IERR)
      IF(IERR.NE.0) WRITE(6,307)
      DO 100 I=1,8
  100 CALL HI2HU(IARRAY(I))
      WRITE(11,1) (IARRAY(I),I=1,8)
      REWIND 11
```

```
   46*          READ(11,2) ISPS,NC,NS,NBLX,ISCALE
   47*        2 FORMAT(21X,I5,I2,2I3,I5)
   48*          NWDS=(FLOAT(NC*8)/6. + 1.)
   49*          ISCALE=10000
   50*          KODE=1
   51*          NC1=NC-2
   52*          NBL=NBLX-2
   53*          TSAMPL=1.0/ISPS
   54*          XMEAN(1)=0.0
   55*          XMEAN(2)=0.0
   56*          FC1=1./(2.*TSAMPL)
   57*          REWIND 11
   58*          CALL IO(3,IARRAY,24,1,2,IERR)
   59*          IF(IERR.NE.0) WRITE(6,307)
   60*          DO 101 I=1,NWDS
   61*      101 CALL HI2HU(IARRAY(I))
   62*          WRITE(11,1) (IARRAY(I),I=1,NWDS)
   63*          REWIND 11
   64*          READ(11,3) ((YMEAS(I,J),J=1,2),I=1,NTIMES)
   65*        3 FORMAT(16X,15(A6,A2))
   66*          CALL IO(3,IARRAY,24,1,2,IERR)
   67*          DO 102 I=1,NWDS
   68*      102 CALL HI2HU(IARRAY(I))
   69*     2000 DO 2001 I=1,4
   70*     2001 NOPTS(I)=0
   71*          NTIMES=2
   72*     C
   73*     C  READ TIME CARD
   74*     C
   75*          READ(5,10) ISTRT,ISTOP,XMEAS(1,1),XMEAS(1,2),XMEAS(2,1),XMEAS(2,2
   76*         1),NDATAS,NLAGS,(NOPTS(I),I=1,4),FC,SIGUS,DELTA,IOMIT1,IOMIT2
   77*       10 FORMAT(2I10,A6,A2,1X,A6,A2,1X,2I5,1X,4I1,   3F5.0,2I6)
   78*          IF(XMEAS(1,1).NE.6HLAST   ) GO TO 35
   79*          GO TO 36
   80*     C
   81*     C  SKIP FILE ON TAPE
   82*     C
   83*       37 CALL IO(3,IARRAY,20,1,2,IERR)
   84*          CALL IO(3,IARRAY,8,1,2,IERR)
   85*          CALL IO(3,IARRAY,24,1,2,IERR)
   86*          CALL IO(3,IARRAY,24,1,2,IERR)
   87*       36 CALL IO(3,IARRAY,300,0,2,IERR)
   88*          IF(IERR.NE.1) GO TO 36
   89*          GO TO 1000
   90*       35 IF(XMEAS(2,1).EQ.6H       ) NTIMES=1
   91*          IF(NTIMES.EQ.2.AND.NDATAS.GT.10000) NDATAS=10000
   92*          IF(NTIMES.EQ.1.AND.NDATAS.GT.20000) NDATAS=20000
   93*          NLAGX=(NDATAS+9)/10
   94*          IF(NLAGS.GT.NLAGX) NLAGS=NLAGX
   95*          L=1
   96*     C
   97*     C  MATCH CARD AND TAPE MEASUREMENT NUMBERS
   98*     C
   99*        6 DO 22 I=1,NC1
*DIAGNOSTIC*  THE TEST FOR EQUALITY BETWEEN NON-INTEGERS MAY NOT BE MEANINGFUL.
  100*          IF(YMEAS(I,1).NE.XMEAS(L,1)) GO TO 22
*DIAGNOSTIC*  THE TEST FOR EQUALITY BETWEEN NON-INTEGERS MAY NOT BE MEANINGFUL.
```

```
101*            IF(YMEAS(I,2).NE.XMEAS(L,2)) GO TO 22
102*            MEAS(L)=I+1
103*            GO TO 13
104*         22 CONTINUE
105*            WRITE(6,5)
106*          5 FORMAT(63H0 CARD MEASURMENT NUMBERS DO NOT MATCH TAPE MEASURMENT N
107*           1UMBERS.    )
108*            IERR=2
109*            GO TO 9999
110*         13 IF(L.GE.NTIMES) GO TO 7
111*            L=L+1
112*            GO TO 6
113*          7 NBL=NBL-2
114*            MDATAS=0
115*          9 CALL IO(3,IARRAY,300,0,2,IERR)
116*            IF(IERR.EQ.1) GO TO 40
117*            IF(IERR.EQ.2) GO TO 400
118*            IF(IERR.NE.0) GO TO 9
119*            ITIME=FLD(1,17,IARRAY(1))
120*            ITIME=(ITIME+(200/ISPS+1))*1000
121*            IF(ITIME.LT.ISTRT) GO TO 9
122*            J=0
123*    C
124*    C  SPLIT WORDS INTO DATA VALUES, STORE IN IDATA
125*    C
126*            DO 11 I=1,300
127*            ISIGN1=0
128*            ISIGN2=0
129*            IDATA(J+1)=0
130*            IDATA(J+2)=0
131*            IDATA(J+1)=FLD(1,17,IARRAY(I))
132*            IDATA(J+2)=FLD(19,17,IARRAY(I))
133*            ISIGN1=FLD(0,1,IARRAY(I))
134*            ISIGN2=FLD(18,1,IARRAY(I))
135*            IF(ISIGN1.EQ.1) IDATA(J+1)=IDATA(J+1)-2**17
136*            IF(ISIGN2.EQ.1) IDATA(J+2)=IDATA(J+2)-2**17
137*            J=J+2
138*         11 CONTINUE
139*    C
140*    C  CHECK FOR START AND STOP TIMES
141*    C
142*         20 DO 30 I=1,NBL,NC
143*            ITIME=IDATA(I)*1000 +IDATA(I+1)/10
144*            IF(ITIME.LT.ISTRT) GO TO 30
145*            GO TO (32,33),KODE
146*         32 ISTRT=ITIME
147*            KODE=2
148*         33 IF(ITIME.GT.ISTOP) GO TO 40
149*            IHOLD=ITIME
150*            MDATAS=MDATAS+1
151*            DO 31 J=1,NTIMES
152*            MEASJ=MEAS(J)
153*    C
154*    C  SCALE AND STORE DATA POINTS IN XARAY
155*    C
156*            XARAY(MDATAS,J)=FLOAT(IDATA(I+MEASJ))/ FLOAT(ISCALE)
157*            XMEAN(J)=XMEAN(J)+XARAY(MDATAS,J)
```

```
158*       31 CONTINUE
159*          IF(MDATAS.GE.NDATAS) GO TO 40
160*       30 CONTINUE
161*          GO TO 9
162*       40 NDATAS=MDATAS
163*          ISTOP=IHOLD
164*          K4=ISTOP/1000
165*          I4=ISTRT/1000
166*          SI4=(ISTRT-I4*1000)/1000
167*          SK4=(ISTOP-K4*1000)/1000
168*          ISTRT=I4
169*          ISTOP=K4
170*          I1=ISTRT/3600
171*          K1=ISTOP/3600
172*          I2=(ISTRT-I1*3600)/60
173*          K2=(ISTOP-K1*3600)/60
174*          I3=ISTRT-I1*3600-I2*60
175*           K3=ISTOP-K1*3600-K2*60
176*          I4=SI4*1000
177*          K4=SK4*1000
178*     C
179*     C  STORE HEADER INFORMATION FOR PLOTS, WRITE HEADER INFORMATION ON LINE PRINTER
180*     C
181*          IF(NTIMES.EQ.1) GO TO 500
182*          REWIND 11
183*          WRITE(11,404) ((XMEAS(I,J),J=1,2),I=1,2)
184*          WRITE(6,404) ((XMEAS(I,J),J=1,2),I=1,2)
185*       404 FORMAT(1H1,21HMEASUREMENT NOS. ARE ,2(A6,A2,4X),50X)
186*          REWIND 11
187*          READ(11,403) (SPACE(I),I=44,50)
188*       403 FORMAT(1X,20A6)
189*          GO TO 501
190*       500 REWIND 11
191*          WRITE(11,402) XMEAS(1,1),XMEAS(1,2)
192*          WRITE(6,402) XMEAS(1,1),XMEAS(1,2)
193*       402 FORMAT(1H1,19HMEASUREMENT NO. IS ,A6,A2,5X,75X)
194*          REWIND 11
195*          READ(11,403) (SPACE(I),I=44,50)
196*       501 REWIND 11
197*          WRITE(11,405) MDATAS
198*       405 FORMAT(1X,17HNUMBER OF POINTS ,I5,10X)
199*          REWIND 11
200*          READ(11,403) (SPACE(I),I=51,54)
201*          REWIND 11
202*          WRITE(11,406) ISPS
203*       406 FORMAT(1X,29HNUMBER OF SAMPLES PER SECOND ,I5,10X)
204*          REWIND 11
205*          READ(11,403) (SPACE(I),I=55,60)
206*          WRITE(6,407) I1,I2,I3,SI4,K1,K2,K3,K4
207*          REWIND 11
208*          WRITE(11,407) I1,I2,I3,SI4,K1,K2,K3,K4
209*       407 FORMAT(1X,14HSTART TIME IS ,I2,2(1H ,I2),1H.,I3,2X,
210*         113HSTOP TIME IS ,I2,2(1H ,I2),1H.,I3,20X)
211*          REWIND 11
212*          READ(11,403) (SPACE(I),I=61,70)
213*          GO TO 106
214*       307 FORMAT(1X,17HERROR IN HEADER 2 )
```

```
215*      308 FORMAT(1X,17HERROR IN HEADER 3 )
216*      400 WRITE(6,401)
217*      401 FORMAT(1X,14HPARITY ERROR     )
218*          STOP
219*      106 NDAT1=NDATAS-1
220*          IJ=-19
221*          IK=20
222*          DO 411 I=1,40
223*      411 TITL(I)=6H
224*    C
225*    C   WRITE OUT THE REQUEST FOR THIS JOB
226*    C
227*      999 WRITE(6,1100) NDATAS,NTIMES,NLAGS
228*     1100 FORMAT(1X ,19HNUMBER OF POINTS = ,I8,
229*         1   26H NUMBER OF TIMES SERIES = ,I5,18H NUMBER OF LAGS = ,I5)
230*          WRITE(6,1007) (NTITLE(I),NOPTS(I),I=1,4)
231*     1007 FORMAT(13H PARAMETER = ,A6,5X,17H OPTION SWITCH = ,I6)
232*          WRITE(6,1200) SIGUS,DELTA,TSAMPL
233*     1200 FORMAT(1X,14HSIGMA UNITS = ,F5.2,5X,14HDELTA SIGMA = ,F5.2,
234*         15X,23HTIME BETWEEN SAMPLES = ,F8.4)
235*    C
236*    C  COMPUTE MEAN, SIGMA, RMS, THIRD AND FOURTH STATISTICAL MOMENTS
237*    C
238*      160 DO 250 I=1,NTIMES
239*          IJ=IJ+IK
240*          IK=IJ+19
241*          M3(I)=0
242*          M4(I)=0
243*          RMS(I)=0.0
244*          SIGMA(I)=0.0
245*          XMEAN(I)=XMEAN(I)/FLOAT(NDATAS)
246*          DO 301 J=1,NDATAS
247*          XARAY(J,I)=XARAY(J,I)-XMEAN(I)
248*          RMS(I)=RMS(I)+(XARAY(J,I)**2)
249*          M3(I)=M3(I)+(XARAY(J,I)**3)/FLOAT(NDATAS)
250*          M4(I)=M4(I)+(XARAY(J,I)**4)/FLOAT(NDATAS)
251*      301 SIGMA(I)=SIGMA(I)+(XARAY(J,I)**2)/FLOAT(NDAT1)
252*          RMS(I)=SQRT(RMS(I)/FLOAT(NDATAS))
253*          M4(I)=M4(I)/(SIGMA(I)**2)
254*          SIGMA(I)=SQRT(SIGMA(I))
255*          M3(I)=M3(I)/(SIGMA(I)**3)
256*          WRITE(6,302) XMEAN(I),RMS(I),M3(I),M4(I),I
257*      302 FORMAT(7H MEAN =,F6.3,1X,6H RMS = ,F6.3,2X,10HSKEWNESS =,F6.3,
258*         12X,10HKURTOSIS =,F6.3,2X,16HFOR TIME SERIES ,I2,50X)
259*          REWIND 11
260*          WRITE(11,302) XMEAN(I),RMS(I),M3(I),M4(I),I
261*          REWIND 11
262*          READ(11,403) (TITL(II),II=IJ,IK)
263*          XMEAN(I)=0.0
264*      250 CONTINUE
265*    C
266*    C  CALL ROUTINES FOR PLOT DATA
267*    C
268*    C
269*    C   NUMBER OF CROSSINGS ROUTINE
270*    C
271*          IF(NOPTS(1).EQ.1) CALL NCROS(NDATAS,NTIMES,SIGUS,DELTA)
```

```
272*    C
273*    C   PROBABILITY DISTRIBUTION ROUTINE
274*    C
275*          IF(NOPTS(4).EQ.1) CALL PDIST(NDATAS,NTIMES)
276*    C
277*    C
278*    C   AUTO CORRELATION ROUTINE
279*    C
280*          IF(NOPTS(2).NE.0.OR.NOPTS(3).NE.0) CALL AUTOC(NDATAS,NTIMES,NLAGS,
281*         1NOPTS(2),IOMIT1,TITLE,TSAMPL,TITL)
282*    C
283*    C   POWER SPECTRAL DENSITY ROUTINE
284*    C
285*          IF(NOPTS(3).NE.0) CALL PDENS(NTIMES,NLAGS,IOMIT2,FC,FC1,TSAMPL)
286*          GO TO 2000
287*    C
288*    C   END-OF-JOB
289*    C
290*      900 WRITE(6,1008)
291*          SPACE(1)=0
292*          WRITE(10) SPACE
293*     1008 FORMAT(15H1 JOB COMPLETED)
294*          ENDFILE 10
295*          REWIND 10
296*          GO TO 2003
297*    C
298*    C   ERROR MESSAGES
299*    C
300*     9999 WRITE(6,8888)
301*     8888 FORMAT(46H0*** ERROR DETECTED IN INPUT, RUN CANCELED ***
302*          SPACE(1)=0
303*          WRITE(10) SPACE
304*    C
305*     2003 STOP
306*          END
```

END OF COMPILATION:

```
1*          SUBROUTINE NCROS(NPTS,NSRS,M,DELTA)
2*    C
3*    C   NUMBER OF CROSSINGS ROUTINE
4*    C
5*          INTEGER FLAG,FF
6*          DIMENSION SPACE(3115)
7*          DIMENSION Y(100,2),U(100),V(100)
8*          DIMENSION UL(10)
9*          EQUIVALENCE (SPACE(76),U(1)),(SPACE(1076),V(1)),
10*        1  (SPACE(2076),Y(1,1)),(UL(1),SPACE(3001))
11*         DIMENSION XARAY(10000,2),SIGMA(2),XMEAN(2)
12*         DIMENSION ARAYX(20000)
13*         EQUIVALENCE (XARAY(1,1),ARAYX(1))
14*         COMMON /ARAY/XARAY,SIGMA,XMEAN
15*         COMMON /STORG/SPACE
16*         DATA UL/10.,50.,100.,200.,500.,1000.,2000.,5000.,10000.,20000./
17*         INTEGER Y
18*         REAL M
19*         WRITE(6,207)
20*     207 FORMAT(//,1X,20HNUMBER OF CROSSINGS ,/)
21*         DO 40 NS=1,NSRS
22*         ITOTV=0
23*         TOTV=0.0
24*         DO 10 I=1,100
25*         DO 10 J=1,2
26*      10 Y(I,J)=0.0
27*    C
28*    C  COMPUTE NUMBER OF CLASS INTERVALS
29*    C
30*         K=2.*M/DELTA+1.00001
31*         VLEVEL=-M* SIGMA(NS)
32*         X1=XARAY(1,NS)
33*    C
34*    C  CALCULATE NUMBER OF CROSSINGS
35*    C
36*         DO 1001 J=1,K
37*         SS=VLEVEL+FLOAT(J-1)*DELTA*SIGMA(NS)
38*         IF(X1-SS) 110,110,130
39*     110 FLAG=1
40*         FF=1
41*         GO TO 141
42*     130 FLAG=2
43*         FF=-1
44*     141 DO 990 I=2,NPTS
45*         XI= XARAY(I,NS)
46*         IF(XI-SS) 200,400,301
47*     200 GO TO (990,400) ,FLAG
48*     301 GO TO (400,990) ,FLAG
49*     400 Y(J,FLAG)=Y(J,FLAG)+1
50*         FLAG=FLAG+FF
51*         FF=-FF
52*     990 CONTINUE
53*    1001 CONTINUE
54*         WRITE(6,2000) XMEAN(NS),SIGMA(NS)
55*    2000 FORMAT(1X,5HMEAN=,F10.5,8H  SIGMA=,F10.5)
56*         WRITE(6,208)
57*     208 FORMAT(1X,5HGROUP,5X,5HSIGMA,5X,18HPOSITIVE CROSSINGS ,5X,
58*        118HNEGATIVE CROSSINGS )
59*         DO 500  J=1,K
60*         U(J)=-M+FLOAT(J-1)*DELTA
```

```
61*           WRITE(6,1000) J,U(J),Y(J,1),Y(J,2)
62*      1000 FORMAT(2X,I3,F11.2,5X,I10,13X,I10)
63*           V(J)=Y(J,1)+Y(J,2)
64*           TOTV=TOTV+V(J)
65*       500 CONTINUE
66*           ITOTV=TOTV
67*           WRITE(6,300) ITOTV
68*       300 FORMAT(1X,24HTOTAL NO. OF CROSSINGS= ,I6,5X)
69*           REWIND 11
70*           WRITE(11,300) ITOTV
71*           REWIND 11
72*           READ(11,303) (SPACE(I),I=71,75)
73*       303 FORMAT(1X,5A6)
74*           IF(M) 30,50,30
75*     C
76*        30 XR=U(1)
77*           XL=U(1)
78*           YT=V(1)
79*           YB=V(1)
80*           DO 11 J=2,K
81*           XL=AMIN1(XL,U(J))
82*           XR=AMAX1(XR,U(J))
83*           YT=AMAX1(YT,V(J))
84*        11 YB=AMIN1(YB,V(J))
85*           DO 140 J=1,10
86*           IF ( YT .LE. UL(J) ) GO TO 150
87*      140  CONTINUE
88*      150  YT=UL(J)
89*           IXL=XL
90*           XL=IXL
91*           IXR=XR+.99
92*           XR=IXR
93*           IYT=YT+.99
94*           YT=IYT
95*           IYB=YB
96*           YB=IYB
97*           DO 1 I=22,36
98*         1 SPACE(I)=6H
99*           SPACE(1)=4
100*          SPACE(22)=6HNUMBER
101*          SPACE(23)=6H OF CR
102*          SPACE(24)=6HOSSING
103*          SPACE(25)=6HS
104*          SPACE(28)=6H   SIG
105*          SPACE(29)=6HMA
106*          SPACE(33)=6H CROSS
107*          SPACE(34)=6HINGS
108*          SPACE(41)=K
109*          SPACE(37)=XL
110*          SPACE(38)=XR
111*          SPACE(39)=YB
112*          SPACE(40)=YT
113*          SPACE(42)=55
114*          WRITE(10) SPACE
115*       40 CONTINUE
116*    C
117*       50 RETURN
118*          END

END OF COMPILATION:        NO  DIAGNOSTICS.
```

```
      C      POWER SPECTRAL DENSITY
      C
            SUBROUTINE PDENS(NSRS,M,NOMIT4,FC,FC1,H)
            DIMENSION XARAY(10000,2),ARAYX(20000),NO(3)
            DIMENSION XMEAN(2),SIGMA(2),A(1000,2,2),B(1000,2,2),F(1000,2,2),
           1  COR(1000,2,2),SPACE(3115),DATA(2000),Q(1000,2,2)
            EQUIVALENCE (ARAYX(1),XARAY(1,1))
            EQUIVALENCE (ARAYX(4001),A(1,1,1)),(ARAYX(8001),B(1,1,1)),(ARAYX(
           1 12001),COR(1,1,1),F(1,1,1)),(ARAYX(17076),DATA(1),SPACE(1076))
            EQUIVALENCE(Q(I,1,1),ARAYX(1))
            COMMON /ARAY/XARAY,SIGMA,XMEAN
            M1=M+1
            K=0
            DO 40 I=1,M1
            DO 40 J=1,NSRS
            DO 40 L=1,NSRS
            K=K+1
         40 COR(I,J,L)=ARAYX(K)
            DO 16 I=1,NSRS
            DO 16 K=1,NSRS
            DO 6 J=1,M1
            B(J,I,K)=.5*(COR(J,I,K)-COR(J,K,I))
          6 A(J,I,K)=.5*(COR(J,I,K)+COR(J,K,I))
            DO 12 L=1,M
            F(L,I,K)=0.0
            MM1=M-1
            DO 11 J=1,MM1
            F(L,I,K )=4.0*H*A(J+1,I,K)*COS(3.14159*FLOAT(J) *FLOAT(L)/FLOAT(M)
           1 ) +F(L,I,K )
         11 CONTINUE
            F(L,I,K )=F(L,I,K )+2.0*H*(A(1,I,K)+(-1.)**(L  )*A(M1,I,K))
         12 CONTINUE
            DO 16 L=1,M1
            Q(L,I,K)=0.0
            DO 17 J=1,MM1
         17 Q(L,I,K)=Q(L,I,K)+4.*H*B(J+1,I,K)*SIN(3.14159*FLOAT(J)*FLOAT(L)
           1  /FLOAT(M))
            F(L,I,K)=SQRT(F(L,I,K)**2+Q(L,I,K)**2)
         16 CONTINUE
      C
      C   PROCESS F ARRAY (CO-SPECTRAL DENSITIES )
      C
      C       NOMIT=00,   PROCESS ALL
      C       NOMIT=11,   SKIP 1-1
      C       NOMIT=12,   SKIP 1-2
      C       NOMIT=21,   SKIP 2-1
      C       NOMIT=22,   SKIP 2-2
      C
            NCNT=0
      C
      C   SET OMIT OPTION SWITCH
      C
            NO(3)=NOMIT4/10000
            NOMIT4=NOMIT4-(NO(3)*10000)
            NO(2)=NOMIT4/100
            NO(1)=NOMIT4-(NO(2)*100)
            NOMIT4=NO(1)
```

```
      WRITE(11,107) NG,XSTEP
  107 FORMAT(I3,2X,18HINTERVALS OF SIZE ,F7.5)
      REWIND 11
      READ(11,108) (SPACE(I),I=71,75)
  108 FORMAT(5A6)
C
C   CALL PLOT PACKAGE
C
      XL=-5.0
      DO 11 I=1,NG
      CP(I)=CP(I)*100.
   11 EP(I)=EP(I)*100.
C
C   DESCRIBE HORIZONTAL AXIS IN TERMS OF DELTA-SIGMAS
C
      YT = AMAX1(EP(1),CP(1))
      YB = 0.0
      DO 10 J=2,NG
   10 YT=AMAX1(EP(J),CP(J),YT)
      IYT=(YT/10.)
      YT=FLOAT(IYT)*10.+10.
      DO 102 I=22,36
  102 SPACE(I)=6H
      SPACE(1)=2
      SPACE(22)=6HPROBAB
      SPACE(23)=6HILITY
      SPACE(24)=6HDENSIT
      SPACE(25)=6HY
      SPACE(28)=6H   SIG
      SPACE(29)=6HMA
      SPACE(33)=6H PERCE
      SPACE(34)=6HNT OF
      SPACE(35)=6HDATA
      SPACE(37)=XL
      SPACE(38)=XR
      SPACE(39)=YB
      SPACE(40)=YT
      SPACE(41)=NG
      SPACE(42)=19
      SPACE(43)=55
      SPACE(76)=XMIN/SIGMA(NS)
      DO 101 I=2,NG
  101 SPACE(I+75)=SPACE(I+74)+XSTEP
      WRITE(10) SPACE
   59 CONTINUE
   60 RETURN
      END

END OF COMPILATION:        NO  DIAGNOSTICS.
```

```
C    AUTO-CORRELATION
C
      SUBROUTINE AUTOC(N,NSRS,M,NOP3,NOMIT3,TITLE,TSAMPL,TITL)
      DIMENSION C(2),NO(3),SPACE(3115),TITL(40)
      DIMENSION DATA(2000),XARAY(10000,2),SIGMA(2),XMEAN(2),COR(1000,2,2
     1  ),ARAYX(20000),CORX(4000),TITLE(75)
      EQUIVALENCE (XARAY(1,1),ARAYX(1)) ,(COR(1,1,1),CORX(1))
     1,(ARAYX(17076),DATA(1),SPACE(1076))
      COMMON /ARAY/XARAY,SIGMA,XMEAN
      WRITE(6,600)
  600 FORMAT(//,1X,12HCORRELATIONS ,/)
      M=M-1
      M1=M+1
      DO 4 I=1,NSRS
      DO 4 J=1,NSRS
      DO 6 L=1,M1
      NR=N-L+1
      COR(L,I,J)=0.0
      DO 5 K=1,NR
      COR(L,I,J)=COR(L,I,J)+ XARAY(K,I)* XARAY(K+L-1,J)
    5 CONTINUE
    6 COR(L,I,J)=(1./FLOAT(NR))*COR(L,I,J)
    4 CONTINUE
      C(1)=SQRT(COR(1,1,1))
      C(2)=SQRT(COR(1,2,2))
      DO 30 J=1,NSRS
      DO 30 I=1,NSRS
      DO 30 L=1,M1
   30 COR(L,J,I)=COR(L,J,I)/(C(J)*C(I))
      DO 599 I=1,75
  599 SPACE(I+1)=TITLE(I)
      DO 598 I=1,40
  598 SPACE(I+3075)=TITL(I)
      WRITE(6,597) COR(1,1,1)
  597 FORMAT(1X,8HR1(0) = ,E15.6)
      IF(NOP3.EQ.0) GO TO 40
C
C   PROCESS COR ARRAY AS PER NOMIT REQUEST
C
C        NOMIT = 00,          PROCESS ALL
C        NOMIT = 11           OMIT 1-1
C        NOMIT = 12           OMIT 1-2
C        NOMIT = 21           OMIT 2-1
C        NOMIT = 22           OMIT 2-2
C
      NCNT=0
C
C   SET OMIT OPTION SWITCHES
C
      NO(3)=NOMIT3/10000
      NOMIT3=NOMIT3-(NO(3)*10000)
      NO(2)=NOMIT3/100
      NO(1)=NOMIT3-(NO(2)*100)
      NOMIT3=NO(1)
      IOUT=1
C
```

```
57*   C
58*   C   CHECK FIRST TIME SERIES AUTO CORRELATION
59*         IF(NOMIT3.NE.11) GO TO 100
60*         IOUT=IOUT+1
61*         NOMIT3=NO(IOUT)
62*         GO TO 200
63*   C
64*   C   PROCESS FIRST TIME SERIES AUTO CORRELATION
65*   C
66*     100 DO 110   K=1,M
67*     110 DATA(K)=COR(K,1,1)
68*         SPACE(26)=6H1-1
69*         SPACE(33)=6H AUTO
70*         NCNT=1
71*         GO TO 500
72*   C
73*   C   CHECK SECOND TIME SERIES AUTO CORRELATION
74*   C
75*     200 IF(NOMIT3.NE.22) GO TO 205
76*         IOUT=IOUT+1
77*         NOMIT3=NO(IOUT)
78*         GO TO 300
79*   C
80*   C   PROCESS SECOND TIME SERIES AUTO CORRELATION
81*   C
82*     205 DO 210  K=1,M
83*     210 DATA(K)=COR(K,2,2)
84*         SPACE(26)=6H2-2
85*         SPACE(33)=6H AUTO
86*         NCNT=2
87*         GO TO 500
88*   C
89*   C   CHECK 1-2 CROSS CORRELATION
90*   C
91*     300 IF(NOMIT3.NE.12) GO TO 305
92*         IOUT=IOUT+1
93*         NOMIT3=NO(IOUT)
94*         GO TO 400
95*   C
96*   C   PROCESS 1-2 CROSS CORRELATION
97*   C
98*     305 DO 310  K=1,M
99*     310 DATA(K)=COR(K,1,2)
100*        SPACE(33)=6HCROSS
101*        SPACE(26)=6H1-2
102*        NCNT=3
103*        GO TO 500
104*  C
105*  C   CHECK 2-1 CROSS CORRELATION
106*  C
107*    400 IF(NOMIT3.NE.21) GO TO 405
108*        GO TO 40
109*  C
110*  C   PROCESS 2-1 CROSS CORRELATION
111*  C
112*    405 DO 410  K=1,M
113*    410 DATA(K)=COR(K,2,1)
114*        SPACE(26)=6H2-1
115*        SPACE(33)=6HCROSS
116*        NCNT=4
```

```
117*    C
118*    C   GENERATE PLOT
119*    C
120*    C
121*    C   DETERMINE MIN AND MAX VALUES FOR X AND Y
122*    C
123*      500 XR=TSAMPL*M
124*          XL = 0
125*          YT=DATA(1)
126*          YB=DATA(1)
127*          DO 61 J=2,M
128*          YT=AMAX1(YT,DATA(J))
129*       61 YB=AMIN1(YB,DATA(J))
130*          IYT=(YT+.19)*10.0
131*          IF(IYT.NE.((IYT/2)*2)) IYT=IYT+1
132*          YT=FLOAT(IYT)/10.0
133*          IYB=(YB-.19)*10.0
134*          IF(IYB.NE.((IYB/2)*2)) IYB=IYB-1
135*          YB=FLOAT(IYB)/10.0
136*    C
137*    C   INITIALIZE HORIZONTAL COORDINATE ARRAY
138*    C
139*          SPACE(1)=1
140*          DO 501 I=22,25
141*      501 SPACE(I)=6H
142*          DO 607 I=27,32
143*      607 SPACE(I)=6H
144*          DO 503 I=34,36
145*      503 SPACE(I)=6H
146*          SPACE(28)=6HTIME I
147*          SPACE(29)=6HN SEC.
148*          SPACE(34)=6HCORREL
149*          SPACE(35)=6HATION
150*          SPACE(37)=XL
151*          SPACE(38)=XR
152*          SPACE(39)=YB
153*          SPACE(40)=YT
154*          SPACE(41)=M
155*          SPACE(42)=55
156*          SPACE(22)=6HCORREL
157*          SPACE(23)=6HATION
158*          SPACE(24)=6HFUNCTI
159*          SPACE(25)=6HON
160*          A=TSAMPL
161*          AA=-A
162*          IF(M.GT.1000) GO TO 504
163*          DO 502 I=1,M
164*          AA=AA+A
165*      502 SPACE(I+75)=AA
166*      504 AREA=0.0
167*          DO 505 K=2,M
168*          IF(DATA(K-1).LE.0.0.AND.DATA(K).GT.0.0) AREA=AREA+.5*(DATA(K)/
169*         1 (-DATA(K-1)+DATA(K)))*(SPACE(K+75)-SPACE(K+74))
170*          IF(DATA(K-1).GT.0.0.AND.DATA(K).GT.0.0) AREA=AREA+(DATA(K-1)+DATA
171*         1 (K))*.5*(SPACE(K+75)-SPACE(K+74))
172*          IF(DATA(K-1).GT.0.0.AND.DATA(K).LE.0.0) AREA=AREA+.5*(DATA(K-1)/
173*         1 (DATA(K-1)-DATA(K)))*(SPACE(K+75)-SPACE(K+74))*DATA(K-1)
174*      505 CONTINUE
```

```
175*            SPACE(71)=6HPOSITI
176*            SPACE(72)=6HVE ARE
177*            REWIND 11
178*            WRITE(11,506) AREA
179*        506 FORMAT(3HA =,E13.6)
180*            REWIND 11
181*            READ(11,507) (SPACE(I),I=73,75)
182*            WRITE(6,508) (SPACE(I),I=71,75)
183*        508 FORMAT(1X,10A6)
184*        507 FORMAT(3A6)
185*            WRITE(10) SPACE
186*            IF(M.LE.1000) GO TO 510
187*            DO 511 I=1,M
188*            AA=AA+A
189*        511 SPACE(I+75)=AA
190*            WRITE(10) SPACE
191*        510 IF(NSRS.EQ.1) GO TO 40
192*            GO TO (200,300,400,40),NCNT
193*    C
194*    C    CHECK FOR NULL REQUEST
195*    C
196*    C
197*         40 K=0
198*            DO 41 I=1,M1
199*            DO 41 J=1,NSRS
200*            DO 41 L=1,NSRS
201*            K=K+1
202*         41 ARAYX(K)=COR(I,J,L)
203*            RETURN
204*            END

END OF COMPILATION:        NO  DIAGNOSTICS.
```

```
      C  PROBABILITY DENSITY ROUTINE
      C
            SUBROUTINE PDIST(N,NSRS)
            DIMENSION EP(100),CP(100)
            DIMENSION SPACE(3115)
            EQUIVALENCE (SPACE(1076),CP(1)),(SPACE(2076),EP(1))
            DIMENSION XARAY(10000,2),SIGMA(2),XMEAN(2)
            DIMENSION ARAYX(20000)
            EQUIVALENCE (XARAY(1,1),ARAYX(1))
            COMMON /ARAY/XARAY,SIGMA,XMEAN
            COMMON /STORG/SPACE
      C
      C  PROBABILITY DISTRIBUTION ROUTINE
      C
            WRITE(6,103)
        103 FORMAT(//,1X,24HPROBABILITY DISTRIBUTION ,/)
            DO 59 NS=1,NSRS
            SS=SIGMA(NS)**2
            XBAR=XMEAN(NS)
            IND=3
      C
      C   COMPUTE STEP SIZE
      C
            XMIN=XARAY(1,NS)
            XMAX=XARAY(1,NS)
            DO 20 I=2,N
            XMIN=AMIN1(XMIN,XARAY(I,NS))
         20 XMAX=AMAX1(XMAX,XARAY(I,NS))
            NG=1.87*(FLOAT(N-1)**.4) +.5
            NG=NG-1
            STEP=(XMAX-XMIN)/FLOAT(NG)
            WRITE(6,56) NG
         56 FORMAT(1X,13HNO. OF GROUPS  ,I10)
            XMAX=AINT((XMAX+SIGN(.5*STEP,XMAX))/STEP)*STEP
            XMIN=AINT((XMIN+SIGN(.5*STEP,XMIN))/STEP)*STEP
            NG=(XMAX-XMIN)/STEP+1.0005
            NG1=NG+1
            DO 57 I=0,NG1
         57 EP(I)=0.0
            DO 58 I=1,N
            K=(XARAY(I,NS)-XMIN)/STEP+1.5000005
            IF(K.LT.0) K=0
            IF(K.GT.NG) K=NG1
         58 EP(K)=EP(K)+1.0
            C=STEP/SQRT(6.283185*SS)
            DO 62 I=0,NG1
            XX=XMIN+(I-1)*STEP
            CP(I)=C*EXP(-((XX-XBAR)**2/(2.*SS)))
         62 EP(I)=EP(I)/N
            WRITE(6,55) XMIN,XMAX
         55 FORMAT(1X,7HXMIN = ,F15.5,5X,7HXMAX = ,F15.5)
            WRITE(6,68)
         68 FORMAT(1X,18HCALCULATED DENSITY ,5X,17HEMPIRICAL DENSITY )
         50 WRITE(6,100) (CP(I),EP(I),I=1,NG)
        100 FORMAT(F13.4,10X,F11.4)
            REWIND 11
            XSTEP=STEP/SIGMA(NS)
            XR=5.0
```

```
      IOUT=1
C
C   CHECK 1-1 COSPECTRAL
C
      IF(NOMIT4.NE.11) GO TO 1100
      IOUT=IOUT+1
      NOMIT4=NO(IOUT)
      GO TO 1200
C
C   PROCESS 1-1 POWER SPECTRUM
C
 1100 DO 1120  K=1,M
 1120 DATA(K)=F(K,1,1)
      SPACE(26)=6HN 1-1
      SPACE(32)=6H   POW
      SPACE(33)=6HER SPE
      NCNT=1
      GO TO 1500
C
C   CHECK 2-2 COSPECTRAL
C
 1200 IF(NOMIT4.NE.22) GO TO 1205
      IOUT=IOUT+1
      NOMIT4=NO(IOUT)
      GO TO 1300
C
C   PROCESS 2-2 POWER SPECTRUM
C
 1205 DO 1210  K=1,M
 1210 DATA(K)=F(K,2,2)
      SPACE(26)=6HN 2-2
      SPACE(32)=6H   POW
      SPACE(33)=6HER SPE
      NCNT=2
      GO TO 1500
C
C   CHECK 1-2 COSPECTRAL
C
 1300 IF(NOMIT4.NE.12) GO TO 1305
      IOUT=IOUT+1
      NOMIT4=NO(IOUT)
      GO TO 1400
C
C   PROCESS 1-2 POWER SPECTRUM
C
 1305 DO 1310 K=1,M
 1310 DATA(K)=F(K,1,2)
      SPACE(26)=6HN 1-2
      SPACE(32)=6H   CRO
      SPACE(33)=6HSS SPE
      NCNT=3
      GO TO 1500
C
C
 1400 IF(NOMIT4.NE.21) GO TO 1405
      GO TO 600
C
```

```
116*    C    CHECK 2-1 COSPECTRAL
117*    C    PROCESS 2-1 POWER SPECTRUM
118*    C
119*     1405 DO 1410 K=1,M
120*     1410 DATA(K)=F(K,2,1)
121*          SPACE(26)=6HN 2-1
122*          SPACE(32)=6H   CRO
123*          SPACE(33)=6HSS SPE
124*          NCNT=4
125*          GO TO 1500
126*    C    GENERATE PLOT
127*    C
128*     1500 SPACE(1)=3
129*          DO 1501 I=22,25
130*     1501 SPACE(I)=6H
131*          DO 1607 I=27,31
132*     1607 SPACE(I)=6H
133*          SPACE(22)=6HSPECTR
134*          SPACE(23)=6HAL DEN
135*          SPACE(24)=6HSITY F
136*          SPACE(25)=6HUNCTIO
137*          SPACE(36)=6HY
138*          SPACE(28)=6H  FREQ
139*          SPACE(29)=6HUENCY
140*          SPACE(30)=6H(CPS)
141*          SPACE(34)=6HCTRAL
142*          SPACE(35)=6HDENSIT
143*    C
144*    C    DETERMINE MIN AND MAX VALUES FOR Y
145*    C
146*          YT=DATA(1)
147*          YB=DATA(1)
148*          MMM=(FC/FC1)*FLOAT(M)
149*          KJ=1
150*          DO 13 J=2,MMM
151*          YT=AMAX1(YT,DATA(J))
*DIAGNOSTIC*  THE TEST FOR EQUALITY BETWEEN NON-INTEGERS MAY NOT BE MEANINGFUL.
152*          IF(YT.EQ.DATA(J)) KJ=J
153*       13 YB=AMIN1(YB,DATA(J))
154*          FMAX=FLOAT(KJ)*FC1/FLOAT(M)
155*          BW=FC1/FLOAT(M)
156*          REWIND 11
157*          WRITE(11,1611) YT,FMAX,BW
158*     1611 FORMAT(3HMAX,F6.3,1X,2HAT,F6.3,5H CPS,,3H BW,F4.2)
159*          REWIND 11
160*          READ(11,1612) (SPACE(I),I=71,75)
161*     1612 FORMAT(5A6)
162*    C
163*    C
164*    C    INITIALIZE HORIZONTAL COORDINATE ARRAY
165*    C
166*          XL=FC1/FLOAT(M)
167*          IF(MMM.GT.1000) GO TO 1503
168*          DO 1502 I=1,MMM
169*     1502 SPACE(I+75)=FLOAT(I)*FC1/FLOAT(M)
170*    C    SET THE MIN AND MAX VALUES FOR X
171*    C
```

```
172*    1503 XR=FC
173*    C
174*         IF(XL) 999,999,20
175*      20 IF(YB) 899,899,21
176*    C
177*    C   DETERMINE THE GRID RANGES IN POWERS OF 10
178*    C
179*      21 DO 22 I=1,12
180*         K=I-8
181*         IF(10.**K-XL) 22,22,23
182*      23 K=K-1
183*         XL1=10.**K
184*         GO TO 24
185*      22 CONTINUE
186*      24 DO 25 I=1,12
187*         K=I-8
188*         IF(10.**K-YB) 25,25,36
189*      36 K=K-1
190*         YB1=10.**K
191*         GO TO 29
192*      25 CONTINUE
193*      29 DO 27 K=1,10
194*         I=K-1
195*         IF(10.**I-XR) 27,28,28
196*      28 XR1=10.**I
197*         GO TO 31
198*      27 NX=K+3
199*      31 DO 32 K=1,10
200*         I=K-1
201*         IF(10.**I-YT) 32,33,33
202*      33 YT1=10.**I
203*         GO TO 34
204*      32 NY=K+3
205*      34 SPACE(37)=XL1
206*         SPACE(38)=XR1
207*         SPACE(39)=YB1
208*         SPACE(40)=YT1
209*         SPACE(41)=MMM
210*         SPACE(42)=55
211*         WRITE(10) SPACE
212*         IF(MMM.LE.1000) GO TO 1507
213*         DO 1508 I=1,MMM
214*    1508 SPACE(I+75)=FLOAT(I)*FC1/FLOAT(M)
215*         WRITE(10) SPACE
216*         GO TO 1507
217*     999 WRITE(6,46) XL
218*      46 FORMAT(19H1 IMPOSSIBLE X-GRID,26H, HORIZONTAL AXIS MINIMUM  ,F10.5
219*        1,/3X,26HLESS THAN OR EQUAL TO ZERO  )
220*         GO TO 1507
221*     899 WRITE(6,48) YB
222*      48 FORMAT(19H1 IMPOSSIBLE Y-GRID,23H, VERTICAL AXIS MINIMUM  ,F10.5,
223*        1/3X,26HLESS THAN OR EQUAL TO ZERO  )
224*    1507 IF(NSRS.EQ.1) GO TO 600
225*         GO TO (1200,1300,1420,620),NCNT
226*    1420 DO 1421 I=1,MMM
227*    1421 DATA(I)=Q(I,1,2)
228*         SPACE(37)=FC1/FLOAT(M)
```

```
229*            SPACE(38)=FC
230*            SPACE(39)=-180.
231*            SPACE(40)=180.
232*            SPACE(1)=1
233*            SPACE(32)=6H   PHA
234*            SPACE(33)=6HSE ANG
235*            SPACE(34)=6HLE IN
236*            SPACE(35)=6HDEGREE
237*            SPACE(36)=6HS
238*            WRITE(10) SPACE
239*            IF(MMM.LE.1000) GO TO 1400
240*            DO 1423 I=1,MMM
241*    1423    SPACE(I+75)=FLOAT(I)*FC1/FLOAT(M)
242*            WRITE(10) SPACE
243*            GO TO 1400
244*     620    DO 1451 I=1,MMM
245*    1451    DATA(I)=Q(I,2,1)
246*            SPACE(37)=FC1/FLOAT(M)
247*            SPACE(38)=FC
248*            SPACE(39)=-180.
249*            SPACE(40)=180.
250*            SPACE(1)=1
251*            SPACE(32)=6H   PHA
252*            SPACE(33)=6HSE ANG
253*            SPACE(34)=6HLE IN
254*            SPACE(35)=6HDEGREE
255*            SPACE(36)=6HS
256*            WRITE(10) SPACE
257*            IF(MMM.LE.1000) GO TO 600
258*            DO 1452 I=1,MMM
259*    1452    SPACE(I+75)=FLOAT(I)*FC1/FLOAT(M)
260*            WRITE(10) SPACE
261*    C
262*    C   CHECK FOR NULL REQUEST
263*    C
264*    C
265*      600   RETURN
266*            END

END OF COMPILATION:
```

```
C
C     THIS PROGRAM FINDS THE HURST RANGE FOR SAMPLES OF SIZE 125*2**N,
C     WHERE N RANGES FROM 0 TO NL-1. NL DIFFERENT SIZES CAN BE CHOSEN.
C
C
C     KK   = SEQUENCE NUMBER OF SAMPLE
C     KL   = SAMPLE SIZE
C     KM   = MAXIMUM SAMPLE SIZE
C     KN   = NUMBER OF SAMPLE
C     NA   = INTERVAL BETWEEN POINTS CHOSEN FROM ORIGINAL DATA
C     NL   = NUMBER OF SAMPLE SIZES BEING USED
C     IDF  = NUMBER OF KM INTERVALS TO USE FOR COMPUTATIONS
C     NYPL= PLOTTING FLAG( NYPL NON-ZERO - PLOT)
C     SUM1(I) = SUM OF DATA VALUES FOR ITH SAMPLE
C     SUM2(I) = SUM OF SQUARES OF DATA VALUES FOR ITH SAMPLE
C
C     NYPL = 0 NO PLOTS
C            1 PLOT
C     NPRNT=  0 PRINT ALL HURST RANGE VALUES
C            1 PRINT ONLY MEAN HURST RANGE
C     NORM = 0 DO NOT NORMALIZE
C            1 NORMALIZE
C
      COMMON /ALL/LTIT(20),NL    ,IEOF(10),AMNHR(20),SAMPSZ(20),
     * JTIM(2),A2(125),SM(20),NYPL,NPRNT,NORM
      DIMENSION EOF(10)
      DATA (EOF(I),I=1,10)/10*6HEOFEOF/
      DO 5 I=1,10
 5    IEOF(I)=EOF(I)
 100  FORMAT(3I1)
      READ(5,100)NYPL,NPRNT,NORM
      IF(NYPL)10,12,10
 10   REWIND 12
 12   CALL MAIN
      IF(NYPL)20,22,20
 20   CALL PLTPOW
 22   STOP
      END
```

```
      SUBROUTINE MAIN
      COMMON /ALL/LTIT(20),NL    ,IEOF(10),AMNHR(20),SAMPSZ(20),
     * JTIM(2),A2(125),SM(20),NYPL,NPRNT,NORM
      COMMON /L1/X(12288)          ,SUM1(2048),SUM2(2048),HURST(    8),N
      COMMON /L2/KK,KN,J,ANI,K2,KL,M,L,KM,LR,KX(20),KLO
      COMMON /L3/KLMN,   ID,IDF,NA,NCHAN,NS,ISTM,IOTCT
      COMMON /L4/IY(300),JY(600),AUM1(2),AUM2(2)
      COMMON /L5/      ILOC,IXCT,JSTMF
      COMMON /L6/IRECT,NBL
 96   FORMAT(20A6)
 98   FORMAT(1H0,13HSAMPLE SIZE =,I6)
 99   FORMAT(1H1,45X,18HHURST RANGE VALUES )
 100  FORMAT(16I5)
 101  FORMAT(19H MEAN HURST RANGE =,F10.4)
 102  FORMAT(8F15.3)
 103  FORMAT(17H MEAN HURST RANGE,F10.3)
 104  FORMAT(2A6,I6,I3,I5,I2,2I3)
 107  FORMAT(12H START TIME ,2A6,10X,I6)
C
C     AT THIS POINT READ IN THE DATA
C
 8    CONTINUE
      ID=0
      ILOC=1
      IXCT=1
      CALL HEDRED(LTIT,20,PARCK,1,EOFCK)
      IF(EOFCK.NE.0.0) GO TO 40
      CALL HEDRED(IY,6,PARCK,1,EOFCK)
      REWIND 99
      WRITE(99,96)(IY(I),I=1,9)
      REWIND 99
      READ(99,104)SERNO,DATE,ITIM1,ITIM2,ISR, CHAN,NS,NBL
      CALL HEDRED(IY,34,PARCK,1,EOFCK)
      CALL HEDRED(IY,34,PARCK,1,EOFCK)
      READ(5,100)   IDF
      READ(5,100)NA,NL,KLO
      IRECT=4
 1    LR=0
      READ(5,100)ISTM
      IF(ISTM   .GE.99999) GO TO 40
      JDFCT=0
      JSTMF=0
      AUM1(1)=0.0
      AUM1(2)=0.0
      AUM2(1)=0.0
      AUM2(2)=0.0
      DO 4 I=1,NL
      SM(I)=0.0
      AMNHR(I)=0.0
 4    KX(I)=0
 2    ANI=KLO
      KN=2**(NL-1)
      AI=KN
      KM=AI*ANI
      KL=KLO
```

```
      CALL READ1(IOK)
      IF(IOK.NE.0) GO TO 40
      IF(ISTM.LT.0) GO TO 1
C
C     COMPUTE HURST RANGE FOR SMALLEST SAMPLES
C
      J=KN/2
      DO 3 I=1,J
      SUM1(I)=0.0
 3    SUM2(I)=0.0
      J=0
      KLMN=0
      KK=0
      WRITE(6,99)
      CALL HMS(ISTM,JTIM)
      WRITE(6,107)(JTIM(I),I=1,2),ISTM
      WRITE(6,98)KL
 5    DO 10 I=1,KL
      KJS=I+J
 10   A2(I)=X(KJS)
      CALL ADRAN1
      IF(MOD(KK,8))12,11,12
 11   IF(NPRNT)7,6,7
 6    WRITE(6,102)(HURST(I),I=1,8)
 7    KK=0
 12   J=J+KL
      IF(J.GE.KM)GO TO 15
      GO TO 5
 15   IF(MOD(KK,8))17,18,17
 17   KK=MOD(KK,8)
      IF(NPRNT)18,16,18
 16   WRITE(6,102)(HURST(I),I=1,KK)
 18   KX(1)=KN + KX(1)
      XK=KX(1)
      HMEAN= SM(1)/XK
      SM(1)=0
      WRITE(6,103)HMEAN
      AMNHR(1)=HMEAN+AMNHR(1)
      SAMPSZ(1)=KL
C
C     COMPUTE HURST RANGE FOR ALL OTHER SAMPLE SIZES
C
      XS=KLO
      DO 20 M=2,NL
      KN1=2**(NL-M)
      KL=2**(M-1)
      AI=KL
      ANI=AI*XS
      KL=ANI
 23   WRITE(6,98)KL
      SAMPSZ(M)=KL
      K2=0
      IOTCT=0
      DO 30 L=1,KN1
      IOTCT=IOTCT+1
      CALL ADRAN2
```

```
      IF(IOTCT-8)30,28,28
 28   IF(NPRNT)27,26,27
 26   WRITE(6,102)(HURST(I),I=1,8)
 27   IOTCT=0
 30   CONTINUE
      IF(IOTCT)32,32,31
 31   IF(NPRNT)32,33,32
 33   WRITE(6,102)(HURST(I),I=1,IOTCT)
 32   KX(M)=KX(M)+KN1
      XK=KN1
      HMEAN=SM(M)/XK
      SM(M)=0.
      WRITE(6,103)HMEAN
      AMNHR(M)=HMEAN+AMNHR(M)
C
C     CREATE PROPER SUMS BY ADDING SUMS FROM TWO SAMPLES OF PREVIOUS
C      SIZE
C
 24   KK=0
      DO 25 I=2,KN1,2
      KK=KK+1
      SUM1(KK)=SUM1(I)+SUM1(I-1)
 25   SUM2(KK)=SUM2(I)+SUM2(I-1)
 20   CONTINUE
      JDFCT=JDFCT+1
      IF(JDFCT-IDF)2,50,50
 50   DF=IDF
      IF(NYPL)51,60,51
 51   DO 52 IJ=1,NL
 52   AMNHR(IJ)=AMNHR(IJ)/ DF
      WRITE(12)LTIT
      WRITE(12)JTIM,(AMNHR(IJ),IJ=1,NL),(SAMPSZ(IJ),IJ=1,NL)
C
C     REFORMAT DATA FOR SELF SIMILARITY
C
 60   IJ=10240
      XMIN=X(10240)-X(10239)
      XTOT=0.0
 65   I=IJ-1
      X(IJ)=(X(IJ)-X(I))
      XTOT=XTOT+X(IJ)
      IF(X(IJ).LT.XMIN)XMIN=X(IJ)
      IJ=IJ-1
      IF(IJ.GT.1) GO TO 65
      IF(X(1).LT.XMIN) XMIN=X(1)
      IF(XMIN)70,74,73
 70   XMIN=-XMIN
      XTOT=0.0
      DO 72 I=1,10240
      X(I )=X(I)+XMIN
 72   XTOT=XTOT+X(I)
      GO TO 74
 73   XMIN=0.0
 74   AVE=XTOT/10240.0
```

```
      STD=0.0
      DO 75 I=1,10240
      ASTD=ABS(X(I)-AVE)
75    STD=STD+ASTD*ASTD
      STD=SQRT(STD/10239.0)
      DO 77 I=1,10240
77    X(I)=(X(I)-AVE)/STD
      X(2)=X(2)+X(1)
      K2=0
      IJ=0
66    K1=K2+1
      K2=K2+10
      IJ=IJ+1
      X(IJ)=0.0
      DO 68 I=K1,K2
68    X(IJ)=X(IJ)+X(I)
      IF(K2.LT.10240) GO TO 66
      CALL SLFSIM
      GO TO 1
40    CALL REWOLD(1,1)
      IF(NYPL)42,44,42
42    DO 55 I=1,2
55    LTIT(I)=IEOF(I)
      WRITE(12)LTIT
      REWIND 12
44    RETURN
      END
```

```
      SUBROUTINE ADRAN1
      COMMON /ALL/LTIT(20),NL    ,IEOF(10),AMN R(20),SAMPSZ(20),
     * JTIM(2),A2(125),SM(20),NYPL,NPRNT,NORM
      COMMON /L1/X(12288)          ,SUM1(2048),SUM2(2048),HURST(    8),N
      COMMON /L2/KK,KN,J,ANI,K2,KL,M,L,KM,LR,KX(20),KLO
      COMMON /L3/KLMN,  ID,IDF,NA,NCHAN,NS,ISTM,IOTCT
      COMMON /L4/IY(300),JY(600),AUM1(2),AUM2(2)
      COMMON /L5/      ILOC,IXCT,JSTMF
      COMMON /L6/IRECT,NBL
C
C     THIS SUBROUTINE FINDS THE HURST RANGE FOR A SAMPLE OF SIZE NI
C     THE SUMS NECESSARY TO FIND THE MEAN AND STANDARD DEVIATION ARE
C     PLACED IN ARRAYS FOR USE IN LARGER SAMPLES
C     DATA COMES IN IN THE A2 ARRAY
C     X ARRAY BECOMES CUMULATIVE VALUES OF ORIGINAL DATA
C     THE HURST RANGE IS STORED FOR PRINTING LATER
C
      KLMN=KLMN+1
      KK=KK+1
      K=1
      IF(MOD(KK,2).EQ.0) K=2
      DO 12 I=1,KL
      AUM1(K )=AUM1(K )+A2(I)
 12   AUM2(K )=AUM2(K )+A2(I)*A2(I)
      AMEAN=AUM1(K )/ANI
      ST=(ANI*AUM2(K )-AUM1( K)*AUM1(K ))/(AN *ANI)
      ST=SQRT(ST)
C
      IF(K-2)16,14,14
 14   K=KLMN/2
      SUM1(K)=AUM1(1)+AUM1(2)
      SUM2(K)=AUM2(1)+AUM2(2)
      DO 15 K=1,2
      AUM1(K)=0.0
 15    AUM2(K)=0.0
 16   CONTINUE
C
      SUP=-456.
      FNF=586.
C
      SUM=A2(1)-AMEAN
      IF(SUM.GT.SUP)SUP=SUM
      IF(SUM.LT.FNF)FNF=SUM
C     COMPUTE Y(MIN) AND Y(MAX)
      DO 18 K=2,KL
      AK=K
      IBB1=K+J
      IBB=K+J-1
      X(IBB1)=X(IBB  )+A2(K)
      SUM=X(IBB1)-AK*AMEAN
      IF(SUM.GT.SUP)SUP=SUM
 18   IF(SUM.LT.FNF)FNF=SUM
C     COMPUTE HURST RANGE
      HURST(KK)=(SUP-FNF)/ST
      SM(1)=SM(1)+HURST(KK)
 20   RETURN
      END
```

```
      SUBROUTINE ADRAN2
      COMMON /ALL/LTIT(20),NL    ,IEOF(10),AMN R(20),SAMPSZ(20),
     * JTIM(2),A2(125),SM(20),NYPL,NPRNT,NORM
      COMMON /L1/X(12288)          ,SUM1(2048), UM2(2048),HURST(   8),N
      COMMON /L2/KK,KN,J,ANI,K2,KL,M,L,KM,LR, X(20),KLO
      COMMON /L3/KLMN,  ID,IDF,NA,NCHAN,NS,IS,M,IOTCT
      COMMON /L4/IY(300),JY(600),AUM1(2),AUM2 2)
      COMMON /L5/      ILOC,IXCT,JSTMF
      COMMON /L6/IRECT,NBL
C
C     THIS SUBROUTINE COMPUTES THE HURST RANGE FOR SAMPLES OF TWICE
C     THE SIZE OF SAMPLES WHICH HAVE BEEN PREVIOUSLY SUMED AND CUMULATED
C     THE HURST RANGE IS STORED FOR PRINTING LATER
C     CUMULATIVE DATA IS IN X ARRAY
C
      AMEAN = SUM1(L)/ANI
      ST=(ANI*SUM2(L)-(SUM1(L)*SUM1(L)))/(ANI*ANI)
      ST=SQRT(ST)
      K1=K2+1
      KL=ANI/2.0
      K2=K2+KL
 5    SUP=-456.
      FNF=586.
      AK=0.
      DO 10 K=K1,K2
      AK=AK+1.0
      SUM=X(K)-AK*AMEAN
      IF(SUM.GT.SUP)SUP=SUM
 10   IF(SUM.LT.FNF)FNF=SUM
      XK2=X(K2)
      K1=K2+1
      K2=K2+KL
      DO 20 K=K1,K2
      AK=AK+1.0
      X(K)=XK2 + X(K)
      SUM = X(K)-AK*AMEAN
      IF(SUM.GT.SUP)SUP=SUM
 20   IF(SUM.LT.FNF)FNF=SUM
      HURST(IOTCT) = (SUP-FNF)/ST
      SM(M)=SM(M) + HURST(IOTCT)
      RETURN
      END
```

```
      SUBROUTINE SLFSIM
      COMMON /ALL/LTIT(20),NL    ,IEOF(10),AMN R(20),SAMPSZ(20),
     * JTIM(2),A2(125),SM(20),NYPL,NPRNT,NORM
      COMMON /L1/X(12288)          ,SUM1(2048), UM2(2048),HURST(   8),N
      DIMENSION S(4)
  100 FORMAT(1H1,20A6,///,16H SELF SIMILARITY  ,15X,10HSTART TIME ,2X,2A6
     *)
  101 FORMAT(//,14H SAMPLE SIZE = ,F8.0,10X,17HNUMBER OF SAMPLES ,I8)
      NK=1024
      DM=2.0**0.6
      DO 10 M=1,11
      WRITE(6,100)LTIT,JTIM
      IF(M.EQ.1) GO TO 15
      K=0
      DO 20 L=2,NK,2
      K=K+1
   20 X(K)=(X(L)+X(L-1))/2.0
      NK=K
      GO TO 25
   15 D=10.0**0.6
      DO 30 L=1,NK
   30 X(L)=X(L)/D
   25 XNK=M-1
      IF (NORM) 50,55,50
   50 CONTINUE
      CW=NK
      S(1)=0.0
      S(2)=0.0
      DO 16 L=1,NK
   16 S(1)=S(1)+X(L)
      S(1)=S(1)/CW
      DO 17 L=1,NK
      S(3)=ABS(X(L)-S(1))
   17 S(2)=S(2)+S(3)*S(3)
      S(2)=S(2)/(CW-1.0)
      IF(S(2))14,14,13
   13 S(2)=SQRT(S(2))
   14 DO 18 L=1,NK
   18 X(L)=(X(L)-S(1))/S(2)
   55 CONTINUE
      SIZE=10.0*2.0**XNK
      SUM2(2000)=SIZE
      XNK=NK
      WRITE(6,101)SIZE,NK
      DO 26 L=1,4
   26 S(L)=0.0
      XMIN=X(1)
      XMAX=X(1)
      DO 27 I=2,NK
      IF(X(I).LT.XMIN)XMIN=X(I)
   27 IF(X(I).GT.XMAX)XMAX=X(I)
      CW=(XMAX-XMIN)/32.0
      CALL FRQDIS(X,NK,CW,XMIN)
      DO 40 J=1,NK
   40 S(1)=S(1)+X(J)
      DO 35 J=2,4
      CW=J
      DO 35 L=1,NK
      XMAX=ABS(X(L))
```

```
35    S(J)=S(J)+XMAX**CW
      FN=NK
10    CALL MOMENT(S,FN)
      RETURN
      END



      SUBROUTINE FRQDIS(X,N,CW,XMIN)
      COMMON /ALL/LTIT(20),NL    ,IEOF(10),AMN R(20),SAMPSZ(20),
     * JTIM(2),A2(125),SM(20),NYPL,NPRNT,NORM
      COMMON /L1/X(12288)          ,SUM1(2048), UM2(2048),HURST(   8),N
100   FORMAT(//,24H FREQUENCY DISTRIBUTION ,//)
101   FORMAT(6X,5HCLASS,11X,9HFREQUENCY,7X,8HREL FREQ,8X,7HDENSITY,7X,
     * 8HCUM FREQ)
102   FORMAT(3X,6H BELOW,F7.2,F15.0,3F15.4)
103   FORMAT(1X,F6.2,2H -,F7.2,F15.0,3F15.4)
104   FORMAT(3X,6H ABOVE,F7.2,F15.0,3F15.4)
      DO 5 I=1,32
5     SUM1(I)=0.0
      DO 10 I=1,N
      K=(X(I)-XMIN)/CW+1.0
      IF(K.LE.0)K=1
      IF(K.GT.32)K=32
10    SUM1(K)=SUM1(K)+1.0
      WRITE(6,100)
      WRITE(6,101)
      CU=XMIN+CW
      FN=N
      RFD=SUM1(1)/FN
      DFD=RFD/CW
      SFD=RFD
      SUM2(1)=SFD
      SUM2(1001)=CU
      WRITE(6,102)CU,SUM1(1),RFD,DFD,SFD
      DO 20 I=2,31
      RFD=SUM1(I)/FN
      DFD=RFD/CW
      SFD=SFD+RFD
      CL=CU
      CU=CU+CW
      SUM2(I)=SFD
      SUM2(I+1000)=CL+CW/2.0
20    WRITE(6,103)CL,CU,SUM1(I),RFD,DFD,SFD
      RFD=SUM1(32)/FN
      DFD=RFD/CW
      SFD=SFD+RFD
      SUM2(32)=SFD
      SUM2(1032)=CU
      WRITE(12)SUM2(2000),(SUM2(I),I=1,32),(SUM2(I),I=1001,1032)
      WRITE(6,104)CU,SUM1(32),RFD,DFD,SFD
      RETURN
      END
```

```
      SUBROUTINE MOMENT(SUMX,FNX)
      DIMENSION MO(4),MM(4),SUMX(4)
      REAL MM,MO
 8051 FORMAT(//,25H MOMENTS ABOUT THE ORIGIN
 8052 FORMAT(8H FIRST =,E15.8,5X,8HSECOND =,E 5.8,5X,7HTHIRD =,E15.8,5X,
     *8HFOURTH =,E15.8)
 8053 FORMAT(//,23H MOMENTS ABOUT THE MEAN)
 8054 FORMAT(/,7H MEAN =,E15.8,5X,10HVARIANCE =,E15.8,5X,20HSTANDARD DEV
     *IATION =,E15.8,//)
 8055 FORMAT(27H COEFFICIENT OF VARIATION = ,E15.8,5X,10HSKEWNESS =,E15.
     *8,5X,8HEXCESS =,E15.8)
      DO 8050 I=1,4
 8050 MO(I)=SUMX(I)/FNX
      MM(1)=0.0
      AMA1=ABS(MO(1))
      MM(2)=MO(2)- AMA1**2.0
      MM(3)=MO(3)-3.0*MO(2)*MO(1)+2.0* AMA1**_.
      MM(4)=MO(4)-4.0*MO(3)*MO(1)+6.0*MO(2)*  MA1**2.-3.0* AMA1**4.0
      VAR=FNX*MM(2)/(FNX-1.0)
      STD=SQRT(VAR)
      COV=STD/MO(1)
      CON=FNX**2./((FNX-1.)*(FNX-2.))
      CSKEW=CON*MM(3)/(VAR*STD)
      CKUR=CON*((FNX+1.0)*MM(4)-3.0*(FNX-1.0)*MM(2)**2.)/((FNX-3.0)*VAR*
     **2.0)
      WRITE(6,8051)
      WRITE(6,8052)(MO(I),I=1,4)
      WRITE(6,8053)
      WRITE(6,8052)(MM(I),I=1,4)
      WRITE(6,8054) MO(1),VAR,STD
      WRITE(6,8055)COV,CSKEW,CKUR
      RETURN
      END
```

```
      SUBROUTINE PLTPOW
      COMMON /ALL/LTIT(20),NL    ,IEOF(10),AMNHR(20),SAMPSZ(20),
     * JTIM(2),A2(125),SM(20),NYPL,NPRNT,NORM
      DIMENSION XPLOT(2002)
      DIMENSION ICHAR(5)
      DIMENSION CFR(46)
      CFR(1)=.5
      CFR(2)=.5199
      CFR(3)=.5398
      CFR(4)=.5596
      CFR(5)=.5793
      CFR(6)=.5987
      CFR(7)=.6179
      CFR(8)=.6368
      CFR(9)=.6554
      CFR(10)=.6736
      CFR(11)=.6915
      CFR(12)=.7088
      CFR(13)=.7257
      CFR(14)=.7422
      CFR(15)=.7580
      CFR(16)=.7734
      CFR(17)=.7881
      CFR(18)=.8023
      CFR(19)=.8159
      CFR(20)=.8289
      CFR(21)=.8413
      CFR(22)=.8531
      CFR(23)=.8643
      CFR(24)=.8749
      CFR(25)=.8849
      CFR(26)=.8944
      CFR(27)=.9032
      CFR(28)=.9115
      CFR(29)=.9192
      CFR(30)=.9265
      CFR(31)=.9332
      CFR(32)=.9394
      CFR(33)=.9452
      CFR(34)=.9505
      CFR(35)=.9554
      CFR(36)=.9641
      CFR(37)=.9713
      CFR(38)=.9772
      CFR(39)=.9821
      CFR(40)=.9861
      CFR(41)=.9893
      CFR(42)=.9918
      CFR(43)=.9938
      CFR(44)=.9965
      CFR(45)=.9981
      CFR(46)=.999
      DO 1 I=1,46
    1 CFR(I)=CFR(I)*100.0
C
```

```
 11   FORMAT(2F6.2)
 12   FORMAT(2I2)
 13   FORMAT(2A2)
 14   FORMAT(F8.0)
 15   FORMAT(2A6)
  16  FORMAT(19H1 IMPOSSIBLE X-GRID,26H, HORIZONTAL AXIS MINIMUM  ,F10.5
     1,/3X,26HLESS THAN OR EQUAL TO ZERO  ,2A6)
 17   FORMAT(13H TIME SLICE  ,2A6,/3X,4HY = ,F12.5,3H + ,F12.5,2H X)
  18  FORMAT(19H1 IMPOSSIBLE Y-GRID,23H, VERTICAL AXIS MINIMUM  ,F10.5,
     1/3X,26HLESS THAN OR EQUAL TO ZERO  ,2A6)
 1006 FORMAT(1H1,15H COEFFICIENTS   )
C
      WRITE(6,1006)
C
C
      ICHAR(1)=24
      ICHAR(2)=38
      ICHAR(3)=16
      ICHAR(4)=55
      ICHAR(5)=44
 5    CONTINUE
      READ(12)LTIT
      IF(LTIT(1).EQ.IEOF(1))GO TO 9999
      READ (12)JTIM,(AMNHR(I),I=1,NL),(SAMPSZ(IJ),IJ=1,NL)
      IF(JTIM(1).EQ.IEOF(1)) GO TO 9999
C
C   DETERMINE MIN AND MAX VALUES FOR Y
C
      YT=AMNHR(1)
      YB=YT
      DO 10  IJ=2,NL
      YT=AMAX1(YT,AMNHR(IJ))
   10 YB=AMIN1(YB,AMNHR(IJ))
C
C   SET THE MIN AND MAX VALUES FOR X
C
      XL=SAMPSZ(1)
      XR=SAMPSZ(NL)
C
C   SET MARGINS FOR LABELS
C
      MT=80
      MB=24
      MR=0
      ML=24
      IF(XL) 999,999,20
   20 IF(YB) 899,899,21
C
C   DETERMINE THE GRID RANGES IN POWERS OF 10
C
   21 DO 22 I=1,10
      K=I-5
      IF(10.**K-XL) 22,22,23
   23 K=K-1
      XL1=10.**K
      GO TO 24
```

```
   22 CONTINUE
   24 DO 25 I=1,10
      K=I-5
      IF(10.**K-YB) 25,25,26
   26 K=K-1
      YB1=10.**K
      GO TO 29
   25 CONTINUE
   29 DO 27 K=1,10
      I=K-1
      IF(10.**I-XR) 27,28,28
   28 XR1=10.**I
      GO TO 31
   27 NX=K+3
   31 DO 32 K=1,10
      I=K-1
      IF(10.**I-YT) 32,33,33
   33 YT1=10.**I
      GO TO 34
   32 NY=K+3
C
C    SET LOG - LOG SCALING MODE
C
   34 CALL SMXYV(1,1)
      CALL SETMIV(ML,MR,MB,MT)
C
C    DRAW GRID LINES
C
      CALL GRID1V(4,XL1,XR1,YB1,YT1,1.0,1.0,1,1,1,1,NX,NY)
C
C    PLOT DATA POINTS
C
      CALL APLOTV(NL,SAMPSZ,AMNHR,1,1,1,55,IER)
C
C    WRITE HORIZONTAL AND VERTICAL TITLES
C
      CALL PRINTV(-11,11HSAMPLE SIZE ,450,8)
      CALL APRNTV(0,-14,-16,16HMEAN HURST RAN E ,15,623)
C
C    WRITE HEADER LABEL
C
      CALL PRINTV(120,LTIT,24,1000)
      CALL PRINTV(-10,10HSTART TIME  ,24,980)
      CALL PRINTV(12,JTIM,114,980)
C
C      FIT DATA
C
      DO 100 IJ=1,NL
      SM(IJ)=1.0
      A=AMNHR(IJ)
      IF(A)103,103,102
  102 AMNHR(IJ)=ALOG10(A)
  103 A=SAMPSZ(IJ)
      IF(A)100,100,101
  101 SAMPSZ(IJ)=ALOG10(A)
  100 CONTINUE
```

```
C
      CALL POLYN(SAMPSZ,AMNHR,SM,NL,2,1,A2)
      A=(XR-XL)/1000.0
      DO 110 IJ=1,1001
      JJ=IJ+1001
      B=IJ-1
      B=B*A+XL
      XPLOT(IJ)=B
      B=ALOG10(B)
      C=A2(1)+A2(2)*B
  109 XPLOT(JJ)=10.0**C
  110 CONTINUE
C
      A=XPLOT(1)
      IX1=IXV(A)
      B=XPLOT(1002)
      IY1=IYV(B)
      DO 120 IJ=2,1001
      A=XPLOT(IJ)
      JJ=IJ+1001
      B=XPLOT(JJ)
      IX2=IXV(A)
      IY2=IYV(B)
C
C     PLOT CURVE
C
      CALL LINEV(IX1,IY1,IX2,IY2)
      IX1=IX2
  120 IY1=IY2
      WRITE(6,17)(JTIM(IJ),IJ=1,2),(A2(IJ),IJ=1,2)
C
C     SECTION TO PLOT SELF-SIMILARITY
C
      CALL SMXYV(0,0)
      DO 200 IJ=1,11
      L=(IJ-1)*64+1
      K=L+63
  200 READ(12)A,(XPLOT(I),I=L,K)
      DO 206 IJ=1,5
      L=(IJ-1)*64+1
      K=L+31
      DO 206 J=L,K
      XPLOT(J)=XPLOT(J)*100.0
      IF(XPLOT(J).LT.0.01)XPLOT(J)=0.01
      IF(XPLOT(J).GT.99.99)XPLOT(J)=99.99
      CALL PRBSC(XPLOT(J))
  206 CONTINUE
      DY=0.01
      CALL PRBSC(DY)
      XL=DY
      DY=99.99
      CALL PRBSC(DY)
      XR=DY
      ML=45
      MR=0
      MB=24
```

```
      MT=80
      CALL FRAMEV(3)
      YB=XPLOT(33)
      YT=XPLOT(64)
      DO 202 I=65,257,64
      YB=AMIN1(YB,XPLOT(I+32))
  202 YT=AMAX1(YT,XPLOT(I+63))
      IF(YT.LT.4.0)YT=4.0
      IF(YB.GT.-4.0)YB=-4.0
      CALL XSCALV(XL,XR,ML,MR)
      CALL YSCALV(YB,YT,MB,MT)
      CALL LINRV(2,30,45,1023,YB,YT,.5,4,-4,2,12)
      A=50.0
      CALL PRBSC(A)
      I=NXV(A)
      CALL LINEV(I,24,I,944)
      CALL LINEV(I,24,I,944)
      IJ=50
      REWIND 99
      WRITE(99,12)IJ
      REWIND 99
      READ(99,13)IJ
      I=I-4
      CALL PRINTV(2,IJ,I,18)
      CALL PRINTV(2,IJ,I,950)
C
C     DRAW AND LABEL LINES FROM 20 - 80
C
      DO 205 I=52,80,2
      A=I
      CALL PRBSC(A)
      B=-A
      J=NXV(A)
      IJ=NXV(B)
      CALL LINEV(J,24,J,944)
      CALL LINEV(IJ,24,IJ,944)
      IF(MOD(I,10))205,240,205
  240 CALL LINEV(J,24,J,944)
      CALL LINEV(IJ,24,IJ,944)
      IX1=100-I
      REWIND 99
      WRITE(99,12)I,IX1
      REWIND 99
      READ(99,13)IY1,IX1
      IX2=J-4
      IY2=IJ-4
      CALL PRINTV(2,IY1,IX2,18)
      CALL PRINTV(2,IX1,IX2,950)
      CALL PRINTV(2,IY1,IY2,950)
      CALL PRINTV(2,IX1,IY2,18)
  205 CONTINUE
C
C     DRAW AND LABEL LINES FROM 10 - 20 AND 8  - 90
C
      DO 250 I=81,90
      A=I
```

```
      CALL PRBSC(A)
      B=-A
      J=NXV(A)
      IJ=NXV(B)
      CALL LINEV(J,24,J,944)
      CALL LINEV(IJ,24,IJ,944)
      IF(MOD(I,5))250,251,250
  251 CALL LINEV(J,24,J,944)
      CALL LINEV(IJ,24,IJ,944)
  250 CONTINUE
      IY1=90
      IX1=10
      REWIND 99
      WRITE(99,12)IY1,IX1
      REWIND 99
      READ(99,13)IY1,IX1
      IX2=J-4
      IY2=IJ-4
      CALL PRINTV(2,IY1,IX2,18)
      CALL PRINTV(2,IX1,IX2,950)
      CALL PRINTV(2,IY1,IY2,950)
      CALL PRINTV(2,IX1,IY2,18)
C
C     DRAW AND LABEL LINES FROM 1 - 10 AND 90 - 99
C
      DO 260 I=90,99
      A=I
      CALL PRBSC(A)
      B=-A
      J=NXV(A)
      IJ=NXV(B)
      CALL LINEV(J,24,J,944)
      CALL LINEV(IJ,24,IJ,944)
      IF(I-95)260,262,261
  261 IF(I-99)260,262,260
  262 CALL LINEV(J,24,J,944)
      CALL LINEV(IJ,24,IJ,944)
      IX1=100-I
      REWIND 99
      WRITE(99,12)I,IX1
      REWIND 99
      READ(99,13)IY1,IX1
      IX2=J-4
      IY2=IJ-4
      CALL PRINTV(2,IY1,IX2,18)
      CALL PRINTV(2,IX1,IX2,950)
      CALL PRINTV(2,IY1,IY2,950)
      CALL PRINTV(2,IX1,IY2,18)
  260 CONTINUE
C
C     DRAW AND LABEL LINES FROM .1 - 1 AND 99 - 99.9
C                          AND .01 - .1 AND  9.9 - 99.99
C
      A=99.0
      AINC=0.1
      DO 265 I=1,2
```

```
      DO 266 L=1,9
      A=A+AINC
      B=A
      CALL PRBSC(B)
      C=-B
      J=NXV(B)
      IJ=NXV(C)
      CALL LINEV(J,24,J,944)
  266 CALL LINEV(IJ,24,IJ,944)
      CALL LINEV(J,24,J,944)
      CALL LINEV(IJ,24,IJ,944)
      B=1000.0-A
      REWIND 99
      WRITE(99,11)A,B
      REWIND 99
      READ(99,15)A,B
      J=J-24
      IJ=IJ-24
      IF(I-2)268,267,268
  267 J=J-16
  268 CONTINUE
      CALL PRINTV(6,A,J,18)
      CALL PRINTV(6,B,J,950)
      CALL PRINTV(6,B,IJ,18)
      IF(I-2)271,270,271
  270 IJ=IJ+18
  271 CALL PRINTV(6,A,IJ,950)
      A=99.90
  265 AINC=0.01
      DO 210 I=1,5
      J=(I-1)*64+1
  210 CALL APLOTV(32,XPLOT(J),XPLOT(J+32),1,1 1,ICHAR(I),IERR)
      CALL PRINTV(120,LTIT,24,1000)
      CALL PRINTV(-10,10HSTART TIME ,24,984)
      CALL PRINTV(12,JTIM,114,984)
      CALL PRINTV(-15,15HSELF-SIMILARITY ,24,968)
      CALL PRINTV(-47,47HSAMPLE SIZE - 10=H   20=0   40=+   80=X   160=*
     *,250,968)
      CALL PRINTV(-20,20HCUMULATIVE FREQUENCY ,430,4)
      CALL APRNTV(0,-14,-14,14HCLASS INTERVAL ,15,630)
C
C     PLOT CUMULATIVE FREQUENCY OF NORMAL DISTRIBUTION
C
      J=1
      A=0.0
      XPLOT(46)=0.0
      XPLOT(246)=0.0
      DO 220 I=47,80
      A=A+0.05
      J=J+1
      B=CFR(J)
      CALL PRBSC(B)
      XPLOT(I)=B
      IX1=92-I
      XPLOT(IX1)=-B
      XPLOT(I+200)=A
```

```
      IX1=292-I
220   XPLOT( IX1 )=-A
      A=1.80
      DO 225 I=81,88
      J=J+1
      B=CFR(J)
      CALL PRBSC(B)
      XPLOT(I)=B
      IX1=92-I
      XPLOT(IX1)=-B
      XPLOT(I+200)=A
      IX1=292-I
      XPLOT( IX1 )=-A
225   A=A+0.1
      A=2.7
      DO 230 I=89,91
      J=J+1
      B=CFR(J)
      CALL PRBSC(B)
      XPLOT(I)=B
      IX1=92-I
      XPLOT(IX1)=-B
      XPLOT(I+200)=A
      IX1=292-I
      XPLOT( IX1 )=-A
230    A=A+0.2
      DO 235 I=2,91
      CALL LINEV(NXV(XPLOT(I-1)),NYV(XPLOT(I+199)),NXV(XPLOT(I)),
     * NYV(XPLOT(I+200)))
235   CONTINUE
      GO TO 5
 899  WRITE(6,18) YB,(JTIM(IJ),IJ=1,2)
      GO TO 5
 999  WRITE(6,16) XL,(JTIM(IJ),IJ=1,2)
      GO TO 5
9999  CONTINUE
      CALL FRAMEV
      CALL PLTND
      REWIND 12
      RETURN
      END
```

* U.S. GOVERNMENT PRINTING OFFICE: 1973 O—543-576/7